



TECHNISCHE
UNIVERSITÄT
WIEN

DISSERTATION

Computational and Empirical Assessment of Ventilation Methods in Buildings

**ausgeführt zum Zwecke der Erlangung des akademischen Grades einer
Doktorin der technischen Wissenschaften unter der Leitung von**

Univ. Prof. Dipl.-Ing. Dr. techn. Ardeshir Mahdavi
E 259/3 Abteilung für Bauphysik und Bauökologie
Institut für Architekturwissenschaften
TU Wien

**eingereicht an der Technischen Universität Wien
Fakultät für Architektur und Raumplanung**

von

Dipl.Ing. Mahnameh Taheri
Matrikelnummer: 1028489
Othmargasse 21/22
A-1200 Wien

Kurzfassung

Der Komfort und die Behaglichkeit von Gebäudenutzern hängen neben den innenklimatischen Bedingungen (Strahlungs- und Lufttemperatur, Luftqualität, Luftbewegung, Feuchtigkeit, etc.) unter anderem auch von den Steuerungsmöglichkeiten der Nutzer ab. In den letzten Jahren konnte beobachtet werden, dass das Ansteigen der Aussen-temperatur in urbanen Bereichen nicht nur zu einem Anstieg der Innentemperaturen in innerstädtischen Gebäuden führt, sondern auch zu einer Verschlechterung der Innenluftqualität in den entsprechenden Räumlichkeiten führt. Damit verbunden kommt es zu einem signifikant höheren Einsatz von mechanischen Lüftungsanlagen und Klimageräten, um ausreichende Luftqualität und akzeptable Innentemperaturen zu gewährleisten. Nachhaltige(re) Methoden, wie beispielsweise passive Kühlung mit natürlicher Belüftung bieten zwar eine zufriedenstellende Effizienz, sind aber - aufgrund nur unsicher vorher-sagbarer klimatischer Gegebenheiten und Nutzungsmuster - in Design und Betrieb nicht trivial umzusetzen. Oft verwendete konventionelle Klimatisierungssysteme sind auch bei aussen-klimatischen Schwankungen in der Lage kontrollierte Innenraumbedingungen zu schaffen. Allerdings werden diese Systeme aufgrund Ihrer - zumeist aus fossilen Energieträgern gespeisten - Energieintensivität, in der Regel nicht als nachhaltig betrachtet. Aktuelle Schätzungen gehen davon aus, dass Lüftungssysteme bis zu 30% des Energiebedarfs von typischen Bürogebäuden ausmachen. Die Performance von Belüftungssystemen hängt von mehreren Faktoren wie der Effizienz des Systems, der Luftverteilung, der Platzierung der Lufteinlässe und der Auslässe, etwaiger Luftleckagen, des Betriebsablaufs, der (angestrebten) Temperatursollwerte, der zu transportierenden Luftmenge sowie einigen weiteren ab. Typischerweise eingesetzte Lüftungssysteme liefern in der Regel frische (und zumeist kühle) Luft in den Innenraum und ersetzen damit die verbrauchte Raumluft. Zumeist werden solche Systeme auf ganze Räume dimensioniert. Die erforderlichen hohen Lüftungsraten und der sich daraus ergebende hohe Energieverbrauch solcher Systeme könnte durch räumlich gezielte Konditionierung wie zum Beispiel mit einer Verdrängungslüftungsanlage erheblich reduziert werden. Eine weitere Möglichkeit stellt ein "persönliches Lüftungssystem" dar, welches frische und kühle Luft in das direkte Umfeld von Nutzern liefert. Solche persönlichen Lüftungssysteme ermöglichen es den Gebäudenutzern die Lüftung gemäss Ihren individuellen Vorlieben

und Bedürfnissen anzupassen und zu kontrollieren.

Im Rahmen dieser Dissertation wurden mit Hilfe von rechnerischen und empirischen Methoden zur Beurteilung der Funktionalität von Lüftungssystemen in Innenräumen Untersuchungen in Bezug auf Raumluftqualität und thermischen Komfort durchgeführt. Es wurden unterschiedliche innovative Lüftungskonzepte, wie Verdrängungslüftungskonzepte oder individuelle Belüftungssysteme, untersucht. Das Ziel dieser Bemühungen war es den persönlichen Komfort und die Produktivität der Nutzer unter Berücksichtigung von Umweltfaktoren und der jeweiligen Systemeffizienz zu verbessern. Die Beurteilung der untersuchten Systeme erfolgte auf Basis von Messdaten (objektive Evaluierung) und mittels Befragungen von Nutzern in Räumen mit entsprechenden Systemen (subjektive Evaluierung). Darauf aufbauend, wird der Nutzen von CFD (Computational Fluid Dynamics) Simulationen und deren Anwendung zur Leistungsbewertung von Lüftungssystemen sowie der Modellierung und Bewertung von Luftströmungen in Innenräumen untersucht. Die vorliegende Arbeit illustriert, wie der Einfluss unterschiedlicher Gestaltungsmöglichkeiten (z. B. Anzahl und Ort der Diffusoren und Luftströmungsraten in einem architektonischen Raum) mittels einer geringen Anzahl von numerischen Simulationen ermittelt werden kann. Das Ergebnis dieser Studie kann für Architekten, Bauingenieure, Bauwissenschaftler und andere Stakeholder nützlich sein, um die Energieeffizienz und den Komfort in (mechanisch) belüfteten Räumen weiter zu verbessern und entsprechende Vorhersagemodelle zu entwickeln.

Abstract

The comfort level and well being of building occupants is affected, among other factors, by radiant and air temperature, air quality, air movement, humidity, as well as the degree to which they can control their environment. In the recent years, due to the temperature increase and air quality decrease in urban areas, ventilation systems became more common, in order to meet the requirements to ensure adequate air quality and acceptable indoor temperature. Sustainable methods, such as passive cooling with natural ventilation, have not been yet successful to be used as the only ventilation system, which can fully provide comfortable indoor environment in every building. Moreover, even though the passive systems are efficient, they are dependent to the parameters, such as wind condition, temperature fluctuations, thermal mass of the building elements, etc., which makes them rather difficult to predict and control. Typical conventional climate control systems, operated by fossil fuels, are able to maintain consistent indoor condition against the changing outdoor climate condition. However, these systems are usually not sustainable. For instance, it is estimated that, ventilation systems account for 30% of the energy demand for office buildings. The energy consumption and comfort level provided by a ventilation system depend on the different factors, including the efficiency of the system, air distribution, placement of the air inlets and outlets, air leakage, operation schedule, temperature set points, airflow rate, etc. Conventional ventilation systems usually supply fresh and cool air into the space and replace the entire stale room air. The high energy consumption and required ventilation rates could be reduced by cooling down the actual occupied zones instead of the entire space, for instance using displacement ventilation system. Another example in this regard is “personal ventilation system”, which has the advantage to deliver the fresh and cool air directly to the occupied breathing zone. Moreover, personal ventilation system offers the occupants the possibility of individual adjustments and control of their own surrounding environment.

This dissertation presents the application of computational and empirical methods to evaluate functionality of ventilation systems in architectural spaces with regard to indoor air quality and thermal comfort. The innovative ventilation systems in office spaces are

investigated, including displacement and personal ventilation systems. The research application is aimed at improving the personal comfort and productivity of occupants, taking into account the environmental factors and efficiency of the systems. Performance of the studied systems is investigated via objective evaluations by measurements and subjective evaluations based on feedback from occupants. This study also illustrates the utility of CFD (Computational Fluid Dynamics) simulations for the performance evaluation of ventilation systems and the estimation of airflow pattern in the space. Furthermore, the present contribution investigates whether a relatively comprehensive impact assessment of various design variables and input assumptions (e.g., number and location of diffusers and airflow rates in an architectural space) can be established based on a detailed but small number of numerical simulations. The outcome of such study is remarkably helpful to architects, building engineers, and building scientists, to further improve energy efficiency and occupants' comfort in ventilated spaces, and to develop and refine prediction models.

Acknowledgments

My deepest gratitude goes to, Professor Ardeshir Mahdavi, for his steadfast support, guidance, inspiration and encouragement. I feel incredibly privileged to have him as my supervisor and mentor. He has taught me more than I could ever give him credit for here.

I am heartily grateful to my examiners, Professor Andrea Gasparella and Professor Milos Kalousek, who accepted to dedicate their precious time to evaluate this work.

I would like to thank the Austrian research promotion agency (FFG) for supporting this research in part (Project No. 834207). Parts of the text in this dissertation are adopted from papers, listed in the final chapter, coauthored with Professor Mahdavi and project team members. My thanks also goes to the companies Exhausto, Kunesch, and Kröswang for their support, as well as my dear colleagues and students, who participated in the experiments.

My sincere thanks goes out to Dr. Matthias Schuss, for his continuous support and guidance throughout this research. I am also grateful to Dr. Alfred Fail, Dr. Ulrich Pont, and Mr. Josef Lechleitner, for their efforts for the benefit of this work. I owe a lot to all of my colleagues at the Department of Building Physics and Building Ecology, and my friends in Vienna, who have supported me along the way.

I would like to remember those who I wish were here today, my grandparents Iran, Mansoor, Mahmood, and grandparents in-law, Doosti, Manidjeh, Ebrahim, and Kazem.

My deepest gratitude goes to my mother and father in-law, Mahboubeh and Madjid, who encouraged me with their love and support. My special regards goes to my grandmother Mehrangiz and my uncle Massoud, whose presence in Vienna was encouraging to start this journey. My heartfelt thanks goes to my lovely brother, Mehrshad, and the best little sister and friend any girl could ask for, Mahkameh.

Last but by no means least, I am deeply grateful to my parents, Mahboubeh and Hassan, for raising me with the believe that I could achieve anything I set my mind to, and providing me unconditional love and care. I wish to also express my warmest appreciation for my love, my life, my Mehrad, who has been a true supporter and gave me the chance to live my life to the fullest by his side, these past years.

*To my beloved Mehrad
for his indefatigable love of learning*

Contents

Kurzfassung	2
Abstract	4
Acknowledgments	5
Contents	7
List of Tables	10
List of Figures	12
Abbreviations and Nomenclature	18
1 Introduction	19
1.1 Motivation	19
1.2 Background	20
1.2.1 Thermal comfort and indoor air quality assessment	20
1.2.2 Displacement ventilation	21
1.2.3 Personal ventilation	22
1.3 Research questions corresponding to dissertation goal	25
1.4 Structure of work	25
2 Empirical Indoor Climate Assessment	27
2.1 Background	27
2.1.1 Building monitoring	27
2.1.2 Subjective evaluations	28
2.2 Method	30
2.2.1 Overview	30
2.2.2 Laboratory experiment	30
2.2.2.1 Surveys	32

2.2.2.2	Monitoring of physical data	36
2.2.3	Field experiment	37
2.2.3.1	Surveys	39
2.2.3.2	Monitoring of physical data	40
2.3	Results and discussions	42
2.3.1	Laboratory experiment	42
2.3.2	Field experiment	47
2.3.3	Concluding observations	57
3	Computational Indoor Climate Assessment	58
3.1	Background	58
3.1.1	Flow and heat transfer	58
3.1.2	Computational Fluid Dynamics (CFD)	58
3.1.3	CFD simulation	59
3.1.3.1	Domain discretization	60
3.1.3.2	Conservation equations	61
3.1.3.3	Navier-Stokes equations	63
3.1.3.4	Turbulence model	64
3.1.3.5	Numerical scheme, iteration and convergence	67
3.1.3.6	Boundary conditions	68
3.1.4	Integrated BES and CFD programs	69
3.1.5	Monitoring-assisted calibration of CFD model	71
3.2	Method	72
3.2.1	Overview	72
3.2.2	The building thermal and CFD simulation	72
3.2.2.1	Geometry modeling and finite volume grid generation	72
3.2.2.2	Simulation input data	73
3.2.2.3	Selected turbulence model	74
3.2.2.4	Selected discretization scheme	74
3.2.2.5	Number of iterations and termination residual	74
3.2.2.6	CFD simulation outcomes	74
3.2.2.7	Calibration of the initial CFD model	75
3.2.3	Computational models	77
3.2.3.1	Laboratory model	77
3.2.3.2	Field office model	83
3.3	Results and discussion	90
3.3.1	Laboratory	90

3.3.2	Field office.	97
3.3.3	Concluding observations.	106
4	An Examination of the Reliability of Common Thermal Comfort Indicators.	109
4.1	Background.	109
4.2	Method	113
4.2.1	Overview.	113
4.2.2	Laboratory experiment	113
4.2.3	Field experiment	114
4.2.4	PMV versus TSV	114
4.3	Results and discussions	114
4.3.1	Laboratory experiment	114
4.3.2	Field experiment	116
4.3.3	Concluding observations.	119
5	Parametric Assessment of Airflow Conditions Based on a Limited Set of CFD-based Simulation Runs	120
5.1	Background.	120
5.2	Method	121
5.2.1	Overview.	121
5.2.2	CFD modelling scenarios	121
5.2.2.1	First scenario	121
5.2.2.2	Second scenario	122
5.2.3	Investigation approach	123
5.3	Results and discussion	124
5.3.1	First scenario	124
5.3.2	Second scenario	127
5.3.3	Concluding observations.	127
6	Conclusions	130
6.1	Contribution	130
6.2	Future research	132
	References.	133
	Curriculum vitae.	141

List of Tables

2.1	ASHRAE 7-point sensation scale	28
2.2	5-point air movement acceptability scale	29
2.3	Survey questions pertained to thermal sensation, comfort and perception of humidity	33
2.4	Survey questions pertained to air speed and air quality acceptability . .	33
2.5	Monitored data	41
3.1	Number of examples regarding the common functionalities of BES and CFD programs in building performance evaluations (Zhai and Chen 2005)	69
3.2	Required input data for CFD simulations and the source providing them	73
3.3	Monitored parameters for CFD model evaluations together with sensor information	76
3.4	Surface temperature sensor information	78
3.5	Properties of the enclosure elements	85
3.6	Properties of the window components	86
3.7	Assumptions regarding the internal gains and air change rate	87
3.8	Boundary conditions of the initial model, defined based on the measure- ments in laboratory test room	90
3.9	Calibration variables in initial model and performed calibration steps . .	93
3.10	Boundary conditions pertain to supply diffusers (<i>SD1</i> to <i>SD7</i>) and extract grilles (<i>EG1</i> to <i>EG7</i>), defined based on measurements in the office space	98
3.11	Boundary conditions pertain to surface temperatures, imported from the thermal simulation outcomes	98
4.1	Main parameters for PMV calculations and their acceptable ranges . . .	113
4.2	Input data required for PMV calculations and respective calculated PMV values for the experiments in lab cell 1 with ducted PV	115
4.3	Input data required for PMV calculations and respective calculated PMV values for the experiments in lab cell 2 with ductless PV	115
4.4	Input data required for PMV calculations together with respective calcu- lated PMV values under the ventilation regime DV	117

List of tables

4.5	Input data required for PMV calculations together with respective calculated PMV values under the ventilation regime DPV	117
5.1	Simulation variants in the first scenario	122
5.2	Simulation variants in the second scenario	123
5.3	R^2 results for comparison of CFD-based and simplified calculations (Equation 5.1) of airflow speed for the four cases of the first scenario . .	127

List of Figures

1.1	Flow pattern in (a) a real experiment versus (b) a computer simulation (source: Rakesh et al. 2014)	21
1.2	Sketch of (a) MV and (b) DV in an office space (source: Aswegan and Pich 2014)	22
1.3	Difference between individuals' perceptions of the air temperature	23
1.4	Example of a PV air terminal device (source: EXHAUSTO 2016)	24
2.1	Schematic illustration of the experimental laboratory cells	30
2.2	PV devices installed in the lab cells, (a) lab cell 1 with ducted PV, and (b) lab cell 2 with ductless PV	31
2.3	External view of the experimental laboratory cells	31
2.4	Survey questionnaire, page 1	34
2.5	Survey questionnaire, page 2	35
2.6	Comfort measurement setup (source: Rogers 2015)	36
2.7	Internal view of the office space	37
2.8	Schematic illustration of the office space with marked location of the monitored workstations (<i>WS1</i> to <i>WS11</i>) as well as the supply diffusers (<i>SD1</i> to <i>SD7</i>) and extract grilles (<i>EG1</i> to <i>EG6</i>)	38
2.9	(a) Ductless PV air intake and (b) PV supply diffuser	38
2.10	(a) Air quality sensor, (b) PIR occupancy sensor, and (c) window contact sensor (Thermokon 2015)	40
2.11	Participants' thermal sensation vote (TSV) versus thermal comfort vote (TCV)	42
2.12	Supply air temperature of DV, ducted/ductless PV, and the room air temperature, averaged over the aforementioned 13 experimental sessions	43
2.13	Participants' perception of humidity (RHV) versus (a) absolute humidity ($g.m^{-3}$) and (b) relative humidity (%)	44
2.14	Participants' air movement sensation (AMS) versus (a) air movement comfort (AMC) and (b) measured air velocity at the workstation ($m.s^{-1}$)	44
2.15	Box plot of air velocity at workstations with ducted and ductless PV	45

2.16	Perception of air quality (AQ) versus measured CO ₂ concentration (ppm) near participants	46
2.17	Box plot of CO ₂ concentration in PV supply air, room air, and exhaust air in the rooms with ducted and ductless PV	46
2.18	Responses to the survey questions (mean votes of all participants over two periods of nine working days each) under the two distinct ventilation regimes (DPNV, NV)	47
2.19	Survey results (one-day winter experiment with visiting participants) at workstations with (a) ducted and (b) ductless PVs	49
2.20	Survey results (one-day summer experiment with visiting participants) at workstations with (a) ducted and (b) ductless PVs	50
2.21	PV actuator adjustment frequency (mean number of daily actions) in different months	52
2.22	Comparison between the PV actuator adjustment frequency (actions per day averaged over the entire observation period) for ducted (WS2 to WS5) and ductless units (WS1, and WS6 to WS11) (see also Figure 2.8)	52
2.23	Frequency distribution of indoor air temperature for two periods in the observation period	54
2.24	Frequency distribution of CO ₂ concentration for two periods in the observation period	54
2.25	Indoor/outdoor air temperature in the 9-day of (a) DPNV and (b) NV regime	55
2.26	Indoor CO ₂ concentrations in the 9-day of (a) DPNV and (b) NV regime	56
3.1	CFD workflow in DesignBuilder (source: Designbuilder 2011c)	60
3.2	Illustration of a supply diffuser model and a possible supply air X and Y discharge angle in DesignBuilder (source: DesignBuilder 2011b)	75
3.3	(a) Data logger, (b) thermoelectric flow sensor, and (c) temperature sensor (Rogers 2015, B+B Thermo-Technik GmbH 2017)	76
3.4	Surface temperature measurement instrument, type 1 (Testo 2015)	78
3.5	Surface temperature measurement instrument, type 2 (Thermokon 2015)	78
3.6	Positions of velocity measurements in lab cell 2, on (a) the plan and (b) a vertical section (Section B-B)	80
3.7	Positions of temperature measurements in lab cell 2, on (a) the plan and (b) a vertical section (Section B-B)	80
3.8	(a) Plan of the lab cell 2 together with a vertical section (Section D-D) presenting the supply diffuser in (b) initial and (c) calibrated models	82
3.9	Plan of the office space together with marked locations of the supply diffusers, extract grilles, monitored workstations, as well as the vertical sections under study	83
3.10	Simulation model of the office space in DesignBuilder	84

3.11	Positions of velocity measurements in the office space (section A-A, Figure 3.9)	89
3.12	Positions of temperature measurements in the office space (section A-A, Figure 3.9)	89
3.13	Measured and initially simulated velocity at positions v_1 to v_{12} in the laboratory test room (see Figure 3.6)	91
3.14	Measured and initially simulated temperature at positions θ_1 to θ_{30} in the laboratory test room (see Figure 3.7)	92
3.15	Measured versus simulated airflow speed in initial and calibrated model	94
3.16	Measured versus simulated temperature in initial and calibrated model .	94
3.17	Cumulative distributions of velocity relative errors	95
3.18	Absolute velocity error distributions	96
3.19	Cumulative distributions of temperature relative errors	96
3.20	Surface boundary conditions, flow balance specifications in DesignBuilder	97
3.21	Importing surface boundary conditions from thermal simulation outcomes to the CFD simulation model in DesignBuilder	99
3.22	Measured values of airflow speed for specific positions in the office space (see Figure 3.11) together with corresponding CFD simulation results (both before and after calibration)	100
3.23	Measured values of air temperature for specific positions in the office space (see Figure 3.9 and Figure 3.12) together with corresponding CFD simulation results (both before and after calibration)	100
3.24	Air temperature in (a) winter and (b) summer conditions (section B-B, Figure 3.9)	102
3.25	Velocity distribution in (a) winter and (b) summer conditions (section B-B, Figure 3.9)	103
3.26	Air temperature and velocity distribution, summer conditions (section C-C, Figure 3.9)	104
3.27	Illustration of the (a) actual and (b) alternative supply diffuser design (section D-D, Figure 3.9)	105
3.28	(a) Air temperature and (b) velocity in summer conditions (with original supply flow rate and temperature), (section B-B, Figure 3.9)	107
3.29	(a) Air temperature and (b) velocity in summer conditions (with modified supply flow rate and temperature), (section B-B, Figure 3.9)	108
4.1	Six factors involved in PMV calculation	111
4.2	The calculated PMV and actual TSV of the participants of the laboratory experiment	116
4.3	The calculated PMV and actual TSV of a small group of visiting participants under the ventilation regime DV	118

4.4	The calculated PMV and actual TSV of a small group of visiting participants under the ventilation regime DPV	118
5.1	Illustration of the model geometry and location of the diffuser and extract grille in three layouts <i>A</i> , <i>B</i> and <i>C</i> , first scenario	122
5.2	Illustration of the model geometry and location of the diffuser and extract grille in three layouts <i>A</i> , <i>B</i> and <i>C</i> , second scenario	123
5.3	Airflow speed at grid nodes in variant 3 and 4 versus the corresponding nodes in variant 1 and 2, respectively	124
5.4	Airflow speed at grid nodes in variant 4 and 5 versus the corresponding nodes in variant 1 and 2, respectively	125
5.5	Cumulative distributions of relative errors of respective cases in the first scenario	126
5.6	Percentage of result within various bins of absolute error (for respective cases in the first scenario)	126
5.7	Airflow speed at grid nodes in layouts <i>A</i> , <i>B</i> , and <i>C</i> for respective variants of the second scenario	128
5.8	Cumulative distributions of relative errors for respective variants of the second scenario	129
5.9	Absolute error distributions for respective variants in the second scenario	129

Abbreviations and Nomenclature

Abbreviations

AMC	Air movement comfort
AMS	Air movement sensation
AQ	Air quality
ASHRAE	American society of heating, refrigerating and air-conditioning engineers
BES	Building energy simulation
CFD	Computational fluid dynamics
DPNV	Combined displacement, personal, and natural ventilation system
DPV	Combined displacement and personal ventilation system
DV	Displacement ventilation system
EG	Extract grille
LES	Large-eddy simulation
MV	Mixing ventilation system
NV	Natural ventilation
PIR	Passive infrared
PMV	Predicted mean vote
PV	Personal ventilation system
RANS	Reynolds averaged Navier-Stokes
RHV	Relative humidity vote
SD	Supply diffuser
TCV	Thermal comfort vote
TSV	Thermal sensation vote
WS	Workstation

Nomenclature

β	Thermal expansion coefficient of air [K^{-1}]
ΔT	Air temperature change [K]
Δt	Time interval [s]
δ	Laplacian operator
δ_{ij}	Kronecker delta
$\frac{D}{Dt}$	Substantial derivative
ℓ	Turbulent length scale
ε	Turbulent dissipation rate [$m^2.s^{-3}$]
Γ	Turbulent diffusivity of heat
Γ_ϕ	Diffusion coefficient
λ	Thermal conductivity [$W.m^{-1}.K^{-1}$]
μ	Air viscosity [$Pa.s$]
μ_t	Turbulent or eddy viscosity
∇	Gradient operator
$\nabla.$	Divergence operator
v	Air velocity in direction y [$m.s^{-1}$]
ρ	Air density [$kg.m^{-3}$]
ϕ	Mean dependent variable
A_i	Area of surface i [m^2]
A_{du}	Dubois body surface area [m^2]
C	Concentration of contaminant [$kg.m^{-3}$]
c_p	Air specific heat [$J.kg^{-1}.K^{-1}$]
c_μ	Standard eddy viscosity model constant
C_{res}	Heat exchange by convection in breathing [$W.m^{-2}$]
D	Molecular diffusion coefficient for the contaminant [$m^2.s^{-1}$]
E_c	Heat exchange by evaporation on the skin [$W.m^{-2}$]
E_{res}	Evaporative heat exchange in breathing [$W.m^{-2}$]
F_B	Body force
f_{cl}	Clothing surface area factor
g	Gravitational acceleration [$m.s^{-2}$]
H	Dry heat loss [$W.m^{-2}$]

Abbreviations and Nomenclature

h_c	Convective heat transfer coefficient [$W.m^{-2}.K^{-1}$]
I_{cl}	Clothing insulation [$m^2.K.W^{-1}$]
k	Air conductivity [$W.m^{-1}.K^{-1}$]
k	Turbulence kinetic energy [$m^2.s^{-2}$]
L	Characteristic length [m]
M	Metabolic rate [$W.m^{-2}$]
N	Number of the surfaces
p	Pressure [Pa]
P_a	Water vapour partial pressure [Pa]
Pe	Peclet number
q	Heat source within the control volume [$W.m^{-3}$]
$Q_{heat-extraction}$	Room heat extraction rate [W]
$q_{i,c}$	Convective flux from surface i [$W.m^2$]
q_{ik}	Radiative heat flux from surface i to surface k [$W.m^2$]
q_{ir}	Radiative heat flux from internal heat sources and solar radiation [$W.m^2$]
q_i	Conductive heat flux on surface i [$W.m^2$]
Q_{other}	Heat gain [W]
S	Volumetric contaminant generation rate [$kg.m^{-3}.s^{-1}$]
S_ϕ	Source
T	Temperature [K]
t	Time [s]
T_∞	Reference temperature [K]
t_a	Air temperature [$^{\circ}C$]
t_r	Mean radiant temperature [$^{\circ}C$]
t_{cl}	Clothing surface temperature [$^{\circ}C$]
u	Air velocity in direction x [$m.s^{-1}$]
U_i	Velocity in the direction i
v_{ar}	Relative air velocity [$m.s^{-1}$]
V_{room}	Room volume [m^3]
W	External work [$W.m^{-2}$]
w	Air velocity in direction z [$m.s^{-1}$]
x_i	Displacement in the direction i

Chapter 1

Introduction

1.1 Motivation

Comfortable healthy indoor environment has become a major concern since people spent majority of their time in indoor environment, including homes, offices, public buildings, etc. In the recent years, due to the rising temperature and decreasing air quality in urban areas, ventilation systems became more common, in order to meet the requirements to ensure adequate air quality and acceptable indoor temperature. Room air distribution and ventilation methods directly affect the occupants health and comfort. This highlights the significance of profound study of the ventilation systems functionality considering the occupants perception of the indoor environment and thermal comfort as well as the indoor air quality.

To increase the indoor air quality and thermal comfort different ventilation methods have been investigated and devolved. Experimental and computational thermal and airflow studies can contribute to progress in this area (Wiercinski and Skotnicka-Siepsiak 2008). For instance, to evaluate the perceived indoor environmental conditions by occupants, surveys can be conducted (Kim et al. 2013). In addition, thermal comfort calculations that use measured environmental variables as input can facilitate, the indoor climate and thermal comfort assessment (Bordass and Leaman 2009). Computational Fluid Dynamics (CFD) represents another potentially effective method for indoor environmental studies (Wiercinski and Skotnicka-Siepsiak 2008). There have been many studies on the potential of CFD to assist building performance analysis and indoor air quality assessments (Chen and Zhai 2004, Meroney 2009). In this context, this dissertation presents a systematic and comprehensive methodology for assessment of the indoor air quality and thermal comfort in ventilated spaces, specially in this case by displacement and personal ventilation

systems. The main attention in this dissertation was drawn to particularly investigate different applicable methods of indoor conditions and thermal comfort assessments, specifically in office spaces. The methods used here have been categorized under two main classes of the *i*) empirical, and *ii*) computational methods. Hopefully, using similar strategies for indoor environmental assessments will support decision making process which leads to the comfortable and healthy living/working environment.

1.2 Background

Basically, ventilation can be defined as the replacement of the stale indoor air with outside fresh air (Awbi 2015). Generally, the ventilation systems have been categorized as the natural ventilation, mechanical ventilation, or mix of the two. Considering the mechanical ventilation system, currently the most common practical method is the so called total volume ventilation and air conditioning of the space. The two main applications of this method are the mixing (MV) and displacement ventilation (DV) systems (Melikov et al. 2002). One of the most recent developments in the ventilation systems is personal ventilation (PV), which aims at providing each occupant with clean fresh air directly at their breathing zone as well as personal control on the local environment (Melikov et al. 2007). In this dissertation, the matter in question is study of the indoor conditions in spaces ventilated by combination of the above-mentioned ventilation systems.

1.2.1 Thermal comfort and indoor air quality assessment

Thermal comfort is defined in ASHRAE 2004 as “*condition of mind which expresses satisfaction with the thermal environment*”. In building performance studies, providing comfortable indoor environment for the occupants is one of the main concerns. Perceived comfort levels and their variance can be interpreted in view of the combined effects of the *i*) physical parameters of indoor environment, or environmental factors, including air temperature, mean radiant temperature, relative humidity and air speed, together with the *ii*) human factors, including metabolic rate and clothing insulation (Hensen 1990, Lechner 2001, Lesbirel 2012). Moreover, physiological and psychological differences from one person to the other also affect their perception of comfortable environment. Thereby, the required conditions to provide comfort in a same space is not the same for all of the occupants (ASHRAE 2004).

The studies in this area typically deploy both empirical and computational methods to determine if the indoor environment meets the desired comfort level and evaluate the functionality of the systems (Figure 1.1). Empirical methods provide valuable insights

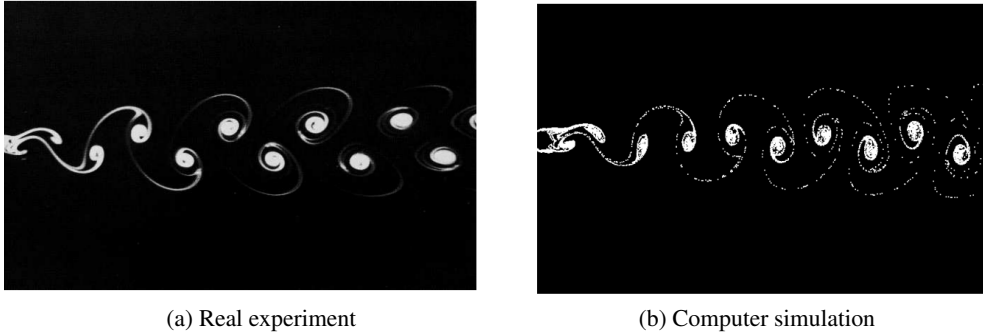


Figure 1.1: Flow pattern in (a) a real experiment versus (b) a computer simulation (source: Rakesh et al. 2014)

and descriptions in the indoor environmental studies, by means of the measurement of environmental parameters and subjective evaluations. Generally, the empirical methods assist the integration of research and practice. These methods are appropriate for investigating certain phenomenon in details and enable researchers to evaluate certain parameters and behaviors under less artificial conditions. However, they have also some restrictions, such as the time and space scale, as well as resources required (the number of available sensors, participants, etc.). On the other hand, the computational methods provide powerful predictions of the fluid flow in indoor environment. Using the computational methods, researchers are able to work with models, which have high resolution of time and space. In fact, computational methods enable virtual modeling of many problems and conditions, for which conducting experiments is not always feasible. However, the errors and limitations involved in mathematical modeling and computational powers are inevitable. Considering the strength and limitations of both methods, neither empirical nor computational methods can replace the other one completely.

1.2.2 Displacement ventilation

Airflow pattern in ventilated spaces depends on the type of the implemented ventilation system. Room mechanical ventilation approaches are commonly categorized as mixing (MV) and displacement (DV) ventilation (Hamilton et al. 2004) (see Figure 1.2). In the more conventional mixing ventilation, the injected fresh air is fully mixed with the stale room air, while displacement ventilation introduces cool air to the zone with low velocity and minimal mixing (Magnier et al. 2012).

The application and principles of DV have been treated in numerous publications (see, for example, Jackman 1991, Hensen and Hamelinck 1995, Emmerich and McDowell

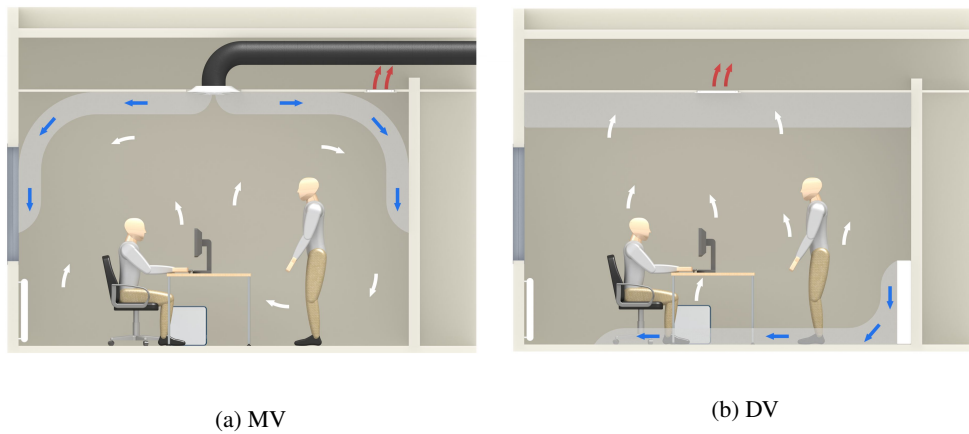


Figure 1.2: Sketch of (a) MV and (b) DV in an office space
(source: Aswegan and Pich 2014)

2005, Lin and Lin 2014). Typically, in DV systems the air suppliers are installed close to the floor level. As low-velocity cool air stream comes into contact with indoor heat sources (e.g., occupants, equipment), it warms up and subsequently exits the space from the air extract grilles near the ceiling (Rees and Haves 2013). A number of issues need to be considered for the proper operation of DV systems. For instance, the minimum height of the ventilated room should be about 2.7 m (EDR 2015). Moreover, in order to facilitate the circulation of the fresh air in the space, cubicle furniture or partitions are not recommended (Titus 2014). In order to avoid the discomfort due to the strong air movement sensation the area near the supply diffuser with the air velocity higher than 0.25 m.s^{-1} is suggested to be not occupied (Loudermilk 1999). If the system is not optimally designed, there is the possibility of local discomfort due to the air draft or vertical temperature differences (Magnier et al. 2012). Laboratory studies simulating office spaces ventilated by DV suggest that the occurrence of discomfort, especially in the winter period, is mostly due to the cold legs and ankles (Wyon and Sandberg 1990, Schiavon et al. 2014).

1.2.3 Personal ventilation

It is not trivial to thermally satisfy multiple occupants who share the same space, such as open plan office spaces (Figure 1.3). This is due to the differences between individuals' perceptions of the air quality, movement and temperature as well as occupants' clothing or activity level (Melikov 2004). Most common ventilation systems currently used

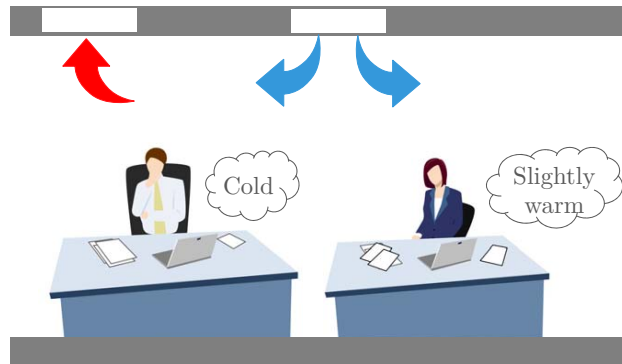


Figure 1.3: Difference between individuals' perceptions of the air temperature

are mixing and displacement ventilation systems. In both cases since the fresh air is delivered to the zone at far distance from the occupants, it can become polluted by the time reaching the occupants' breathing zone (Russo 2011). Personal ventilation system (PV) intends to improve the air quality by delivering clean and cool air with low velocity to occupants' breathing zone (Melikov et al. 2002, Dalewski et al. 2014). Moreover, PV systems (Figure 1.4) are meant to facilitate individual adjustments (Schiavon and Melikov 2009). Previous studies have shown that the cool airflow supplied at occupants' breathing zone by PV system allows increasing the average zone air temperature and consequently this may reduce the total building energy consumption (Schiavon et al. 2010, Chakroun et al. 2011, Dalewski et al. 2012, Veselý and Zeiler 2014). However, the air quality improvement provided by PV highly depends on the PV airflow rate and direction as well as the temperature difference between the PV air jet and the room air temperature (Faulkner et al. 1999, Melikov et al. 2002, Russo 2011, Junjing et al. 2014).

The idea of combining DV and PV systems (DPV) can be implemented by means of either ducted or ductless PVs. In ducted PV system the fresh air is brought directly to the breathing zone, while the PV nozzle is directly connected to the air distribution ducts. In case of ductless PV, the air layer close to the floor is mechanically moved up to the occupants' breathing zone. In fact, the air supplied to the zone by diffusers of the displacement ventilation, creates a stratified flow of cool and clean air close to the floor. For a more efficient use of the fresh air layer, PV transports it to the breathing zone (Halvonova and Melikov 2010c).

Numerous experimental investigations on indoor environmental comfort in spaces ventilated by either ducted or ductless PVs combined with displacement or mixing ventilation have been carried out. The results of literature review on this subject suggest that this concept have been tested mainly assisted by thermal manikins (Cermak et al. 2006, Niu



Figure 1.4: Example of a PV air terminal device
(source: EXHAUSTO 2016)

et al. 2007, Conceição et al. 2010, Halvonova and Melikov 2010b, Melikov and Kaczmarczyk 2012, Dalewski et al. 2014). Studies with participation of human subjects have been developed under fully controlled laboratory conditions or special environmental conditions, such as hot and humid climate. To provide some examples, Kaczmarczyk et al. 2004 studied the response of 60 human participants among university students to a PV system compared to MV system. Sekhar et al. 2005 investigated the impact of PV use on thermal comfort and indoor air quality assisted by subjective evaluations under 17 different controlled environmental conditions. Kaczmarczyk et al. 2010 evaluated the influence of PV system operation on perception of 32 students, in a climate chamber under different air temperature and relative humidity. Li et al. 2010 investigated the response of 30 human subjects to PV system combined with under-floor air distribution system in a field environmental chamber in hot and humid climate. Yang et al. 2010 presented the results of thermal environment, air quality and air movement assessments based on the response of 32 subjects in a field environmental climate chamber with ceiling mounted PV system. Melikov and Kaczmarczyk 2012 evaluated the perception of indoor air quality and air movement in two climate chambers at different combinations of room air temperature, relative humidity and pollution level, with and without facially applied airflow.

1.3 Research questions corresponding to dissertation goal

The intention behind the research design in this dissertation was to address a number of pertinent questions, which can be categorized in five groups:

- **Research question 1**
How do users evaluate different ventilation options, i.e. various combinations of natural ventilation (NV), displacement ventilation (DV), and personal ventilation (PV), with regard to thermal comfort and air quality?
- **Research question 2**
What is the interaction level of the occupants with PV devices? What is the frequency of PV actuator (valve) adjustments by users? Does PV type (ducted versus ductless) affect the PV valve manipulation frequency? Is there a relationship between PV usage frequency and indoor conditions (e.g., indoor air temperature, CO₂ concentration)?
- **Research question 3**
What are the requirements to perform virtual (numerical) experiments, specifically CFD simulations, for assessment of the indoor environment? To which extent can monitoring-based calibration improve the reliability of CFD models to support indoor environmental studies?
- **Research question 4**
Does predicted mean vote (PMV) represent a viable criteria for the evaluation of DV and PV systems?
- **Research question 5**
How can a relatively comprehensive impact assessment of various design variables and input assumptions (e.g., number and location of diffusers, air change rates) be based on a detailed but small number of numeric simulations?

1.4 Structure of work

To address the above mentioned research questions and outlines, this dissertation is divided into six chapters:

- Chapter 1 presents the motivation of the research, gives a summary of existing studies and current achievements relating to the topic of the dissertation and describes the problem along with the research questions.

- Chapter 2 intends to address the research questions 1 and 2. It begins with a summarized background information and goes on with detailed methodology and results of the empirical research conducted in this dissertation. The research presented in this chapter benefits from both laboratory and field experiments. The monitored data and user surveys provide the basis to document the indoor conditions and their implications for the occupants. By this way, the functionality of the ventilation systems in the case studies are evaluated with regard to indoor air quality and thermal comfort.
- Chapter 3 is enriched with computational investigations. The intention behind the research design here was to address the research question 3 and benefit from CFD-based airflow simulations to support a better understanding of the complex nature of airflow phenomena in the space. A brief description of computational fluid dynamics as a potentially effective method for indoor environmental studies is presented. This is followed by describing the methodology to develop, validate and calibrate CFD models in this research. Calibrated CFD models assist reliable estimation of the airflow velocity and temperature fields, as well as systematic investigation of design alternatives and their implications for indoor environmental variables. This chapter proceeds with detailed results of the methodology together with discussions.
- The dissertation continues with Chapter 4 to address the research question 4. Calculated predicted mean votes, PMVs, and actual thermal sensation votes, TSVs, represent common and widely used thermal comfort indicators. In this chapter, the viability of PMV for the evaluation of DV and PV systems is studied, as compared to the actual TSV.
- Chapter 5 addresses the research question 5 and investigates the possibility to obtain the basic airflow field information for a large variety of design configurations based on a small number of full-fledge CFD simulation runs. The approach presented in this chapter would allow for an efficient deployment of advanced numerical simulation pertaining to the evaluation of airflow patterns in indoor environments.
- This dissertation then closes with final conclusions and future research suggestions in Chapter 6.

Chapter 2

Empirical Indoor Climate Assessment

2.1 Background

2.1.1 Building monitoring

Building automation and control systems have been widely used for variety of purposes including monitor and control of the building indoor environment, system operation and occupants' thermal comfort assessment. Indoor environment measurements assist the building performance studies in different ways, including *i*) determination of the level of agreement between the desired and actual performance of the building, considering both energy use and indoor environmental conditions, *ii*) assessment of the building performance simulation predictions and generating calibrated simulation models.

In case of new buildings, simulations-based performance evaluations are the only plausible option. However, to study the performance of the existing buildings, building monitoring is a valuable option. Thermal comfort and indoor air quality, aside from the human factors, depends on several environmental factors including air temperature, mean radiant temperature, relative humidity, and air speed. Regular monitoring of the environmental conditions provides the basis for the assessment of comfort in indoor environment. Measurements are required in occupied zones in the space, such as workstations, at which the occupants are expected to stay during the time they spend in the building (ASHRAE 2004).

2.1.2 Subjective evaluations

To evaluate the indoor environmental conditions as perceived by the occupants, surveys can be conducted. Surveys have been used commonly as part of the post occupancy evaluations, to evaluate whether the occupied environment is comfortable for majority of the occupants (Kim et al. 2013). Surveys are required to be performed to evaluate every designed ventilation system and system's operation condition. These assessments enable the evaluation of the main aspects relevant to the comfort such as indoor temperature, humidity and air speed (ASHRAE 2004). Thereby, surveys should cover occupant's feedback regarding the above mentioned criteria. In the following, some commonly-used models to evaluate occupants' perception of indoor temperature, humidity and air speed, which has been used in this study, are provided.

People's perception of the warm or coldness is in fact different from the actual sense of the air temperature. Different human beings have different rating for what they perceive based on the temperature in a space, which ranges from cold, to neutral, to hot (Zhang 2003). To evaluate this sensation the 7-point scale presented in Table 2.1, which was developed by ASHRAE, assists the quantification of occupants' thermal sensation (ASHRAE 2004). The ASHRAE thermal sensation scale has been also used as a reference to generate a 7-point humidity sensation scale. For instance, Shaharon and Jalaludin 2012 presented a humidity perception scale, including very dry (-3), dry (-2), slightly dry (-1), just right (0), slightly humid (+1), humid (+2) and very humid (+3) (Shaharon and Jalaludin 2012).

Table 2.1: ASHRAE 7-point sensation scale

Value	Description
+3	Hot
+2	Warm
+1	Slightly warm
0	Neutral
-1	Slightly cool
-2	Cool
-3	Cold

Note that, thermal sensation will not always be necessarily also representative of subjects' comfort level. For instance, different individuals don't have necessarily same perceived comfort in different temperature, which is due to different preferences. Therefore, thermal comfort is required to be studied in addition to the thermal sensation. In this regard, different studies used different scales for thermal comfort evaluations. For instance, Hagino and Hara 1992 presented a 7-point scale, ranging from very comfortable (+3), comfortable (+2), slightly comfortable (+1), to neutral (0), to slightly uncomfortable (-1), uncomfortable (-2), and very uncomfortable (-3). Zhang 2003 used a thermal comfort scale ranging from very uncomfortable to comfortable, without neutral. This scale forces the subjects to select their perceived comfort level from the category of generally either "*comfortable*" or "*uncomfortable*".

Considering the comfort level of occupants, another indicator which can be studied is the perception of air speed in the space. Part of the heat losses from the human body relates to the air movement in their surroundings. Thus, the air velocity affects the thermal comfort perception. Candido et al. 2010 presented the results of a study on effect of air movement on thermal comfort. For the purpose of subjective evaluations the prepared questioners included a question related to the air movement, focusing on the acceptability as well as the sensation of the air speed (Table 2.2).

Table 2.2: 5-point air movement acceptability scale

Value	Description	Acceptability
+2	Too high air velocity	Unacceptable
+1	High air velocity	
0	Enough air velocity	Acceptable
-1	Low air velocity	
-2	Too low air velocity	Unacceptable

2.2 Method

2.2.1 Overview

This section explores laboratory and field experiments concerning indoor conditions in office spaces equipped with DV system, as well as ducted and ductless PV systems. The main objective of the study was to assess the functionality of the ventilation systems, with regard to indoor air quality and thermal comfort, by means of empirical methods. In this section, monitored data and user surveys provide a basis to document the indoor conditions and their implications for the occupants.

2.2.2 Laboratory experiment

Two lab cells (mock-up office spaces) of the Department of Building Physics and Building Ecology, TU Wien, Vienna, Austria, were used for the purpose of this research (see, Figure 2.1). The lab cells are identical in dimensions (width = 3 m, length = 4 m, and height = 2.5 m).

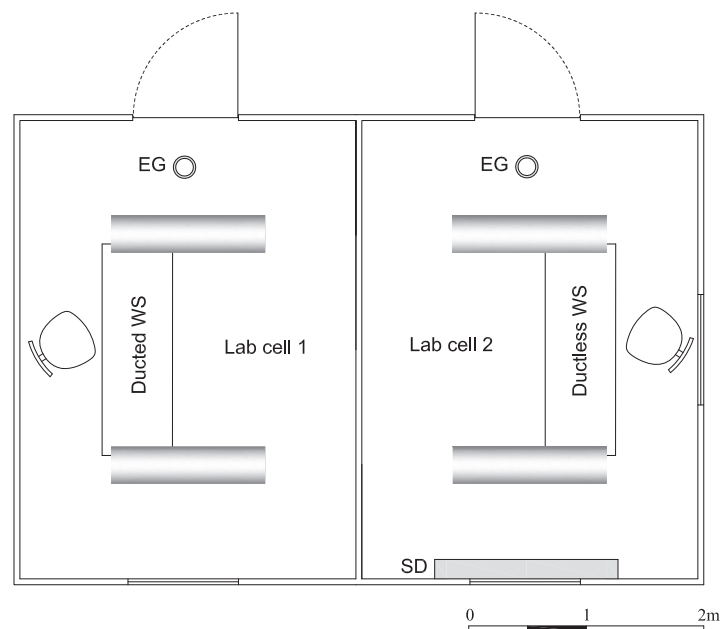


Figure 2.1: Schematic illustration of the experimental laboratory cells

2. Empirical indoor climate assessment

“*Lab cell 1*” is equipped with a ducted PV system, and “*lab cell 2*” with combined DV and ductless PV system (DPV). In this room a linear enclosure displacement supply diffuser (Figure 2.1, SD) is installed on the southern wall of the room at the height of 0.07 m above the floor level (width = 0.165 m, length = 1.56 m, and height = 0.205 m). A circular ceiling extract grille (Figure 2.1, EG) is attached to the ceiling of each lab cell. Figure 2.2 and 2.3 depict the interior and exterior of the laboratory.

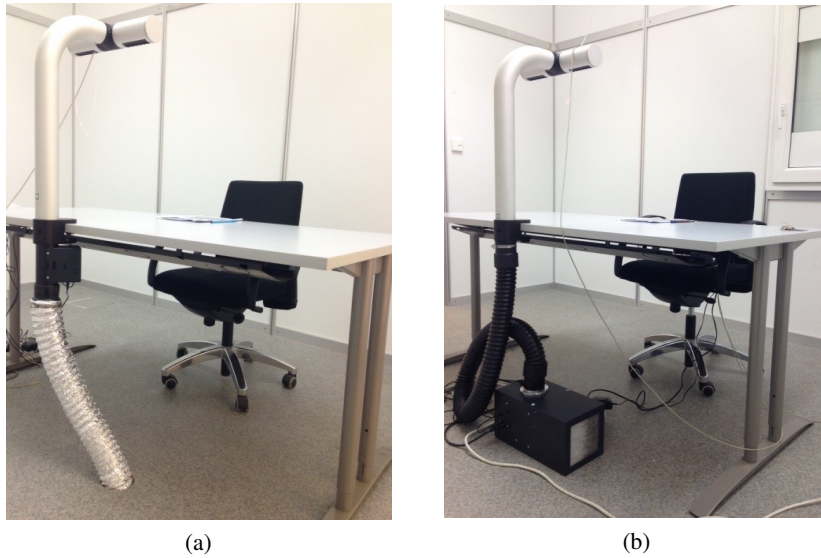


Figure 2.2: PV devices installed in the lab cells, (a) lab cell 1 with ducted PV, and (b) lab cell 2 with ductless PV

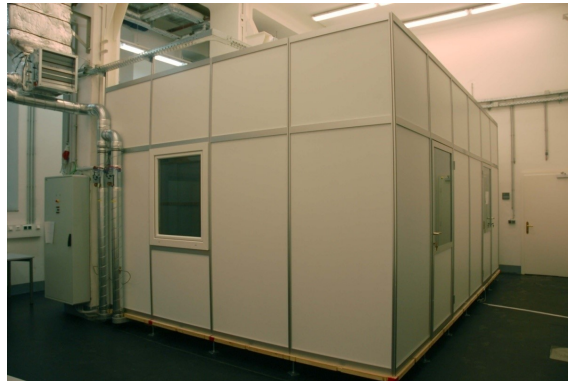


Figure 2.3: External view of the experimental laboratory cells

2.2.2.1 Surveys

Efforts were made to collect data pertaining to the subjective assessment of the ventilation systems and indoor environmental conditions. 26 students (13 male and 13 female, average ages of 23 years old) participated in the laboratory experiment. Each round of experiment involved 2 participants, each sitting in one of the lab cells for one hour. The composition of the groups was random in principle. However, to the extent possible, an equal number of male and female participants were assigned to each lab cell. During each session, participants were requested to work on a task (preparation of energy certificate for a building) unrelated to the experiment's objectives. In intervals of 20, 40, and 60 minutes after the onset of the experiment, participants expressed their thermal perception via a standard questionnaire. Note that post-change adaptation phases of 10 to 20 minutes have been found appropriate in the literatures (see, for example, Arens et al. 2006).

Subjective evaluations pertained to thermal sensation and comfort votes (TSV, TCV), perception of humidity (RHV), air movement sensation and comfort (AMS, AMC), and air quality (AQ). The 7-point ASHRAE scale is used to obtain the TSVs (ASHRAE 2004). In addition, TCVs and RHVs were obtained using a 6-point (Zhang 2003), and a 7-point scale (Shaharon and Jalaludin 2012), respectively. Evaluations of AMS, AMC and AQ (indicators of air speed and air quality acceptability) were captured via 5-point scales with a numeric range from -2 to +2 (Candido et al. 2010). Tables 2.3 and 2.4 demonstrate the corresponding scales applied to generate the survey questionnaires. Moreover, Figures 2.4 and 2.5 present the questionnaires used in this research.

Table 2.3: Survey questions pertained to thermal sensation, comfort and perception of humidity

Scale	TSV	TCV	RHV
+3	Hot	Very comfortable	Very humid
+2	Warm	Comfortable	Humid
+1	Slightly warm	Just comfortable	Somewhat humid
0	Neutral		Neither dry nor humid
-1	Slightly cool	Just uncomfortable	Somewhat dry
-2	Cool	Uncomfortable	Dry
-3	Cold	Very uncomfortable	Very dry

Table 2.4: Survey questions pertained to air speed and air quality acceptability

Scale	AMS	AMC	AQ
+2	Very strong	Very pleasant	Very fresh
+1	Strong	Pleasant	Rather fresh
0	Moderate	All right	Acceptable
-1	Weak	Unpleasant	Rather stale
-2	Barely perceptible	Very unpleasant	Very stale

2. Empirical indoor climate assessment

Date and Time:

Workstation:

Gender:

Age:

Weight:

Height:

■ **How is your current thermal sensation?**

- Cold
- Cool
- Slightly cool
- Neutral
- Slightly warm
- Warm
- Hot

■ **How would you describe the current room temperature?**

- Very uncomfortable
- Uncomfortable
- Slightly uncomfortable
- Slightly comfortable
- Comfortable
- Very comfortable

■ **I think the air is:**

- Very dry
- Dry
- Somewhat dry
- Neither dry nor humid
- Somewhat humid
- Humid
- Very humid

■ **How strong is the current air movement:**

- Very strong
- Strong
- Moderate
- Weak
- Barely perceptible

■ **The current air movement feels:**

- Very unpleasant
- Unpleasant
- All right
- Pleasant
- Very pleasant

■ **How is the current air quality:**

- Very stale
- Rather stale
- Acceptable
- Rather fresh
- Very fresh

Figure 2.4: Survey questionnaire, page 1

■ Describe your current clothing:		Check
Shirts	Turtleneck	<input type="checkbox"/>
	Tube top	<input type="checkbox"/>
	Short sleeves(T-shirt)	<input type="checkbox"/>
	Long sleeves	<input type="checkbox"/>
Trousers	Shorts	<input type="checkbox"/>
	Normal trousers	<input type="checkbox"/>
Skirts, dresses	Short skirt	<input type="checkbox"/>
	Long skirt	<input type="checkbox"/>
	Light dress sleeveless	<input type="checkbox"/>
	Winter dress long sleeves	<input type="checkbox"/>
Sweaters	Sleeveless vest	<input type="checkbox"/>
	Thin sweater	<input type="checkbox"/>
	Thick sweater	<input type="checkbox"/>
Overcoat	Jacket	<input type="checkbox"/>
	Coat	<input type="checkbox"/>
Sundries	Socks	<input type="checkbox"/>
	Thick long socks	<input type="checkbox"/>
	Thin soled shoes	<input type="checkbox"/>
	Thick soled shoes	<input type="checkbox"/>
	Boots	<input type="checkbox"/>

■ Comments / personal comments?

Figure 2.5: Survey questionnaire, page 2

2.2.2.2 Monitoring of physical data

A precise thermal comfort sensor setup (Figure 2.6) captured air temperature, mean radiant temperature, relative humidity, and air velocity near occupants in the laboratory experiment. This measurement setup includes a globe thermometer, humidity/temperature sensor and thermo-anemometer. The ventilation system in the laboratory is connected to an online control, monitoring and safety system in the course of a previous research project. Therefore, the airflow rate (in/out) and airflow temperature data were provided for the period of the experiment. Ducted/ductless PV supply air temperature were also monitored during the experiment. Moreover, CO₂ concentration of PV supply air, room air and the exhaust air were monitored. In addition, the overall laboratory cells' condition were monitored by means of wireless air quality sensors.



Figure 2.6: Comfort measurement setup (source: Rogers 2015)

2.2.3 Field experiment

The field experiment concerns an open plan office space in Grieskirchen, Upper Austria. The studied space (width = 7.5 m, length = 17.3 m, height = 3.1 m) is located in the ground floor of a building, and used as a call center (Figure 2.7). Workstations are organized in this space in terms of five star-shaped hubs, each accommodating up to five workers. The office is equipped with DV as well as PV systems. Figure 2.8 presents a schematic illustration of the office space with marked location of the monitored workstations (WS1 to WS11) as well as the supply diffusers (SD) and extract grilles (EG). The supply air diffusers are installed at the height of 0.38 m from the floor level. Return outlets are positioned 0.11 m below the ceiling. The maximum airflow in the room through the suppliers is about 82 l.s^{-1} . The discharge angle of the air diffusers is downward. Moreover, the supply air is preheated depending on the room temperature to fulfill a constraint of being 2 to 3 K lower than the room air temperature. The space can also be naturally ventilated through the manual operation of windows (NV).

One of the hubs, accommodating workstations 2, 3, 4 and 5 on Figure 2.8, is provided with ducted PV, whereas the others have ductless PVs, as illustrated in Figure 2.9. The air terminal device of the PV system is attached to an arm and the user can change the flow direction in horizontal or vertical plane. The airflow volume out of the PV system unit can be modulated by occupants, using an adjustable valve (from zero to 100%) installed under each desk. The PV system is designed for the maximum supply capacity of 15 l.s^{-1} and the minimum of 0 l.s^{-1} (i.e., completely closed valve) (Melikov et al. 2007). Note that, based on the ventilation system design in the office, the operation of ducted PVs are possible in combination with DV.



Figure 2.7: Internal view of the office space

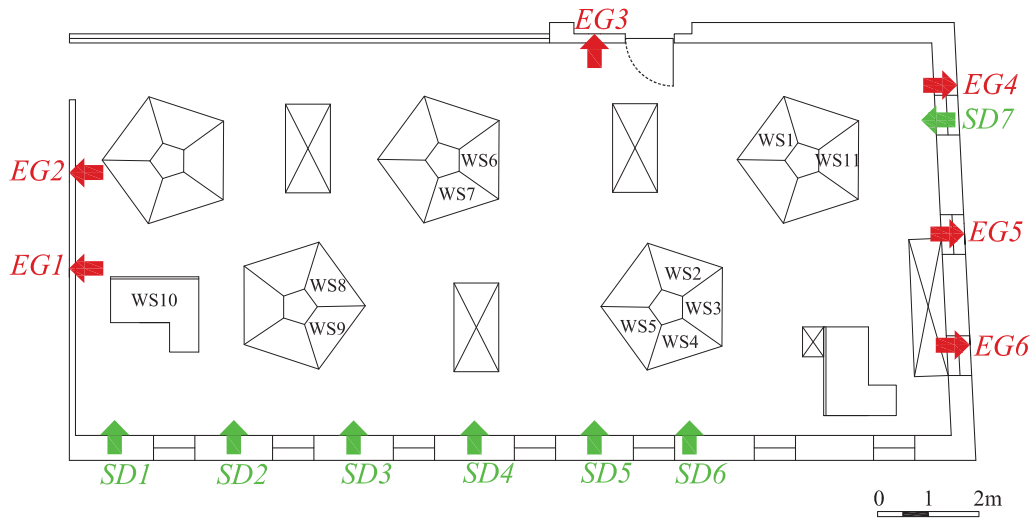


Figure 2.8: Schematic illustration of the office space with marked location of the monitored workstations (WS1 to WS11) as well as the supply diffusers (SD1 to SD7) and extract grilles (EG1 to EG6)



Figure 2.9: (a) Ductless PV air intake and (b) PV supply diffuser

2.2.3.1 Surveys

In case of the field experiment, related data for the subjective assessment of the ventilation systems and indoor environmental conditions was obtained in two different ways:

- The office's regular occupants were requested to participate in a web-based assessment of the indoor environmental conditions under two ventilation configurations, i.e. NV (natural ventilation only) and DPNV (the combined operation of DV and PV, plus natural ventilation). The assessment of each configuration covered a period of 9 working days. The DPNV assessment was conducted in month August. Thereby, DV was continuously activated, whereas PVs and windows could be operated by occupants. The NV assessment was conducted in month October. In this phase, NV was the sole option for office space ventilation. Seven female employees, on average, participated in each survey (online questionnaires were filled once every day, roughly around 10:00 am). Given the voluntary nature of the process (a strict regime could not be imposed upon the employees) questionnaires were not filled at exactly the same time every day.
- Full-day experiments were performed on two occasions (12.01.2013 and 10.08.2013, 09:00 am to 04:00 pm) involving a small group of visiting individuals (students and staff of the Department of Building Physics and Building Ecology, TU Wien, Vienna, Austria). These targeted short-term experiments were necessary, as employee-based surveys' beyond the above-mentioned online surveys' could not be carried out on a continuous basis due to organizational constraints. The visitors were requested to occupy the workplaces, engage in typical office work and twice per day fill in the prepared questionnaires. On each day, two distinct ventilation schemes were compared in view of participants' perception of thermal comfort and air quality. One scheme involved DV alone, whereas the second scheme involved DV plus PV (DPV). The participants (four females and two males, age between 25-35 years similar to regular occupants of the office) were equally divided between workstations with ducted and ductless PVs. Note that, these experiments were conducted under controlled condition with closed windows thus excluding natural ventilation and potential related influences on ventilation regimes under study.

Subjective evaluations pertained to TSV, TCV, RHV, AMS, AMC, and AQ (see also Tables 2.3 and 2.4, as well as Figures 2.4 and 2.5).

2.2.3.2 Monitoring of physical data

A monitoring system was installed in the facility presented in Section 2.2.3 to continuously obtain indoor environmental parameters (air temperature, relative humidity and CO₂ concentration) on a continuous basis. At eleven locations, marked in Figure 2.8 as WS1 to WS11, conditions near occupants were monitored by means of wireless air quality sensors (Figure 2.10a). The eleven workstations include four workstations at the ducted hubs (i.e., WS2 to WS5) and seven workstations at the ductless hubs (i.e., WS1 as well as WS6 to WS11). At the same locations the state of occupancy (presence/absence) was also monitored with wireless PIR (passive infrared) sensors (Figure 2.10b). This type of sensor detects the occupants' motion by measuring the illuminance (*lux*) in the radius of 5 m from the sensor. The windows in this office are single casement with horizontal and vertical-tilt opening system. The window opening (i.e., state of window being open or closed) was detected by means of window-contact sensors (Thermokon 2015) (Figure 2.10c). All these sensors have wireless transmitters. Sending the data points will be either when a change happens in the values or after a maximum pre-set interval.

This research includes PMV-based thermal comfort assessments. For this purpose, short-term spot measurements of the required physical parameters have been conducted by means of the comfort measurement setup (Figure 2.6) at different workstations. These measurements were conducted on two occasions, on 12.01.2013 and 10.08.2013, under the DPV ventilation condition.

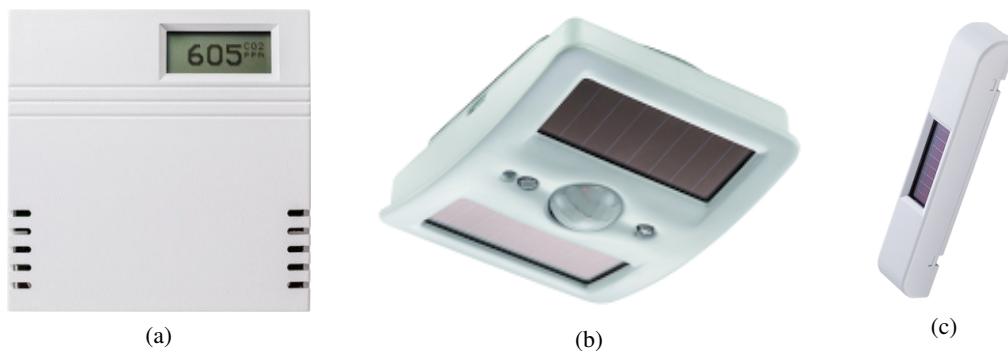


Figure 2.10: (a) Air quality sensor, (b) PIR occupancy sensor, and (c) window contact sensor (Thermokon 2015)

2. Empirical indoor climate assessment

The airflow volume out of the PV system units can be modulated by occupants using a valve (from zero to 100%). Hence, the state of valve was also monitored for the entire period of the study. Table 2.5 summarizes the monitored data points and corresponding sensor information. All the installed sensors were integrated in the online monitoring system of the Department of Building Physics and Building Ecology, TU Wien, and data was automatically stored in real time in a central database. For this purpose, an EnOcean - IP gateway, which is connected via a Virtual Private Network (OpenVPN) to the database server, has been used. The monitoring stretched over a period of eleven months (from July 2012 to May 2013).

Table 2.5: Monitored data

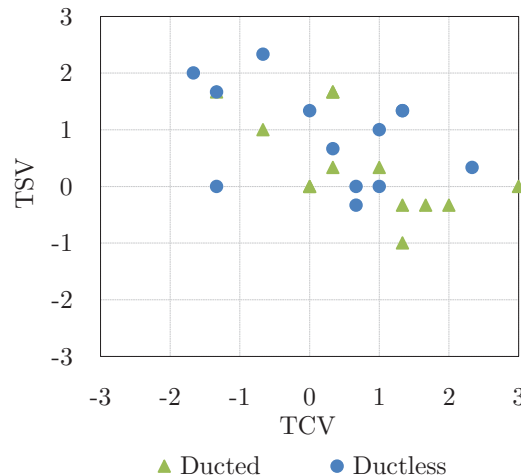
Parameter	Sensor range	Unit	Sensor accuracy
Air temperature	0 to 50	°C	±1%
Relative humidity	0 to 100	%	±2%
CO ₂ concentration	0 to 2000	ppm	±75ppm or±10%
Presence/absence	0 to 512	lux	
State of PV valves	0 to 100	%	
State of doors and windows	0/1	-	

2.3 Results and discussions

2.3.1 Laboratory experiment

The main results of the laboratory experiments are shown in a number of Figures below. Figure 2.11 compares participants' expressed thermal sensation vote (TSV) and the corresponding thermal comfort votes (TCV). Note that, each dot in this Figure (as well as in Figure 2.13, 2.14, and 2.16) represents the mean value of each participant's three votes during each session. As compared to the ductless PV, the room with the ducted PV is judged to be thermally somewhat more comfortable. Moreover, the room with the ductless PV is judged to be somewhat warmer than the one with the ducted PV. This is consistent with the measured temperatures at the breathing zones (see Figure 2.12), which were generally higher in the ductless PV case.

Figure 2.12 shows the average supply air temperature of DV, supply air temperature of ducted and ductless PV as well as the air temperature in rooms. Ducted PV brings air with lower temperature to the occupants breathing zone. In the room with DV and ductless PV, the PV supply air temperature is close to the room air temperature, even though the DV supply is 2 to 3 K below room air temperature. As mentioned previously, this circumstance explains the prevalence of "slightly warm" or "warm" thermal sensation votes in case of the ductless PV. Therefore, ductless PVs may require lower supply temperature. This in turn could translate into comparatively higher energy demand.



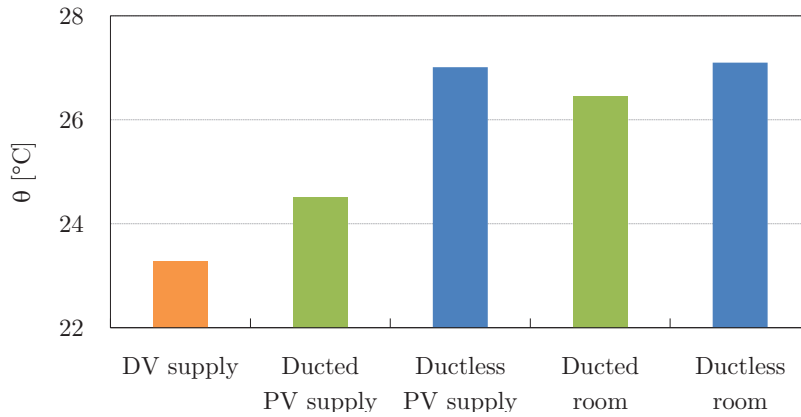


Figure 2.12: Supply air temperature of DV, ducted/ductless PV, and the room air temperature, averaged over the aforementioned 13 experimental sessions

Figure 2.13a and 2.13b contrast subjective assessment of the rooms' humidity level with measured absolute humidity ($g.m^{-3}$) and relative humidity (%), respectively. Both rooms are perceived as rather dry. But, the perceived humidity does not display a clear relationship to the measurement results.

Figure 2.14a compares participants' air movement sensation (AMS) and the corresponding air movement comfort (AMC) votes. With ducted PV, the air movement sensation is generally higher compared to the ductless one. However, this does not translate into a more pronounced perception of discomfort. Figure 2.14b shows a comparison between participants' air movement sensation (AMS) and corresponding measured air velocity ($m.s^{-1}$) values at ducted and ductless workstations. Interestingly, perceived velocity at the ducted PV workstation is higher than the ductless PV workstation, even though the measured velocities were higher at the latter. This may be due to the lower temperature as well as the more pronounced directionality of the flow pattern of the ducted PV. The latter conjecture is consistent with the results shown in Figure 2.15, which includes box plots of the measured airflow velocity at the workstations with ducted and ductless PVs. As this Figure shows, both the median and the spread of measured velocities are higher for the ductless workstation.

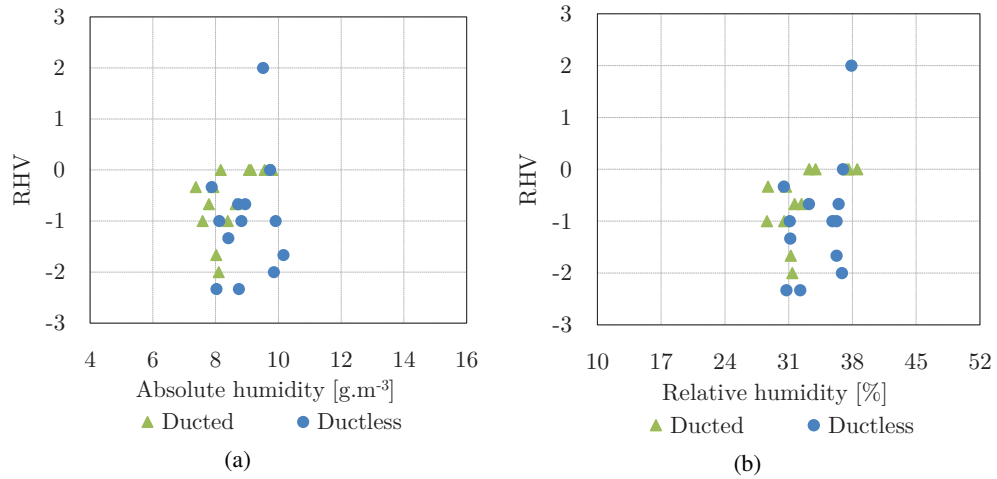


Figure 2.13: Participants' perception of humidity (RHV) versus (a) absolute humidity ($g.m^{-3}$) and (b) relative humidity (%)

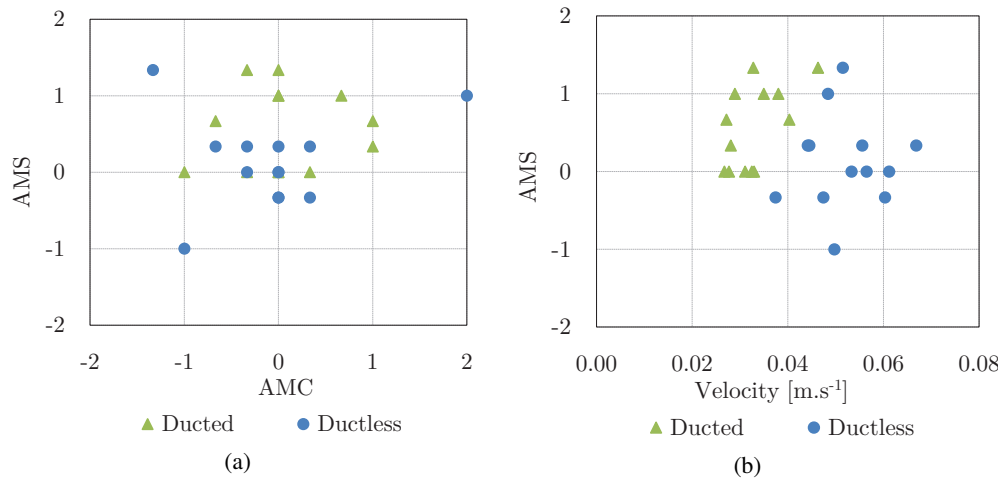


Figure 2.14: Participants' air movement sensation (AMS) versus (a) air movement comfort (AMC) and (b) measured air velocity at the workstation ($m.s^{-1}$)

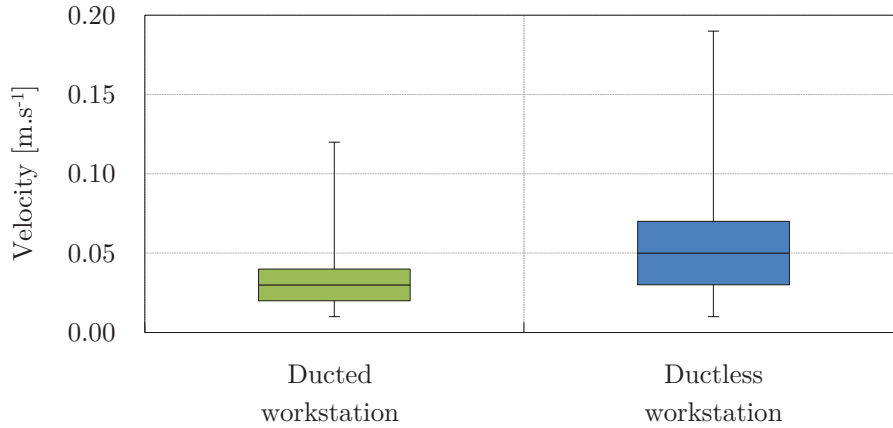


Figure 2.15: Box plot of air velocity at workstations with ducted and ductless PV

Figure 2.16 shows participants' air quality (AQ) votes and the corresponding measured CO₂ concentration at workstations. Ducted PVs achieve significantly lower CO₂ concentration levels at the breathing zones. However, there does not appear to be a significant difference in participants' subjective assessment of the air freshness in the two rooms.

Figure 2.17 compares the CO₂ concentration in PV supply air, room air, and exhaust air for both rooms. As expected, the CO₂ concentration was considerably lower in the ducted PV's supply air. However, even the ductless PV can improve the air quality at occupants breathing zone, as evidenced by a CO₂ concentration almost 200 ppm below the room air. The overall room air quality and the CO₂ concentration in the exhausted air are somewhat similar in both rooms.

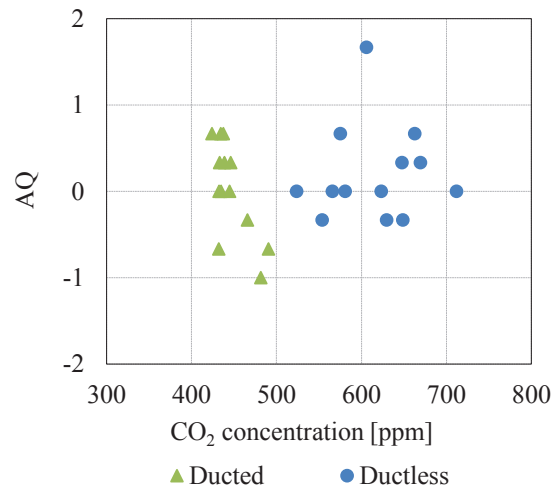


Figure 2.16: Perception of air quality (AQ) versus measured CO₂ concentration (ppm) near participants

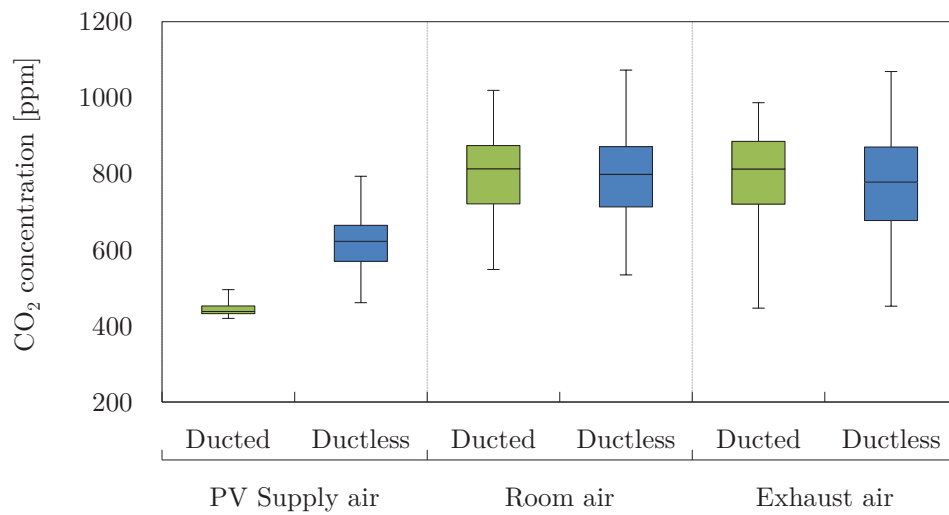


Figure 2.17: Box plot of CO₂ concentration in PV supply air, room air, and exhaust air in the rooms with ducted and ductless PV

2.3.2 Field experiment

Figure 2.18 shows the results of the aforementioned online questionnaire including the mean values of the employees' responses over the course of two periods of each nine working days. Data is plotted separately for the two relevant ventilation regimes, i.e. DPNV (first period, August) and only NV (second period, October). Note that, the very small number of participants (seven employees, on average) and the rather short overall duration of the study pose limits on the general validity of the following discussion of its results. Participants judge the room to be cooler in case of DPNV. This "slightly cool" vote is accompanied with a "just uncomfortable" evaluation. The measurement results suggest that the average indoor temperature was in DPNV case indeed slightly lower (Figure 2.25). In NV case, both thermal sensation and thermal comfort are perceived as neutral. Both ventilation regimes lead to similar evaluations of air movement and air quality (neutral range). However, the air movement sensation under DPNV was stronger than under NV. The survey outcome thus suggests that while both ventilation configurations provide generally acceptable indoor environment, the NV regime received a slightly better evaluation. A better modulation of the supply flow rate and temperature is likely to improve the thermal sensation and comfort vote in DPNV.

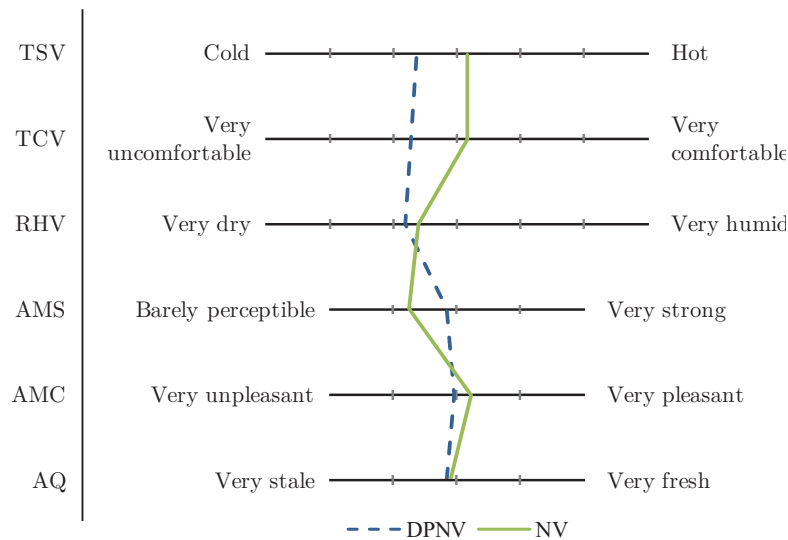
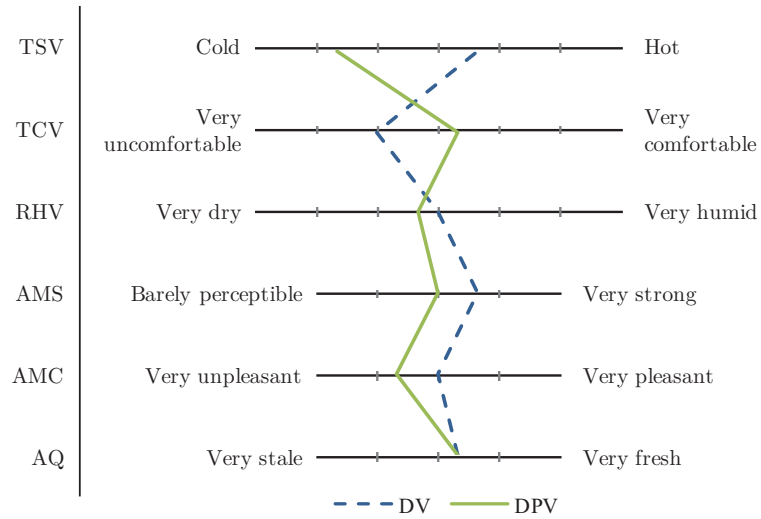


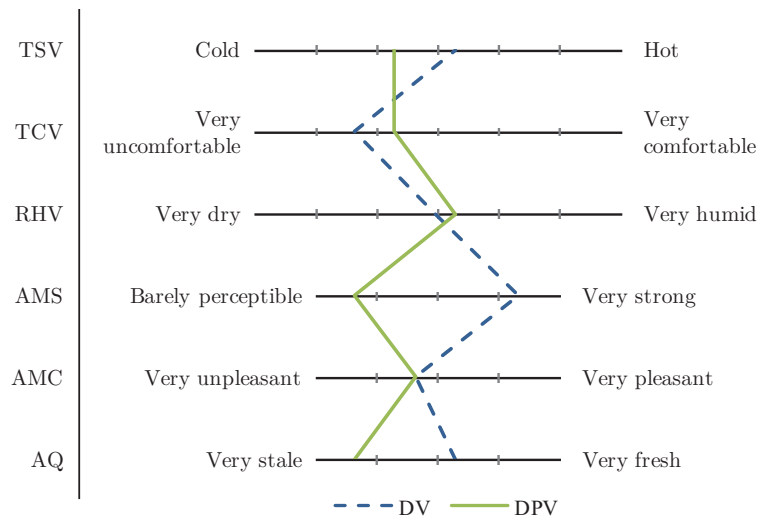
Figure 2.18: Responses to the survey questions (mean votes of all participants over two periods of nine working days each) under the two distinct ventilation regimes (DPNV, NV)

Figure 2.19 and 2.20 illustrate the results (mean votes of visiting participants with regard to the survey questions) of the two one-day experiments. The responses are separately grouped based on the PV type (ducted versus ductless) and ventilation operation options DV (displacement ventilation only) and DPV (both displacement and personal ventilation). Participants occupying workstations with operating PV appear to judge the room to be cooler than those without operating PV (i.e., only DV). This effect is more pronounced for ducted PVs. Measurements of the air entering the breathing zone in this case has a temperature of about 3 K below ambient air temperature (i.e., around 20°C in Winter and 22°C in Summer). Even in case of ductless PVs, the ducted air supply can be assumed to be cooler than the ambient temperature, given the proximity of the workstations to the DV system's outlets. Therefore, it can be argued that changing the PVs' supply air temperature would shift the users' evaluation accordingly. The results presented here are also in the line with previous researches suggesting that PV can provide more cooling by directly delivering cooler air to the occupied zone (Halvonova and Melikov 2010a,b,c).

Regarding the perception of airflow, DV operation alone appears to create a stronger sensation, especially in the case of workstations with ductless PVs (see AMS votes in Figure 2.19b and 2.20b). According to the literature, one problem of the DV systems can be the sensation of the draught (cold air movement) felt at the feet level. It has been proposed that the combination of ductless PV and DV would reduce this risk (Melikov 2004, Halvonova and Melikov 2010c). The higher perceived thermal comfort (both winter and summer) at workstations with PVs (ducted and ductless) could be also related in part to this observation. With regard to the perception of the air quality, ducted PVs appear to at least slightly improve the impression of freshness of the ambient air, whereas ductless PVs appear to have a negative effect. Anecdotal evidence (remarks by regular occupants of the office) points in this case to potentially relevant psychological issues, given that in case of the ductless PVs, supply air is extracted from the "feet and shoes level". Note that, the results presented here are not meant to establish statistical credence, given the rather small number of participants.

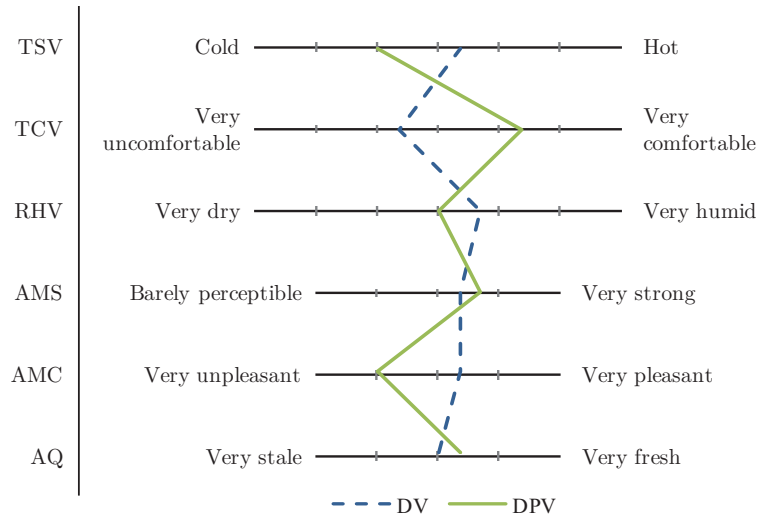


(a) Workstations with ducted PV

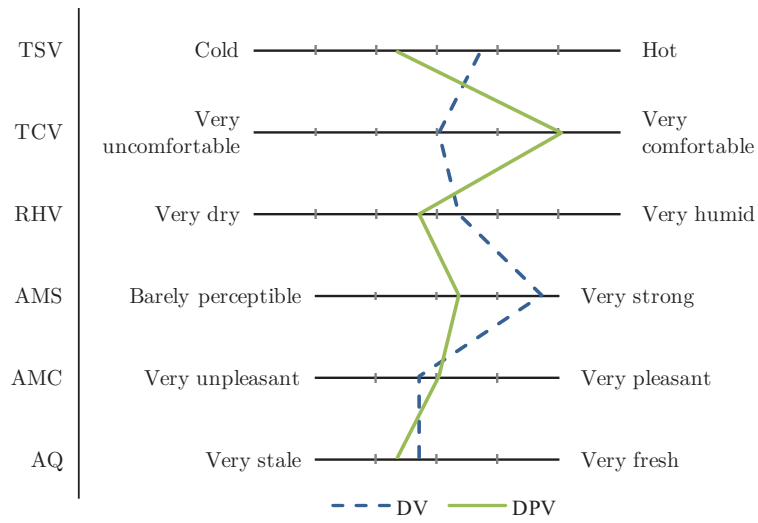


(b) Workstations with ductless PV

Figure 2.19: Survey results (one-day winter experiment with visiting participants) at workstations with (a) ducted and (b) ductless PVs



(a) Workstations with ducted PV



(b) Workstations with ductless PV

Figure 2.20: Survey results (one-day summer experiment with visiting participants) at workstations with (a) ducted and (b) ductless PVs

As noted before, the office workers have the possibility to control airflow volume from the PV diffusers using a valve. The operation of PV is always combined with activated DV. Figure 2.21 summarizes the related results in terms of mean daily number of valve adjustments (total for all workstations) for each month in the observation period. This Figure includes in addition the subset of daily adjustment number that could be characterized as intermediate actions (i.e., actions occurring at least 20 minutes after occupying the workstation or 20 minutes before leaving the workstation). Note that, the data in this Figure is already normalized with regard to working hours. These results suggest that 70% of the adjustments can be categorized as intermediate actions. Note that, adjustments entail "in equal numbers" both actions toward increasing and decreasing the PV volume flow.

To explore the PV valve manipulation frequency in the context of the PV type (ducted versus ductless), Figure 2.22 compares the PV actuator adjustment frequency (actions per day averaged over the entire observation period) for ducted and ductless units. These results suggest that ductless PV units are rarely operated. Ducted workstations show a mean valve manipulation frequency of 2.5 actions per day. For ductless units, the mean value drops to 0.29 actions per day. Five out of seven ductless workstations display zero action frequency. The latter result may also help explain the higher frequency of PV usage in the months of August and September (Figure 2.22). In these warmer months, the capacity of ducted PV stations to supply cooler and fresh air could render them more attractive to the occupants.

Monitoring results pertaining to indoor conditions can support the analysis of ventilation options. For instance, Figure 2.23 and 2.24 shows the frequency distribution of indoor air temperature and CO₂ concentration levels (measured at workstations) averaged over all workstations. The results in this figure are separated for two time periods namely July to December and January to May (PV use frequency was higher in first period).

For a further evaluation of the indoor air temperature and quality, the results were compared to the ASHRAE standards. The metabolic rate of occupants (office work, seated) was considered to be 1.2 *Met* (ASHRAE 2005). The thermal resistance of the occupants' clothing was assumed to be 0.5 and 1.0 *clo* in summer and winter, respectively. According to the measurements, the average relative humidity in the office was about 50% during the period of July to December and 30% in January to May. Given these assumptions and the measurements (see Figure 2.23 and 2.24), the actual conditions in the office can be compared with applicable standards (ASHRAE 2004). The comparison suggests that the thermal conditions were in the period of July to December 80% of the occupied time and in the period of January to May 75% of the time in the acceptable range. Moreover, the results appear to suggest the air quality (as represented via CO₂ concentration monitoring) was somewhat better in the July to December period, when the PV systems were more frequently operated. In this period for around 95%

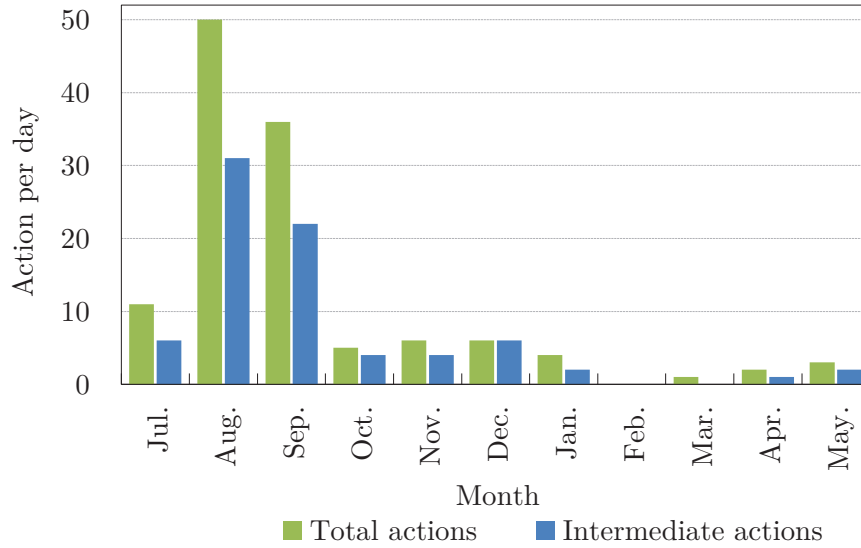


Figure 2.21: PV actuator adjustment frequency (mean number of daily actions) in different months

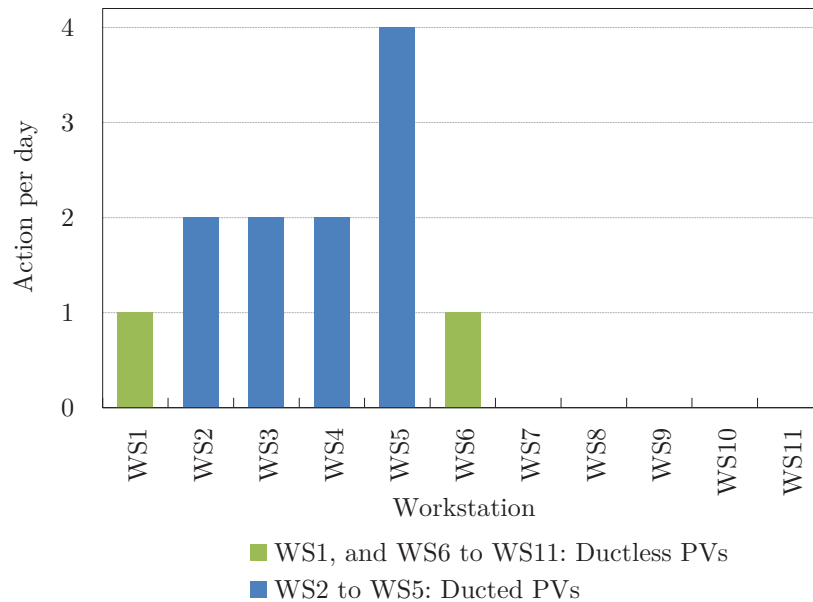


Figure 2.22: Comparison between the PV actuator adjustment frequency (actions per day averaged over the entire observation period) for ducted (WS2 to WS5) and ductless units (WS1, and WS6 to WS11) (see also Figure 2.8)

of the occupied time the CO₂ concentration was below the threshold of 1000 ppm suggested by the ASHRAE standard 62.1 for office buildings (ASHRAE 2007). For the period of January to May this percentage dropped to 55%. The presented results are in agreement with those in literatures. In fact PV systems by directing the supply air to the breathing zone and lower the mixing rate, even compare to DV system, reduces the local concentration (Xu 2007, Halvonova and Melikov 2010a).

Figure 2.25 and 2.26 illustrate indoor (and outdoor) air temperature and indoor CO₂ concentration (averaged over all workstations) during two distinct 9-day periods. The corresponding ventilation regimes for these periods were DPNV (the combined operation of DV and PV, plus Natural Ventilation) and NV (Natural Ventilation only). Based on the monitored data, during the period with DPNV ventilation configuration one window was open 18% of the occupied time. During the NV period two windows were open 18% of the occupied time with at least one open window 25% of the time. The indoor temperature in both cases is roughly in the same range. However, with natural ventilation, the trends appear to be more fluctuating. The results also present slightly higher (and more strongly fluctuating) CO₂ concentrations under the NV regime. Therefore, it can be concluded that the combined regime (DPNV) provides a more uniform indoor environment.

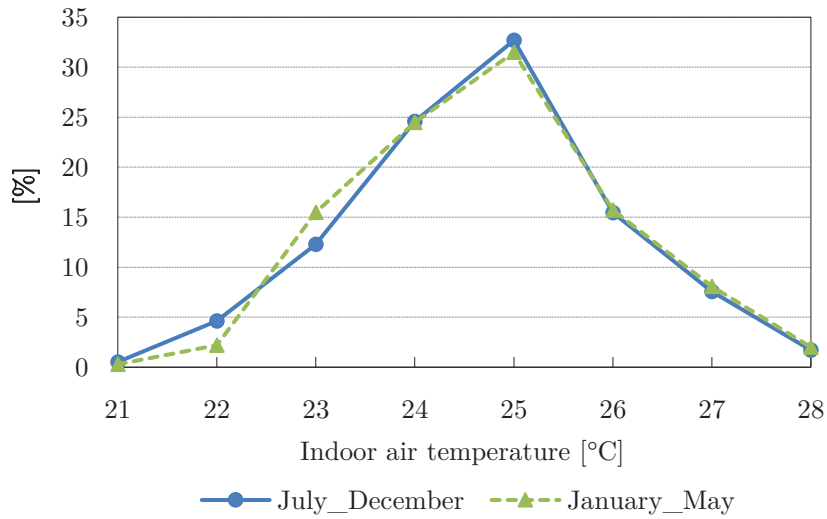


Figure 2.23: Frequency distribution of indoor air temperature for two periods in the observation period

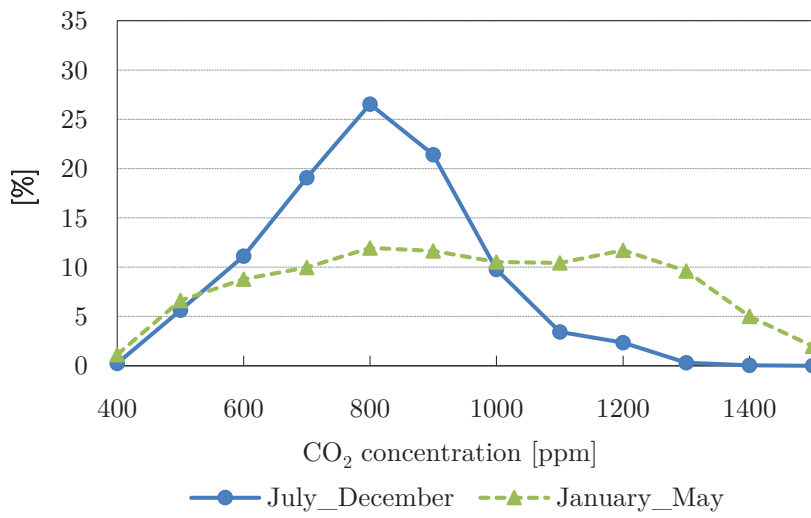
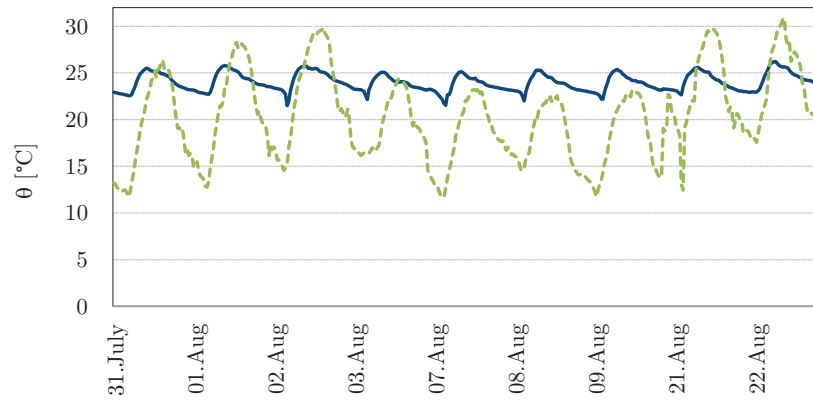
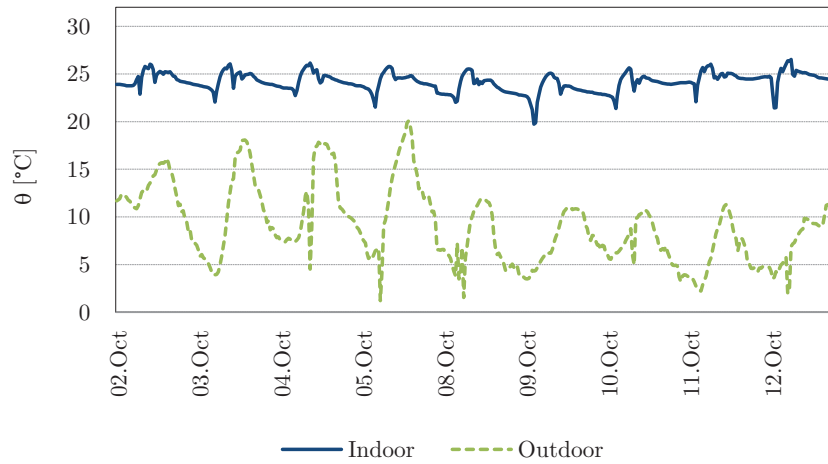


Figure 2.24: Frequency distribution of CO₂ concentration for two periods in the observation period

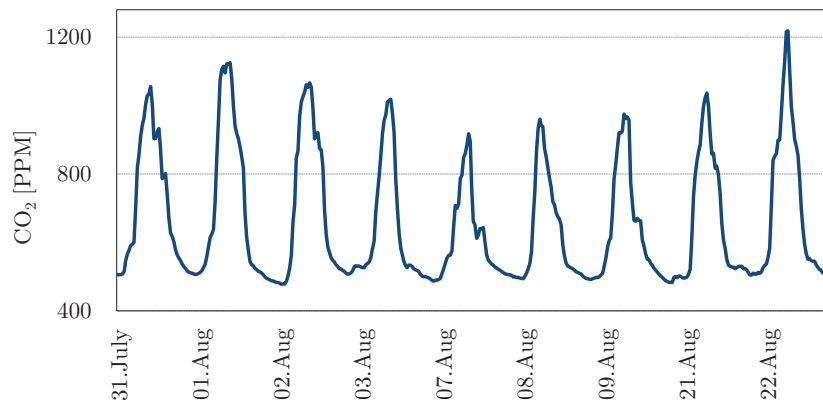


(a) DPNV

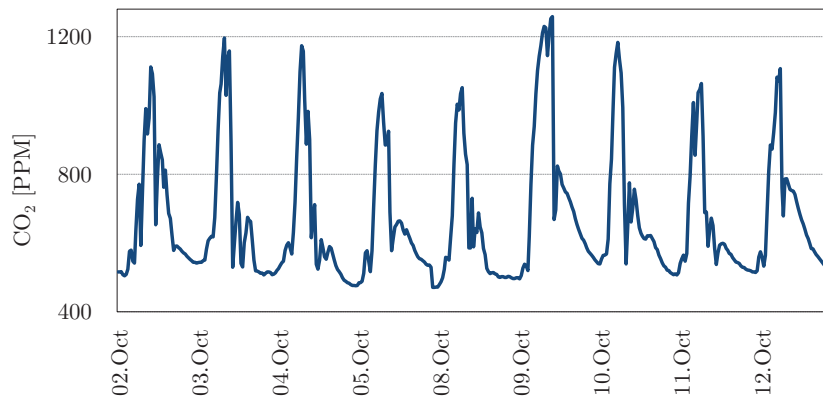


(b) NV

Figure 2.25: Indoor/outdoor air temperature in the 9-day of (a) DPNV and (b) NV regime



(a) DPNV



(b) NV

Figure 2.26: Indoor CO₂ concentrations in the 9-day of (a) DPNV and (b) NV regime

2.3.3 Concluding observations

The results of the performed subjective and objective evaluations suggest that operation of the above-mentioned ventilation systems can generally provide acceptable indoor environmental conditions. According to the measurements the combined operation of the ventilation systems, i.e. DPNV, provides a more uniform indoor environment as compared to the natural ventilation, i.e. NV. Furthermore, the thermal perception of the occupants in the field experiment (room being warm or cold) shows that the office is judged cooler with the combined ventilation DPNV as compared to NV mode. Survey results suggest that the combined DV and PV result in cooler thermal sensation votes in comparison with displacement ventilation alone. Evaluation of the ducted and ductless PVs in both laboratory and field experiments shows that ducted PVs can provide a more desirable indoor environment. The frequency of the PV operation (modulation of volume airflow by the users) was found to be rather low, in case of the ductless PVs compared to the ducted ones. PV usage frequency was found to be somewhat higher in the warmer months of the year, when PV stations supply cooler air to the occupants' breathing zone. In fact, thermally speaking, in case of ductless PVs, sufficiently low supply air temperatures are of great importance in view of required indoor environmental conditions. With regard to air quality considerations, this study suggests that ducted PVs and - to a certain extent - ductless PVs appear to improve the air quality in occupants' breathing zone.

Chapter 3

Computational Indoor Climate Assessment

3.1 Background

3.1.1 Flow and heat transfer

Flow and heat transfer in indoor spaces involves convection, diffusion, conduction, and radiation. Convection refers to the mass and energy transfer in the space caused by flow and temperature gradient. Diffusion relates to the turbulent and molecular movements. Heat loss from the room air through the building elements (solid materials) in the cold season is an example of conduction. Moreover, radiation happens between the objects at different temperature when they have only a transparent medium between them. For indoor environmental analyses, a method, code or tool is required, which is capable of modeling the above-mentioned physical phenomena. For instance, for the indoor environmental studies in a space with a radiator, radiation modeling is required. In case of a space with a fresh air supplier, modeling the mixed convection is necessary. Thus, depending on the defined problem, the analyses should be able to address one or all of the flow and heat transfer features (Chen and Srebric 2002).

3.1.2 Computational Fluid Dynamics (CFD)

Computational Fluid Dynamics (CFD) represents a potentially effective method for indoor environmental studies, to simulate flow and heat transfer in indoor/outdoor envi-

ronment (Wiercinski and Skotnicka-Siepsiak 2008). CFD is a branch of fluid mechanics that have been used in building sciences to “*predict thermal-fluid physical phenomenon in an indoor space*” (Chen and Srebric 2002). Basically, CFD enables calculation of fluid properties such as temperature, velocity, etc., in the space, by means of numerical methods (DesignBuilder 2011a). The physical phenomenon which affects the indoor thermal environment involves, (Chen and Srebric 2002) *i*) heat flow, including for instance conduction through building elements, radiation through the glazing elements, heat gain from heat sources such as occupants and furniture, etc., *ii*) material phase change (between solid, liquid, and gas), for instance when condensation occurs, *iii*) chemical reactions, such as combustion reaction in fire, *iv*) mechanical movements, such as the inhabitants’ movements in a space.

CFD has been used in building indoor environment assessments with a very wide application (see, for instance, Chen and Zhai 2004, Chanteloup and Mirade 2009, Catalina et al. 2009, Laborda et al. 2012), such as, heating, ventilation and air-conditioning system design and assessment, airflow pattern and velocity fields analysis, thermal comfort evaluations, indoor air quality assessments, air change rate effectiveness, age of air, chemical species transport, building safety studies, fire and smoke prediction. In fact, some of the above-mentioned areas of indoor environment studies are only feasible by CFD simulations (Wiercinski and Skotnicka-Siepsiak 2008). Thereby, in the recent years CFD has been widely applied in building performance studies and became very popular in this field. As Clarke 2001 summarizes, a building-integrated CFD modeling includes, model geometry discretization, applying the boundary conditions, a set of equations representing the conservation of mass, energy, momentum and species, an equation solver, a method to link the CFD, thermal and network airflow models, and a method to represent the results in a meaningful way to a user. The following sections describe the elements of CFD simulation ¹.

3.1.3 CFD simulation

Different CFD simulation software has been developed to assist the building engineers in a better understanding of the complex nature of airflow phenomena and heat transfer in the space. Different researches available present the results of studies assisted by CFD simulation packages, such as ANSYS Fluent, CLIMA 3D, PHOENICS, STREAM, etc. The specialist CFD packages provide solutions for a wide range of fluid flow studies and advanced fluid mechanics problems. One concern using some of the advanced-conventional CFD packages is the vast amount of required expertise, time and work to

¹The author would like to start this part by noting that, the information presented here has been presented numerously in the archival literature. This section relies heavily on literature including, Clarke 2001, Ren 2002, Chen and Srebric 2002, Hirsch 2007, McDonough 2003, DesignBuilder 2011b, etc.

generate the initial CFD model (Chowdhury et al. 2010). In some researches, including the present research, with a view over the research scope and objectives, an easy-to-use CFD modelling package, which assists the building engineer and architect to analyze the airflow network and ventilation problems, will be more convenient and encouraging to use. In some literature the CFD module of DesignBuilder software has been presented for analysing the building indoor environment and ventilation systems (Sheta and Sharples 2010, Chowdhury et al. 2010, Laborda et al. 2012, Prajongsan and Sharples 2012, Webb 2013, Ahmed A. Saleem et al. 2014, Chung et al. 2014). Compared to the conventional CFD packages, DesignBuilder “*provides detailed design data on airflow and 3-D temperature distribution ... using the same methods as general purpose CFD packages, but at a fraction of the cost and without the need for specialist knowledge*” (DesignBuilder 2011a). Figure 3.1 illustrates the CFD workflow in Designbuilder (Designbuilder 2011c).

3.1.3.1 Domain discretization

Basically, CFD relates to solve of the equations pertain to fluid flow by means of numerical techniques (Zhai et al. 2001). These set of equations are second order highly nonlinear partial differential equations (PDE). It is almost not possible to solve the non-linear, coupled, partial differential equations analytically, in a turbulent three-dimensional flow field. Therefore, numerical techniques are required to obtain a solution. A straightforward numerical method is the discretization of continues space (and time) into finite elements (Chen and Srebric 2002).

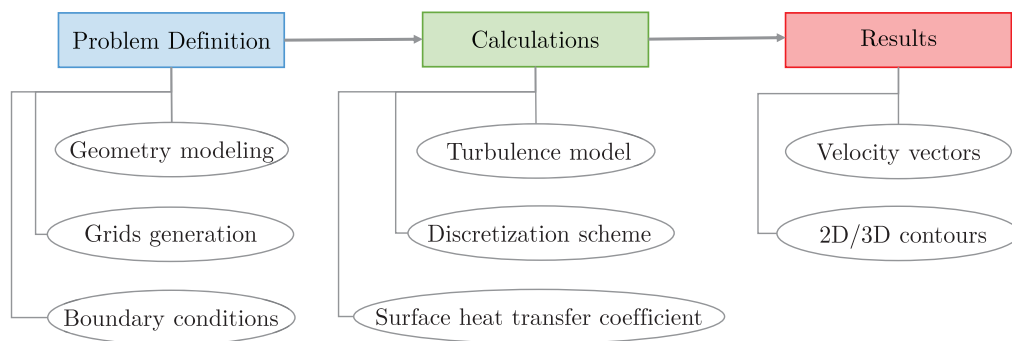


Figure 3.1: CFD workflow in DesignBuilder (source: Designbuilder 2011c)

The space under study should be sub-divided into finite elements or intervals. Commonly used discretization techniques are finite-difference, finite-volume and finite element methods (Chen and Srebric 2002). By this way, the studied volume, for instance a room, is discretised to small cells, or the so-called “grids”. As an example, DesignBuilder uses the finite volume method for 3D CFD calculations. In this case the building space will be divided to finite volume grid which is composed of a set of non-overlapping adjacent rectilinear cells (DesignBuilder 2011b). Thus, linear equations will be assigned to each cell of the grid. The calculation will be iterated until the set of equations are solved, i.e., the equation coefficients are constant and a predefined “convergence” criterion is met. Note that, the convergence of the solutions as well as the speed and accuracy of the calculations is highly affected by the size and distribution of the grids (Ren 2002). However, due to overall non-linear equations set as well as the dependent variables being involved in equation coefficients, convergence will not be achieved in all cases. Numerical grids are categorized in two groups of structured and unstructured grids. The difference between two will appear, for instance, in case of geometries with slopes and curves where the structured grid cannot precisely represent the geometry (Chen and Srebric 2002).

3.1.3.2 Conservation equations

The following partial differential equations (Equations 3.1 to 3.6) describe the airflow, heat transfer and pollutant transfer in a three-dimensional Cartesian coordinate system. There are six equations as well as six unknowns, including three velocity components, temperature, pressure and concentration, which makes the problem a so-called “closed” problem.

- Conservation of momentum in direction x

$$\begin{aligned} \frac{\partial}{\partial t}(\rho u) + \frac{\partial}{\partial x}(\rho uu) + \frac{\partial}{\partial y}(\rho vu) + \frac{\partial}{\partial z}(\rho wu) = & -\frac{\partial p}{\partial x} + \frac{\partial}{\partial x} \left[\mu \left(\frac{\partial u}{\partial x} + \frac{\partial u}{\partial x} \right) \right] \\ & + \frac{\partial}{\partial y} \left[\mu \left(\frac{\partial u}{\partial y} + \frac{\partial v}{\partial x} \right) \right] + \frac{\partial}{\partial z} \left[\mu \left(\frac{\partial u}{\partial z} + \frac{\partial w}{\partial x} \right) \right] \end{aligned} \quad (3.1)$$

- Conservation of momentum in direction y

$$\begin{aligned} \frac{\partial}{\partial t}(\rho v) + \frac{\partial}{\partial x}(\rho uv) + \frac{\partial}{\partial y}(\rho vv) + \frac{\partial}{\partial z}(\rho wv) = & -\frac{\partial p}{\partial y} + \frac{\partial}{\partial x} \left[\mu \left(\frac{\partial v}{\partial x} + \frac{\partial u}{\partial y} \right) \right] \\ & + \frac{\partial}{\partial y} \left[\mu \left(\frac{\partial v}{\partial y} + \frac{\partial v}{\partial y} \right) \right] + \frac{\partial}{\partial z} \left[\mu \left(\frac{\partial v}{\partial z} + \frac{\partial w}{\partial y} \right) \right] \end{aligned} \quad (3.2)$$

- Conservation of momentum in direction z

$$\begin{aligned} \frac{\partial}{\partial t}(\rho w) + \frac{\partial}{\partial x}(\rho uw) + \frac{\partial}{\partial y}(\rho vw) + \frac{\partial}{\partial z}(\rho ww) = & -\frac{\partial p}{\partial z} + \frac{\partial}{\partial x} \left[\mu \left(\frac{\partial w}{\partial x} + \frac{\partial u}{\partial z} \right) \right] \\ & + \frac{\partial}{\partial y} \left[\mu \left(\frac{\partial w}{\partial y} + \frac{\partial v}{\partial z} \right) \right] + \frac{\partial}{\partial z} \left[\mu \left(\frac{\partial w}{\partial z} + \frac{\partial w}{\partial z} \right) \right] - \rho g \beta (T_{\infty} - T) \end{aligned} \quad (3.3)$$

- Conservation of mass

$$\frac{\partial}{\partial x}(\rho u) + \frac{\partial}{\partial y}(\rho v) + \frac{\partial}{\partial z}(\rho w) = 0 \quad (3.4)$$

- Conservation of energy

$$\begin{aligned} \frac{\partial}{\partial t}(\rho c_p T) + \frac{\partial}{\partial x}(\rho c_p u T) + \frac{\partial}{\partial y}(\rho c_p v T) + \frac{\partial}{\partial z}(\rho c_p w T) = & \frac{\partial}{\partial x} \left(k \frac{\partial T}{\partial x} \right) \\ & + \frac{\partial}{\partial y} \left(k \frac{\partial T}{\partial y} \right) + \frac{\partial}{\partial z} \left(k \frac{\partial T}{\partial z} \right) + q \end{aligned} \quad (3.5)$$

- Conservation of contaminants

$$\begin{aligned} \frac{\partial C}{\partial t} + \frac{\partial}{\partial x}(uC) + \frac{\partial}{\partial y}(vC) + \frac{\partial}{\partial z}(wC) = & \frac{\partial}{\partial x} \left(D \frac{\partial C}{\partial x} \right) + \frac{\partial}{\partial y} \left(D \frac{\partial C}{\partial y} \right) \\ & + \frac{\partial}{\partial z} \left(D \frac{\partial C}{\partial z} \right) + S \end{aligned} \quad (3.6)$$

where:

u is the air velocity in direction x [$m.s^{-1}$],

v is the air velocity in direction y [$m.s^{-1}$],

w is the air velocity in direction z [$m.s^{-1}$],

ρ is air density [$kg.m^{-3}$],

μ is air viscosity [$Pa.s$],

β represents the thermal expansion coefficient of air [K^{-1}],

g is the gravitational acceleration [$m.s^{-2}$],

t is time [s],

p is pressure [Pa],

T is temperature [K],

T_∞ is reference temperature [K],

c_p is air specific heat [$J.kg^{-1}.K^{-1}$],

k is air conductivity [$W.m^{-1}.K^{-1}$],

q is the heat within the control volume due to a chemical reaction or a heat source located within the room [$W.m^{-3}$],

C is the concentration of contaminant [$kg.m^{-3}$],

D is the molecular diffusion coefficient for the contaminant [$m^2.s^{-1}$], and

S is the volumetric contaminant generation rate [$kg.m^{-3}.s^{-1}$].

Note that, all these equations contain transient, convection, diffusion and source terms.

3.1.3.3 Navier-Stokes equations

Equations 3.1 to 3.3 describe the motion of transient fluid flow in the Navier-Stokes formulation. Navier-Stokes equation is named after Claude Louis Marie Henri Navier and George Gabriel Stokes and characterizes the motion of viscous fluid substances. For the sake of indoor environment studies, the room airflow can be considered as incompressible, while the velocities tend to be low and in the order of meters or centimeters per second. In such cases the Navier-Stokes equations can be formulated as momentum equation (Equation 3.7) and divergence-free condition (Equation 3.8):

$$\rho \frac{Du}{Dt} = -\nabla p + \mu \delta u + F_B \quad (3.7)$$

$$\nabla .u = 0 \quad (3.8)$$

where:

u is the velocity vector¹,

¹which we write as (u, v, w) .

F_B represents a body force,

$\frac{D}{Dt}$ is the substantial derivative,

∇ is the gradient operator,

δ is the Laplacian operator, and

$\nabla \cdot$ is the divergence operator.

Note that, this equation is Newton's second law of motion applied to a fluid. The left side is mass (per unit volume) times acceleration and the right is the sum of forces acting on the fluid element. The dependent variables in the Navier-Stokes equations are the velocity vector u , and the pressure p , which are the so-called "*primitive*" variables. This is due to the fact that typically in the experiments these physical variables can be directly measured. Additionally, rest of the studied quantities in a fluid flow, can be calculated from these variables. Note that, the body force F_B can contain other dependent variables, such as temperature, and for this case additional equations are required. The solution of the Navier-Stokes equations is a flow velocity and when the velocity field is calculated other quantities, such as pressure or temperature, can be found using additional equations.

3.1.3.4 Turbulence model

The random 3D velocity fluctuations in the fluid flow cause turbulence, which is the property change in the fluid flow with a chaotic-stochastic manner. Random turbulent fluctuations are very common in the airflow, and therefore, should be considered in the analysis and different methods are developed in order to address this issue. Naturally, counting the small scale velocity fluctuations in turbulence simulations is computationally expensive (Russo 2011). Generally, the method to overcome this issue is to solve the governing equations by using approximations, namely using turbulence models in turbulence simulation and eliminating the small scale fluctuations (Chen and Srebric 2002). The exact governing equations are averaged or manipulated to remove the small scales. Modification of the equations adds more variables, and therefore, turbulence models are required to determine the additional variables. Turbulence models can be called "*simpler mathematical models*", which are used in order to physically model the Navier-Stokes equations and predict the turbulence. It is assumed that the stochastic properties of the flow will vanish in an averaging scheme, after a long-enough period of time (Russo 2011).

Turbulence models are categorized in two groups of large-eddy simulations (LES), and Reynolds averaged Navier-Stokes (RANS) equations. LES models are computationally more expensive in comparison with RANS and have been rarely used for indoor environment modelling. RANS models are classified to different categories, among which the $k - \varepsilon$ is a widely used and popular model (Chen and Srebric 2002). Numerous studies are available in literature that can help the CFD users to select appropriate turbulence models for the indoor airflow studies (for instance, see, Nielsen 1998). In general, Chen and Srebric 2002 concluded, the use $k - \varepsilon$ model mostly turns out to the satisfactory results for indoor air simulations. Therefore, in the following the focus will be on the $k - \varepsilon$ model, which is one of the widely tested turbulence models, and also has been used in this study.

$k - \varepsilon$ is a two partial differential equation model to describe the turbulence, the first equation relates to the turbulent kinetic energy (k) and the second one, the turbulent dissipation (ε):

$$k = \frac{1}{2}(\overline{u_i'^2} + \overline{v_i'^2} + \overline{w_i'^2}) \quad (3.9)$$

$$\varepsilon = c_\mu^{3/4} k^{3/2} l^{-1} \quad (3.10)$$

in which:

k is turbulence kinetic energy [$m^2 \cdot s^{-2}$],

ε is turbulent dissipation rate [$m^2 \cdot s^{-3}$],

l is the turbulent length scale, and

c_μ is the standard eddy viscosity model constant, equal to 0.09.

In the $k - \varepsilon$ model, the “instantaneous values” in Equations 3.1 to 3.3 and Equation 3.5 are replaced with the sum of a mean value and a fluctuating component. By adding the new terms, additional unknown, i.e. Reynolds terms ($-\rho \overline{u_i' u_j'}$ and $-\rho c_p \overline{u_j' T'}$), are introduced (Ren 2002). The term $-\rho \overline{u_i' u_j'}$ presents the Reynolds stress τ_{ij} . Assuming that the turbulent stresses are proportional to the mean velocity gradients, one can get:

$$\tau_{ij} = -\rho \overline{u_i' u_j'} = -\mu_t \left(\frac{\partial \overline{u_i}}{\partial x_j} + \frac{\partial \overline{u_j}}{\partial x_i} \right) - \frac{2}{3} \delta_{ij} \rho k \quad (3.11)$$

while:

μ_t is the turbulent or eddy viscosity ¹,
 δ_{ij} is the Kronecker delta ².

This new term in the momentum equation represents the high-frequency fluctuating velocity components. Moreover, assuming that the turbulent heat fluxes are proportional to the mean temperature gradients, we have:

$$-\rho c_p \overline{T'u'_j} = -c_p \Gamma \frac{\partial \bar{T}}{\partial x_i} \quad (3.12)$$

where Γ represents the turbulent diffusivity of heat ³,

The turbulent viscosity and the turbulent diffusivity of heat are related by the turbulent Prandtl number σ_t :

$$\sigma_t = \frac{\mu_t}{\Gamma} \quad (3.13)$$

In the standard $k - \varepsilon$ the eddy viscosity will be calculated by k and ε , according to the following equation:

$$\mu_t = c_\mu \rho \frac{k^2}{\varepsilon} \quad (3.14)$$

By substituting Equations 3.11 to 3.14 into Equations 3.1 to 3.5 :

$$\frac{\partial}{\partial t}(\rho\phi) + \frac{\partial}{\partial x_i}(\rho U_i \phi) = \frac{\partial}{\partial x_i}(\Gamma_\phi \frac{\partial \phi}{\partial x_i}) + S_\phi \quad (3.15)$$

¹ μ is a property of the fluid, but μ_t is a property of the flow and can be different for different flows or throughout a flow.

²Kronecker delta is a function of two variables. If the variables are equal, $i = j$, $\delta_{ij} = 1$, otherwise $\delta_{ij} = 0$.

³ Γ is a property of the flow.

where:

φ denotes the mean dependent variable, such as air velocity and temperature,

x_i is displacement in the direction i ,

U_i is velocity in the direction i ,

Γ_φ is diffusion coefficient, and

S_φ represents a source.

3.1.3.5 Numerical scheme, iteration and convergence

In CFD analysis, the second order partial differential equations are solved by using discretization methods that convert the equations to a set of numerically solvable equations. For this purpose, different techniques can be considered, such as central differencing scheme, upwind scheme, hybrid scheme, power law scheme, etc. The selected numerical schemes have great importance in CFD calculations, in order to achieve accurate and fast solutions. Therefore, the modelers should consider the limitations of each scheme to select the one appropriate for their specific problem (Chen and Srebric 2002). For example, central differencing scheme is used when the ratio of convection over conduction, namely the Peclet number (Pe), is small (i.e., $Pe < 2$), and the upwind scheme is employed for a high Pe (Equation 3.16).

$$Pe = \frac{\text{heat transported by convection}}{\text{heat transported by conduction}} = \frac{L u \rho c_p}{\lambda} \quad (3.16)$$

where,

L is the characteristic length, such as room height or diffuser height,

λ represents the thermal conductivity [$W.m^{-1}.K^{-1}$].

⁴ “Transient + Convection = Diffusion + Source” (Chen and Srebric 2002)

In the upwind scheme, the convective term is calculated assuming that the values of dependent variable on the cell interface and at the upwind side of the interface are equal. The so-called hybrid scheme uses central differences or upwind scheme based on Pe . This scheme is computationally more expensive than upwind scheme. The power law scheme is similar to hybrid scheme, where diffusion is set to zero for $Pe > 10$. This scheme is more accurate compared to hybrid scheme but also computationally more expensive (McDonough 2003, Tawani 2008, DesignBuilder 2011b, Webb 2013).

CFD calculation is an “*iterative*” process which is completed when the “*convergence*” is achieved. As noted before, the domain under study will be sub divided into a set of non-overlapping connected volumes or cells, for each of which the differential equations are expressed in the form of a set of linear algebraic equations and the overall set of equations is then solved by an iterative scheme. The equations set related to each of the dependent variables, such as velocity components, temperature, etc., are iteratively solved within an overall outer iterative loop. The recent value of each dependent variable is used as the new dependent variable coefficient at the end of each outer iteration termination. This outer iterative loop continues up to the point that, the finite difference equations are satisfied by the latest values of the dependent variables in all cells. This is when the convergence is achieved. When in a CFD calculation a maximum number of iterations is reached, no matter if the solution has converged or not, the calculation will terminate at this iteration number. Moreover, the solution is considered as converged for each dependent variable, if the maximum residual quantity for the equation balance through all cells in the space is smaller than the defined termination residual (DesignBuilder 2011b).

3.1.3.6 Boundary conditions

Specification of the boundary conditions is one of the requirements for solving Equation 3.15. In fact, the governing equations presented previously are the same for CFD simulations in every environment. What makes the difference in the outcome is different boundary conditions (Chen and Srebric 2002).

To conduct CFD simulations with regard to indoor airflow patterns, a certain number of boundary conditions are required. Boundary conditions for an indoor CFD simulation usually pertain to the space enclosure, inlets and outlets. Furthermore, fluid flow through the space is influenced by internal obstructions in the fluid flow path or by heat transfer caused by the internal boundary conditions (Zhai et al. 2001, Webb 2013). For instance, in a CFD simulation package like DesignBuilder internal boundary conditions are defined by: *i*) temperature of building envelope, e.g. wall, windows, floor, ceiling, etc., *ii*) temperature or heat flux of internal obstructions and heat sources, including

radiators, furniture, occupants, etc., *iii*) airflow rate, speed, direction and temperature of diffusers, extracts, vents, etc. (DesignBuilder 2011*b*). Part of the boundary conditions pertains to the supply diffusers and extract grilles are defined based on either actual measurements or assumptions. In case of the rest, such as surface temperatures, when actual measurements are not feasible, there is the possibility of conveniently importing them from the building simulation results (see section 3.1.4 below).

3.1.4 Integrated BES and CFD programs

Building Energy Simulation (BES) and CFD programs have been widely used to provide the required information for building performance evaluations. BES and CFD each are capable of addressing certain problems, providing certain categories of information and complement each other (see, for instance, Table 3.1 presented by Zhai and Chen 2005). Integration of these two will result in the more reliable outcomes by omitting part of the initial assumptions. For example, indoor surface temperature and heat flux are part of the required boundary conditions for CFD simulations and BES is capable of providing this input data for CFD. On the other hand, detailed room air temperature distribution predictions and accurate convective heat transfer by CFD assists the total energy consumption calculations by BES (Zhai et al. 2002). By integration of the results of these two, the building engineers can overcome some of the limitations involved in the simulations.

Table 3.1: Number of examples regarding the common functionalities of BES and CFD programs in building performance evaluations (Zhai and Chen 2005)

Functionality	BES	CFD
Weather and solar impact	✓	-
Thermal performance of the enclosure	✓	-
HVAC system capacity	✓	-
Energy consumption analysis	✓	-
Thermal comfort analysis	-	✓
Air distribution	-	✓
Indoor air quality assessments	-	✓

Two of the equations solved by a BES program are energy balance for room air (Equation 3.17) and surface heat transfer (Equation 3.18) (Zhai et al. 2001), which are given below:

$$\sum_{i=1}^N q_{i,c}A_i + Q_{other} - Q_{heat-extraction} = \frac{\rho V_{room}c_p\Delta T}{\Delta t} \quad (3.17)$$

$$q_i + q_{ir} = \sum_{k=1}^N q_{ik} + q_{i,c} \quad (3.18)$$

where,

$\sum_{i=1}^N q_{i,c}A_i$ represents the convective heat transfer from enclosure surfaces to room air,

$q_{i,c}$ is the convective flux from surface i [$W.m^2$],

A_i is area of surface i [m^2],

N is number of the surfaces,

Q_{other} is heat gains (e.g., from lights, people, appliances, etc.) [W],

$Q_{heat-extraction}$ is room heat extraction rate [W],

$\frac{\rho V_{room}c_p\Delta T}{\Delta t}$ is the energy change in room air,

V_{room} is room volume [m^3],

ΔT is the room air temperature change [K],

Δt is time interval [s],

q_i is conductive heat flux on surface i ,

q_{ir} is radiative heat flux from internal heat sources and solar radiation [$W.m^2$], and

q_{ik} is radiative heat flux from surface i to surface k [$W.m^2$].

In order to calculate the heat fluxes, the unknown parameter is the convective heat transfer coefficient h_c required for the calculation of convective heat flux from surface i ($q_{i,c}$). h_c is mostly determined in the BES programs by assuming a constant or the empirical models. Moreover, as previously discussed in section 3.1.3, numerical techniques are applied in CFD simulation to solve the Navier-Stokes (N-S), the conservation of mass, and conservation of energy equations. The accuracy of CFD outcomes is highly dependent to the defined boundary conditions. Thus, accurate determination of the boundary conditions is crucial for the accuracy of the CFD predictions. It is presented in section 3.1.3.6, that the boundary conditions for internal CFD analyses relates to the enclosure surfaces, internal objects, air suppliers and exhausts.

Coupling BES and CFD programs provides accurate convective heat transfer coefficient and room air temperature for BES that can be determined by CFD, and interior surface temperatures for CFD that can be calculated by BES. This emphasizes the necessity of integrating the two programs to improve the accuracy of the simulation results (Zhai et al. 2002). Different available literature outline the coupled BES and CFD programs with various coupling methods (for instance, see, Zhai et al. 2001, 2002, Zhai and Chen 2005, Sheta and Sharples 2010, Iizuka et al. 2011).

3.1.5 Monitoring-assisted calibration of CFD model

Due to the involved simplifications and uncertainties of the assumptions, simulation results are not always reliable. A conventional method to evaluate the credibility of simulation predictions is comparing the simulation outcomes with actual measurements (Chen and Srebric 2002, Cetin and Mahdavi 2015). Chen and Srebric 2002 argue that CFD results and experimental data both have better accuracy for the parameters such as air velocity and temperature (i.e. first-order parameters), as compared to the parameters including turbulence kinetic energy, Reynolds-stresses, and heat fluxes (i.e. second-order parameters). Therefore, it is suggested to conduct the comparison for the first-order parameters. The comparison should clearly state the uncertainties and errors which are known. After comparing the measured and predicted values the initial CFD model can be calibrated to minimize the difference between the measured and simulated parameters. The Calibration process should continue until an acceptable accordance between the measurements and CFD results is achieved. The motivation of generating a calibrated CFD model is to firstly provide a reliable prediction of the indoor environment condition and secondly reuse of the calibrated model to accurately investigate different design alternatives and their implications for indoor environmental variables. Note that the option of calibrating the simulation model based on observed data might not have relevance to scenarios pertaining to building design support, but is of interest for control scenarios in existing buildings.

3.2 Method

3.2.1 Overview

CFD-based airflow simulations were performed in this section to support a better understanding of the complex nature of airflow phenomenon in the space. This section benefits from both laboratory and field office models. In order to evaluate the CFD predictions, simulated airflow velocity and temperature were compared with measured data at multiple locations in the space. The initial CFD model was then calibrated to minimize the difference between the measured and simulated indoor air temperature and velocity. Assisted by the calibrated model, potential alternative design improvements can be investigated. Moreover, airflow velocity at different locations in the space as an output from the CFD simulation can be used as the input data for thermal comfort calculations, specifically in this case PMV, where the actual measurement is missing.

3.2.2 The building thermal and CFD simulation

Advanced whole-building simulation tool DesignBuilder has been used in this study. Among different packages provided for engineers by DesignBuilder, the 3-D modeler, simulation and CFD packages have been used in this dissertation (DesignBuilder 2011a). DesignBuilder uses the EnergyPlus code (EnergyPlus 2011) as its energy performance computational core engine.

3.2.2.1 Geometry modeling and finite volume grid generation

Using DesignBuilder, the same modeled geometry will be used for both thermal performance and CFD simulations. For the sake of CFD simulations, the geometry of the studied space will be divided into non-overlapping adjacent volumes. When the geometry model is created, the volume discretization for the CFD simulation will be done by automatic generation of the so-called grid lines. The user can define the desired maximum grid spacing value, and also edit the automatically generated grids in the more critical regions in the space. In this research, in order to create block-structured grids, the grid spacing was specified and where required manually modified, based on the specific case study. For instance, wherever very narrow grid regions were not necessary, the grid lines were merged in order to reduce the high calculation times and excessive memory use. On the other hand, an opposite instance is in the regions near to the supply diffusers, where grid spacing was reduced to improve further evaluation of the temperature and air

speed in this area. The feedback from CFD grid statistics provided by DesignBuilder in each simulation proved an acceptable grid mesh considering the cell aspect ratio and the memory required for the simulations.

3.2.2.2 Simulation input data

The modeled geometry was fed with the required thermal performance simulation input data (e.g., construction details and associated thermal properties, internal loads, HVAC system, weather data), which were defined based on the available plans, observations and measurements.

To conduct CFD simulations with regard to airflow patterns in a room, a certain number of boundary conditions are required, including surface temperature of walls, windows, floor, ceiling, component blocks and assemblies, etc., as well as the supplied airflow rate, direction and temperature and extract flow rate. The boundary conditions pertains to supply diffusers and extract grilles are defined based on either actual measurements or assumptions. In case of the rest of the boundary conditions, such as surface temperatures, when actual measurements are not feasible, there is the possibility to conveniently import them from the building simulation results.

The CFD calculations are steady state, i.e. the CFD simulation involves an instance of time in a single design day. Therefore, the boundary conditions are required to be defined for the selected particular snap-shot in the time. Table 3.2 summarizes the methods to provide the required input data for CFD simulations in this study.

Table 3.2: Required input data for CFD simulations and the source providing them

Input data	Source
Surface temperatures	Thermal simulation/Measurement
Supply airflow rate	Measurement
Supply airflow direction	Assumption
Supply air temperature	Measurement
Extracted airflow rate	Measurement

3.2.2.3 Selected turbulence model

Two turbulence models are offered by DesignBuilder for the CFD simulations, namely the $k - \epsilon$ model, and the *constant effective viscosity* model. Even though the *constant effective viscosity* model is numerically stable and computationally less expensive, but it is less accurate. Therefore, for the purpose of this study the $k - \epsilon$ model is selected.

3.2.2.4 Selected discretization scheme

Three discretization schemes are available in DesignBuilder, i.e., *upwind*, *hybrid*, and *power-law* discretization schemes. In this research the *upwind* scheme is selected, due to the simplicity of the calculations in this discretization method for the studies with air as the only involved fluid with non-extreme conditions.

3.2.2.5 Number of iterations and termination residual

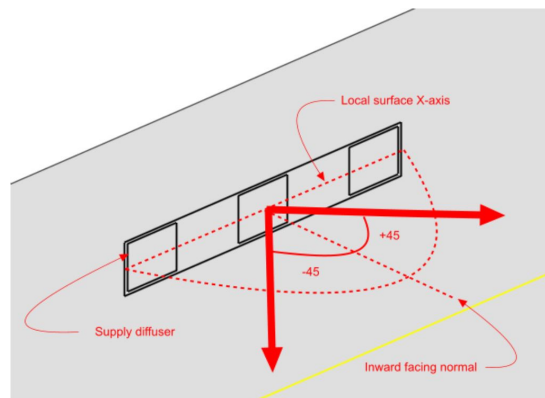
As discussed before, considering the non-linearity of the equations involved in the calculations, the equation set cannot be solved analytically. The numerical method utilized in DesignBuilder is basically based on replacing the differential equations with a set of finite difference equations. In fact, the equation set is transferred to a set of linear algebraic equations and is solved using an iterative scheme. Each dependent variable in the equation set is solved iteratively withing an iterative loop. The maximum number of the iterations of the overall iterative loop as well as inner iterative dependent variable calculations is defined by user. The outer iterative calculation loop will repeat unless the current values of the dependent variables satisfies the finite difference equations for all cells. At this stage the calculation has converged. The convergence is achieved when for each dependent variable the residual is less than a defined termination residual (DesignBuilder 2011b). The calculation settings of the CFD simulations in this study include maximum dependent variable residual (iterative convergence error) of 10^{-5} .

3.2.2.6 CFD simulation outcomes

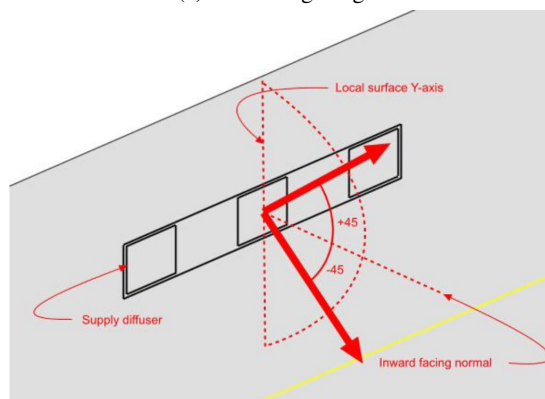
Following the CFD simulation, detailed temperature, airflow, and comfort data within the model are provided. Air temperature and velocity can be plotted at slices along any grid axes in the space. Moreover, by specifying the metabolic rates and clothing levels of the inhabitants comfort calculations will be conducted to display, for instance, the PMV values in the model.

3.2.2.7 Calibration of the initial CFD model

Because of the uncertainties of the assumptions and simplifications involved in CFD simulation, results are not always reliable. An example of an assumption in this study (see also Table 3.2) is the supply airflow direction. In the initial model the discharge angle of the air diffuser, i.e., the discharge angle between the X/Y axis of the supply diffuser's surface and an inward facing normal (Figure 3.2), was assumed to be zero. This means that in the initial model the simulated supply air is injected to the room parallel with the normal line to the supply diffuser's surface. The flow direction can be defined with positive or negative discharge angles. For instance, see Figure 3.2a and 3.2b demonstrating positive and negative X and Y discharge angles, respectively (DesignBuilder 2011b).



(a) X discharge angle



(b) Y discharge angle

Figure 3.2: Illustration of a supply diffuser model and a possible supply air X and Y discharge angle in DesignBuilder (source: DesignBuilder 2011b)

3. Computational indoor climate assessment

One method to evaluate the credibility of simulation predictions is comparing the CFD outcomes with actual measurements. Thus, the CFD predictions of air speed and temperature at certain locations in the space are compared with the corresponding measured values. For the purpose of these measurements, *ALMEMO* multi-function measuring instrument and data logger, together with thermoelectric flow sensor and temperature sensor were used (Figure 3.3). The measured values are stored on the data logger which has an internal memory or can be used with a memory card. Table 3.3 shows details of the measured parameters and sensor information.

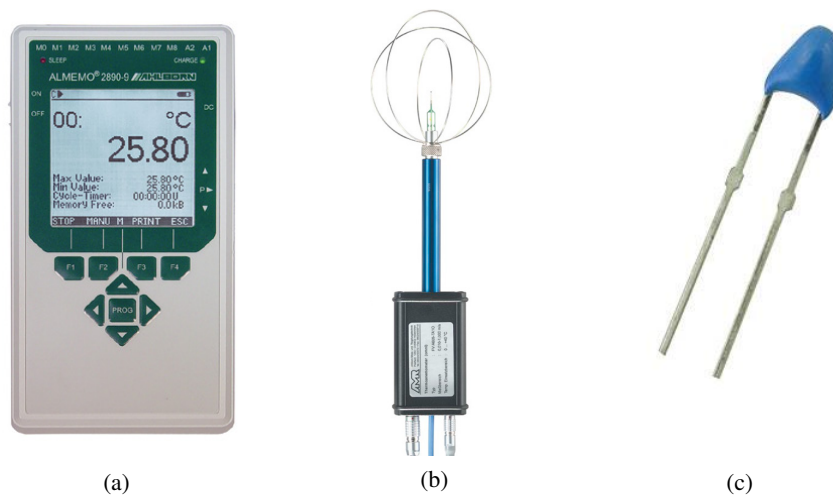


Figure 3.3: (a) Data logger, (b) thermoelectric flow sensor, and (c) temperature sensor (Rogers 2015, B+B Thermo-Technik GmbH 2017)

Table 3.3: Monitored parameters for CFD model evaluations together with sensor information

Measurement type	Symbol	Unit	Sensor range	Sensor accuracy
Thermoelectric flow	v	$m.s^{-1}$	0.01 to 1	$\pm 1 \%$
Temperature	θ_i	$^{\circ}C$	-60 to +150	$\pm 0.5 \%$

The simulation results were meant to be compared with the measured values under the condition that only DV operates (i.e., deactivated PVs and closed windows). Consequently, the simulated ventilation system also involves DV operation only (without PVs and natural ventilation). After comparing the measured and predicted values it was attempted to calibrate the initial CFD model to minimize the difference between the measured and simulated indoor air temperature and velocity. The Calibration process was continued until an acceptable accordance between the measurements and CFD results was achieved. Assisted by the CFD calibrated model, potential alternative design improvements were investigated in one of the case studies. In fact, the implications of alternative design configurations for indoor environmental variables could be computationally evaluated. The idea behind the design suggestions was to alter the geometry and location of the air supply diffusers as well as the airflow rate in a way that provides the requirements for DPV system operation.

3.2.3 Computational models

3.2.3.1 Laboratory model

The first case study in this chapter is the “*lab cell 2*” from the laboratory set up explained in Section 2.2.2. Under fully controlled conditions, during 18 hours of measurements, the input data required for CFD simulations (except the supply flow direction) have been measured.

In order to measure the surface temperatures of walls, windows, floor and ceiling two types of surface temperature measurement instruments (Figure 3.4 and 3.5), have been used. Four humidity/temperature measuring instrument *Testo 635*, together with surface probes (Figure 3.4) were installed on door, window, adiabatic wall and one outside wall. This measurement instrument offers high accuracy measurement of temperature, air humidity, material equilibrium moisture, pressure dew point, absolute pressure and U-value (Testo 2015). The temperature probe with triple sensor system, shown in Figure 3.4b, is suitable for surface temperature measurements and U-value determination. Due to the limitations in the number of available *Testo* measuring instruments, wireless *Thermokon* temperature sensors have been used (Figure 3.5) (Thermokon 2015). The measured values were stored through a wireless system in the online database of the department of Building Physics and Building Ecology, TU Wien. The temperature sensors were installed on the ceiling, floor and outside walls. The following table presents details of the measured parameters and sensor information. Note that, however the sensors illustrated in Figure 3.4 are more suitable for the type of surface temperature measurements required here, considering the number of surface temperature measurements (i.e., eight surfaces) and the availability of the sensors, the second temperature sensors have been used.

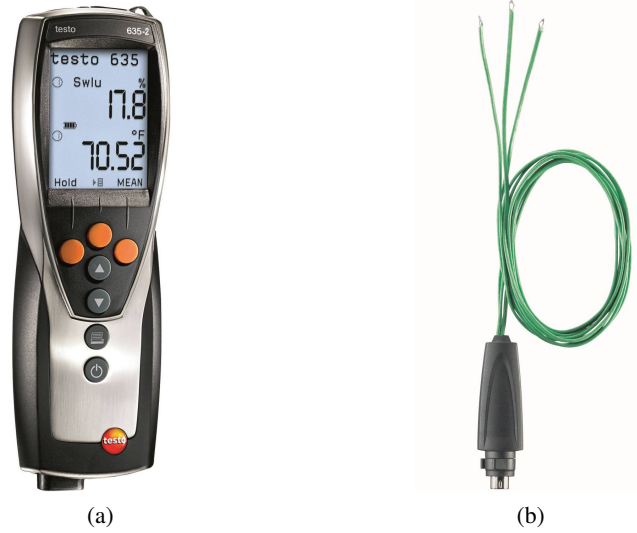


Figure 3.4: Surface temperature measurement instrument, type 1 (Testo 2015)



Figure 3.5: Surface temperature measurement instrument, type 2 (Thermokon 2015)

Table 3.4: Surface temperature sensor information

Measurement type	Symbol	Unit	Sensor type	Sensor range	Sensor accuracy
Surface temperature	θ_i	°C	1	-20 to 60	$\pm 0.5 \text{ } ^\circ\text{C} \pm 1 \text{ digit}$
			2	-20 to 70	$\pm 1\%$

The ventilation system in the test room is connected to an online control, monitoring and safety system in the course of a previous research project. Therefore, the airflow rate (in/out) and airflow temperature data were provided for the period of the experiment. The supply air temperature of the installed control system is measured at a distant from the supply air inlet in the room. The supply air temperature input of the simulations is the temperature of the air at the time entering the space. Plausible change of the air temperature caused by flowing through the ducts, may affect the simulation results. Therefore, an additional air temperature sensor was installed inside the supply air inlet in the room to measure the actual supply air temperature entering the room. Note that, the performed CFD simulation was steady state. Thus, an average of the measured values of each parameter has been used as the CFD simulation input value.

In order to add the internal loads to the laboratory cell (for instance an occupant with a computer) a heat source of 180 W was installed on the desk, which was modelled in CFD simulation as a component block with the respective boundary. Other equipment (i.e. luminaires, office desk and chair) were also included in the simulation model.

As mentined before, because of the involved simplifications and input data uncertainties, CFD simulation results are not always reliable. To examine the accuracy of the simulation outcomes, CFD predictions of airflow speed and air temperatures are compared with measurements at multiple locations in the space. The locations of airflow speed (v_1 to v_{12}) and air temperature (θ_1 to θ_{30}) measurements are shown in Figure 3.6 and 3.7, respectively. Air speed was measured at a distance of 0.1, 0.35, 0.6, and 0.85 m from the supply diffuser and at height of 0.1, 0.6, and 1.1 m above the floor level. Temperature was measured at a distance of 0.25 to 1.75 m (every 0.25 m) from the supply diffuser and at a height of 0.1, 0.3, 0.6, and 1.1 m above the floor level. Each set of measurements stretched over two hours providing air speed and temperature data at 36 and 90 locations, respectively. Following the CFD simulations, temperature and velocity were plotted in terms of planar slices through the space. Predictions of airflow speed and air temperature were compared with the measured values at each corresponding location (average value of the two hours measurement). The initial CFD model was calibrated to minimize the difference between the measured and simulated indoor air temperature and velocity. Calibration process was continued until an acceptable agreement between the measurements and CFD results was achieved.

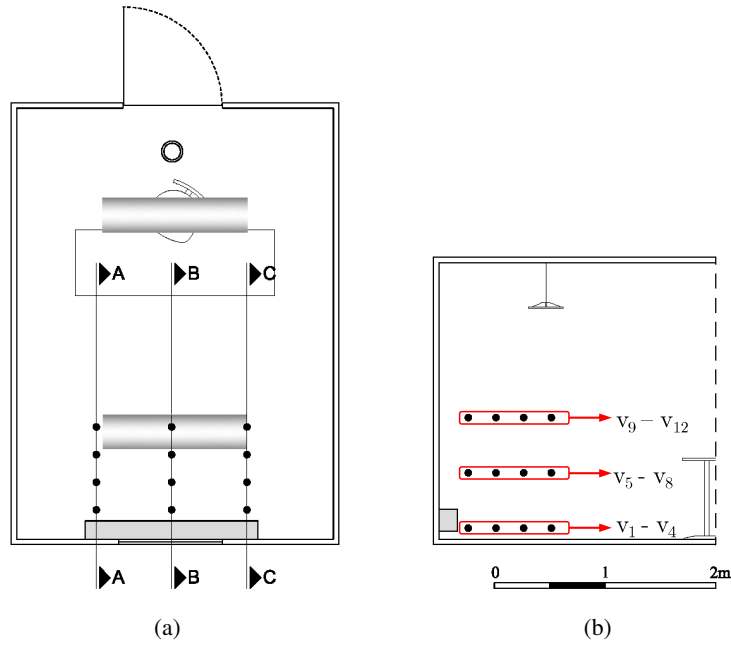


Figure 3.6: Positions of velocity measurements in lab cell 2, on (a) the plan and (b) a vertical section (Section B-B)

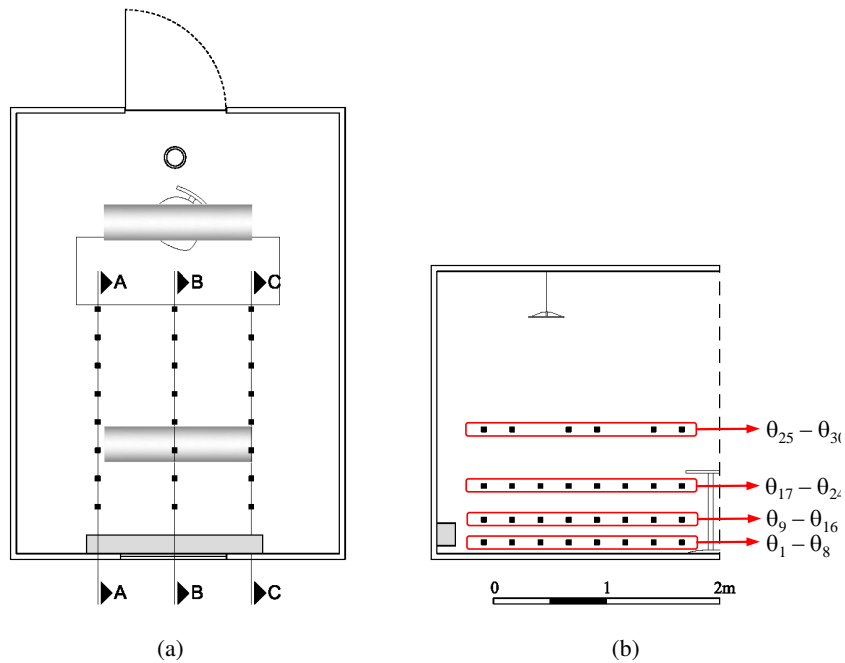


Figure 3.7: Positions of temperature measurements in lab cell 2, on (a) the plan and (b) a vertical section (Section B-B)

The calibration variables and their associated variation are selected considering the input parameters which were not directly measured. To arrive at a calibrated simulation model, the following calibration sequence is followed:

- Figure 3.8b demonstrates the linear supply diffuser (*SD*) in the initial simulation model. Modelling a single supply diffuser means assuming a uniform flow along the diffuser's face. However, in reality the airflow velocity varies at different sections at the face of the diffuser (for instance in the middle of the diffuser compared to the sides). As Figure 3.8c demonstrates, in the first step of the calibration, the single supply diffuser in the initial model, *SD*, was replaced with three supply diffusers, namely *SD1*, *SD2* and *SD3*. The total flow rate was divided between the *SD1*, *SD2* and *SD3* considering the ratio between the measured velocities of point v_1 (Figure 3.6) at each section.
- The flow direction in the CFD model is defined with positive or negative discharge angles (see Figure 3.2). Initially, the simulated supply air was injected to the room parallel with the normal line to the supply diffuser's surface. In the second step, the *X* and *Y*-discharge angle of the airflow from *SD1*, *SD2* and *SD3* were calibrated. This step of calibration process included 52 simulation runs.
- Supply air temperature input for the CFD model was measured at one location inside the enclosure displacement diffuser. The temperature of the low-velocity cool air stream may change in the diffuser box as soon as it comes in contact with warmer air. The third step of the calibrations involves modifying the supply air temperature and required 14 simulation runs.

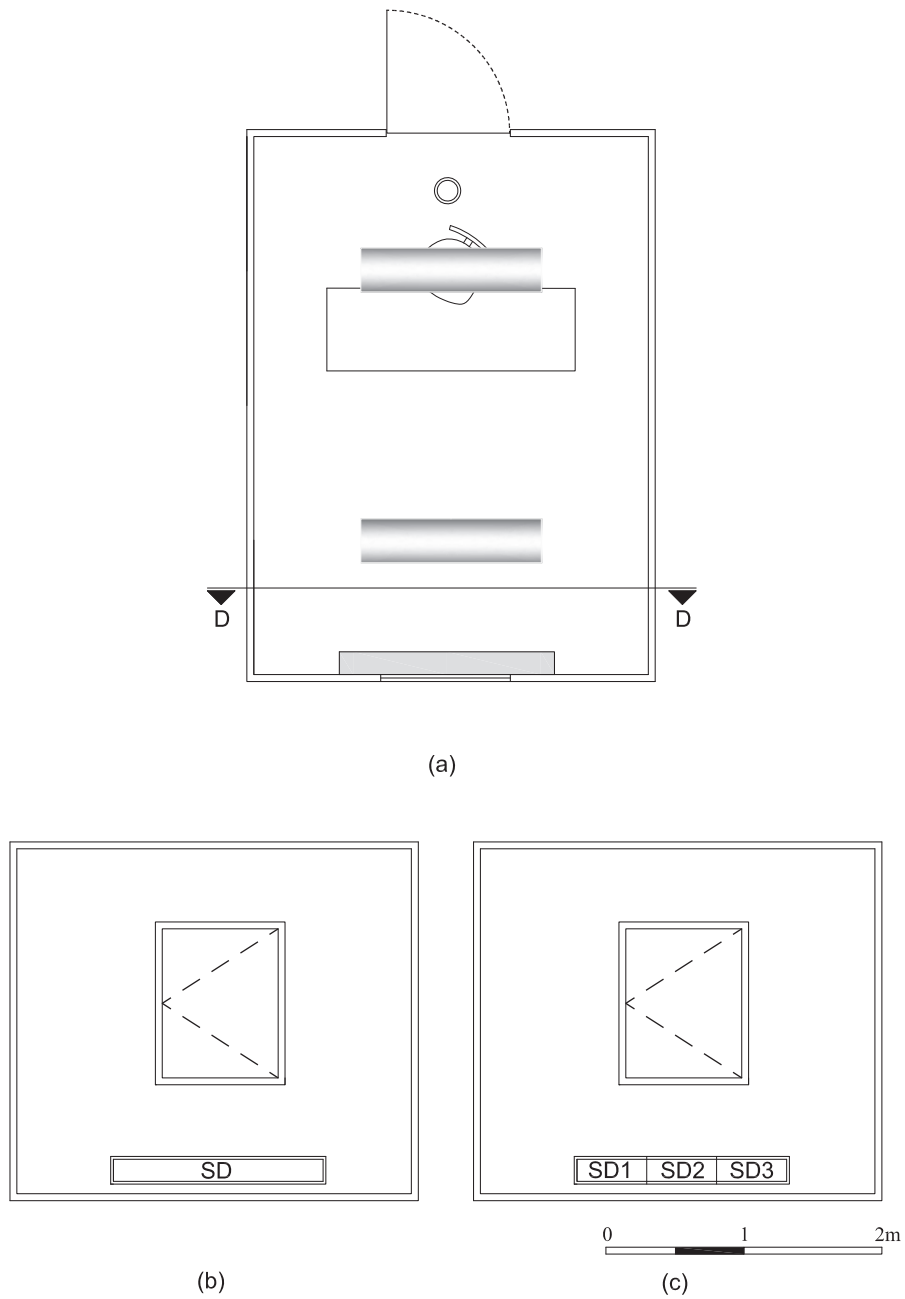


Figure 3.8: (a) Plan of the lab cell 2 together with a vertical section (Section D-D) presenting the supply diffuser in (b) initial and (c) calibrated models

3.2.3.2 Field office model

The second case study in this chapter is the open plan office space presented in Section 2.2.3. Figure 3.9 demonstrates the office plan together with marked locations of the supply diffusers, extract grilles, monitored workstations, as well as the vertical sections which will be referred later in this section. A thermal simulation model of the office space was generated in DesignBuilder using the office geometry, construction details, operation schedules, and weather data. Thermally the office is modeled together with its adjacent zones (Figure 3.10). Tables 3.5 and 3.6 demonstrate properties of different opaque, glazing and gas layers of the building elements. Simulation input assumptions pertain to internal gains (such as, occupancy, lighting, etc.), and systems operation schedules were defined based on the information provided by the project partners and are presented in Table 3.7.

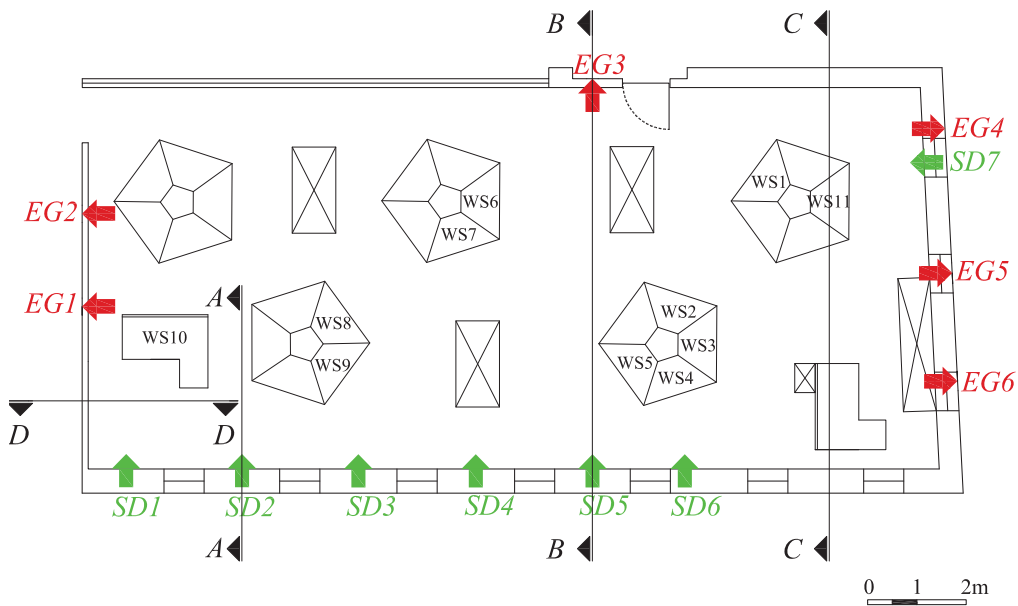


Figure 3.9: Plan of the office space together with marked locations of the supply diffusers, extract grilles, monitored workstations, as well as the vertical sections under study

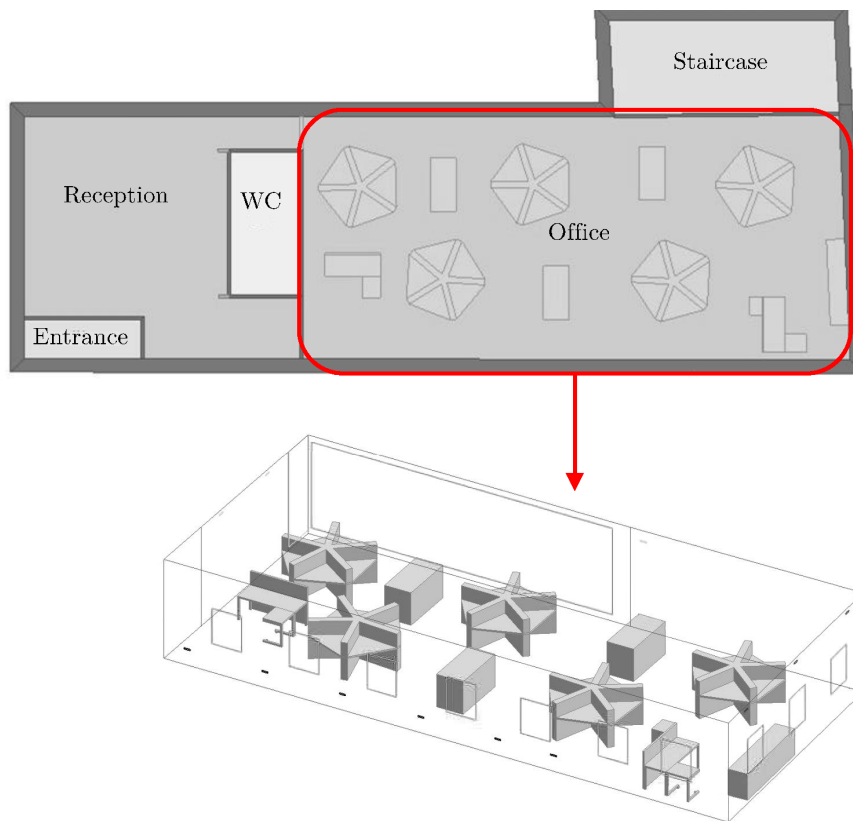


Figure 3.10: Simulation model of the office space in DesignBuilder

Table 3.5: Properties of the enclosure elements

Building component	Layers (Outside to inside)	Thickness [m]	Thermal conductivity [$W \cdot m^{-1} \cdot K^{-1}$]	Specific Heat [$J \cdot kg^{-1} \cdot K^{-1}$]	Density [$kg \cdot m^{-3}$]
Floor	Reinforced Concrete	0.25	2.300	1000	2300
	Cement bonded polystyrene	0.08	0.085	1000	200
	Sound insulation panel	0.03	0.040	900	180
	Cement screed	0.07	1.330	1110	2000
	Timber flooring	0.02	0.140	1200	650
Ceiling	Timber flooring	0.02	0.140	1200	650
	Cement screed	0.07	1.330	1110	2000
	Sound insulation panel	0.04	0.040	900	180
	Reinforced concrete	0.25	2.300	1000	2300
	Exterior plaster	0.01	1.400	1110	2000
Outside wall	EPS Expanded Polystyrene (Standard)	0.16	0.040	1400	15
	Hollow brick	0.25	0.580	1000	1400
	Interior plaster	0.015	0.700	900	1200
Partitions	Gypsum plasterboard	0.025	0.250	1000	900
	Air gap	0.100	1	1	1
	Gypsum plasterboard	0.025	0.250	1000	900

Table 3.6: Properties of the window components

Window component			
Glazing	Outermost pane	Thickness [mm]	6
		Solar transmittance	0.69
		Thermal conductivity [$W.m^{-1}.K^{-1}$]	0.90
	Innermost pane	Thickness [mm]	6
		Solar transmittance	0.43
		Thermal conductivity [$W.m^{-1}.K^{-1}$]	0.90
Gas	Type	Krypton	
	Thickness [mm]	20	
Shading	Type	Blind with high reflectivity slats	
	Blind to glass distance [m]	0.015	
	Slat orientation	Horizontal	
	Slat width [m]	0.025	
	Slat separation [m]	0.0188	
	Slat thickness [m]	0.001	
	Slat angle [°]	45	
	Slat conductivity [$W.m^{-1}.k^{-1}$]	0.9	
	Minimum slat angle [°]	0	
	Maximum slat angle [°]	180	
Frame/Divider	U-value [$W.m^{-2}.k^{-1}$]	1.101	
	Frame width [m]	0.04	
	Divider width [m]	0.02	

Table 3.7: Assumptions regarding the internal gains and air change rate

Input data category		
Air tightness	Infiltration [$ach.h^{-1}$]	0.1
Minimum Fresh Air	Fresh air [$L.s^{-1}$ per person]	7
Environmental Control	Heating set point [$^{\circ}C$]	20
	Heating set back [$^{\circ}C$]	10
	Cooling set point [$^{\circ}C$]	26
	Cooling set back [$^{\circ}C$]	30
	Natural ventilation cooling set point temperature [$^{\circ}C$]	18
	Mechanical ventilation cooling set point temperatures [$^{\circ}C$]	18
Occupancy	Density [people per m^2]	0.1500
	Activity	Office work, seated
	Metabolic factor	1.2
	Clothing [clo]	1 (Winter)
		0.5 (Summer)
Computers	Load [$W.m^{-2}$]	5
	Radiant fraction	0.2
	Schedule	8:00-18:00 (Mon-Fri)
Office equipment	Load [$W.m^{-2}$]	30
	Radiant fraction	0.2
	Schedule	8:00-18:00 (Mon-Fri)
General lighting	Lighting energy [$W.m^{-2}$]	8
	Schedule	8:00-18:00 (Mon-Fri)
	Luminaire type	Suspended
	Radiant fraction	0.420
	Visible fraction	0.180

In tandem with the thermal simulation, a CFD model of the office space was generated using the respective computational application in DesignBuilder. Thermal simulation provided the external and internal surface temperatures as well as zone mean temperature as the boundary conditions for the CFD simulations. Rest of the required boundary conditions pertain to supply air diffuser and extract grilles have been defined based on the measurements of airflow rate and temperature. In fact, the central ventilation device was integrated into the existing monitoring network of TU Wien in order to capture all relevant system parameters of the ventilation system. Only the supply airflow direction definition was defined based on the assumptions.

The calibration process of the initial CFD simulation model involved an instance of time (i.e. 12 *pm*) of a single design day, 12.01.2013. Note that, this instance of time was under controlled measurement condition. Hence, small motion of occupants, if there was any, is negligible in the simulations. CFD predictions of airflow velocities and air temperatures were compared with measurements at multiple locations in the space (12 locations for air velocity and eight locations for air temperature). These locations of velocity and air temperature measurements (point v_1 to v_{12} , and θ_1 to θ_3 , respectively) are shown in Figure 3.11 and 3.12, respectively, which represent a vertical section through the space (section A-A, as marked in Figure 3.9). In addition, measured air temperature at workstations 1, 4, 6, 9, and 10 (Figure 3.9, *WS1*, *WS4*, *WS6*, *WS9*, and *WS10*) were also compared with the corresponding simulation results. The initial model was calibrated mainly by modifying the definition of the Y -discharge angle of the air diffusers.

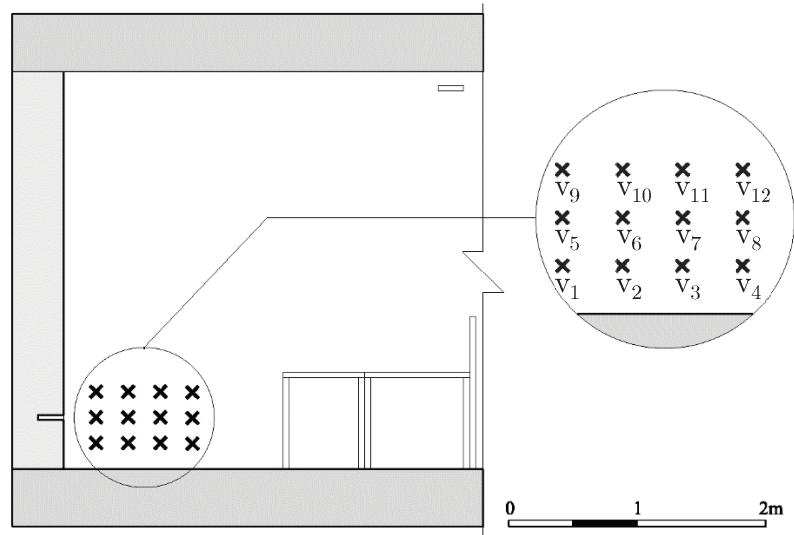


Figure 3.11: Positions of velocity measurements in the office space (section A-A, Figure 3.9)

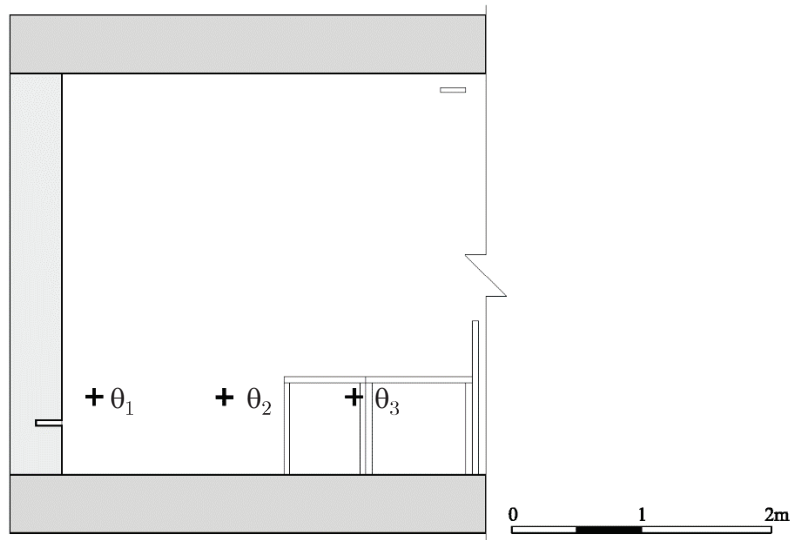


Figure 3.12: Positions of temperature measurements in the office space (section A-A, Figure 3.9)

3.3 Results and discussion

3.3.1 Laboratory

The airflow rate (in/out) and airflow temperature data was available for the duration of the study in the laboratory test room, i.e. lab cell 2. Table 3.8 demonstrates the measured boundary conditions for the CFD model generation. Note that, the CFD simulation is steady state, i.e. essentially the calculations involve a snap-shot in time. Thus, an average of the measured values of each measured boundary condition during the experiment period was used as the input value for the simulations.

Figure 3.13 and 3.14 illustrate the measured airflow speed and air temperature together with the corresponding initial simulation outcomes (see also Figure 3.6 and 3.7). Based on Figure 3.13 the measured air speed considerably differs at section B-B, in the middle of the diffuser, compared to the sides, i.e., section A-A and C-C. According to Figure 3.14 the simulated temperature is consistently lower than the actual air temperature. These results informed the aforementioned selection of the calibration variables and sequences.

Table 3.8: Boundary conditions of the initial model, defined based on the measurements in laboratory test room

Boundary type	Temperature [°C]	Flow rate [$\text{l}\cdot\text{s}^{-1}$]
Floor	21.7	-
Ceiling	24.6	-
Walls N	22.9	-
S	22.9	-
E	22.9	-
W	22.7	-
Window	22.9	-
Door	22.9	-
Supply diffuser	18.9	99
Extract grille	-	99

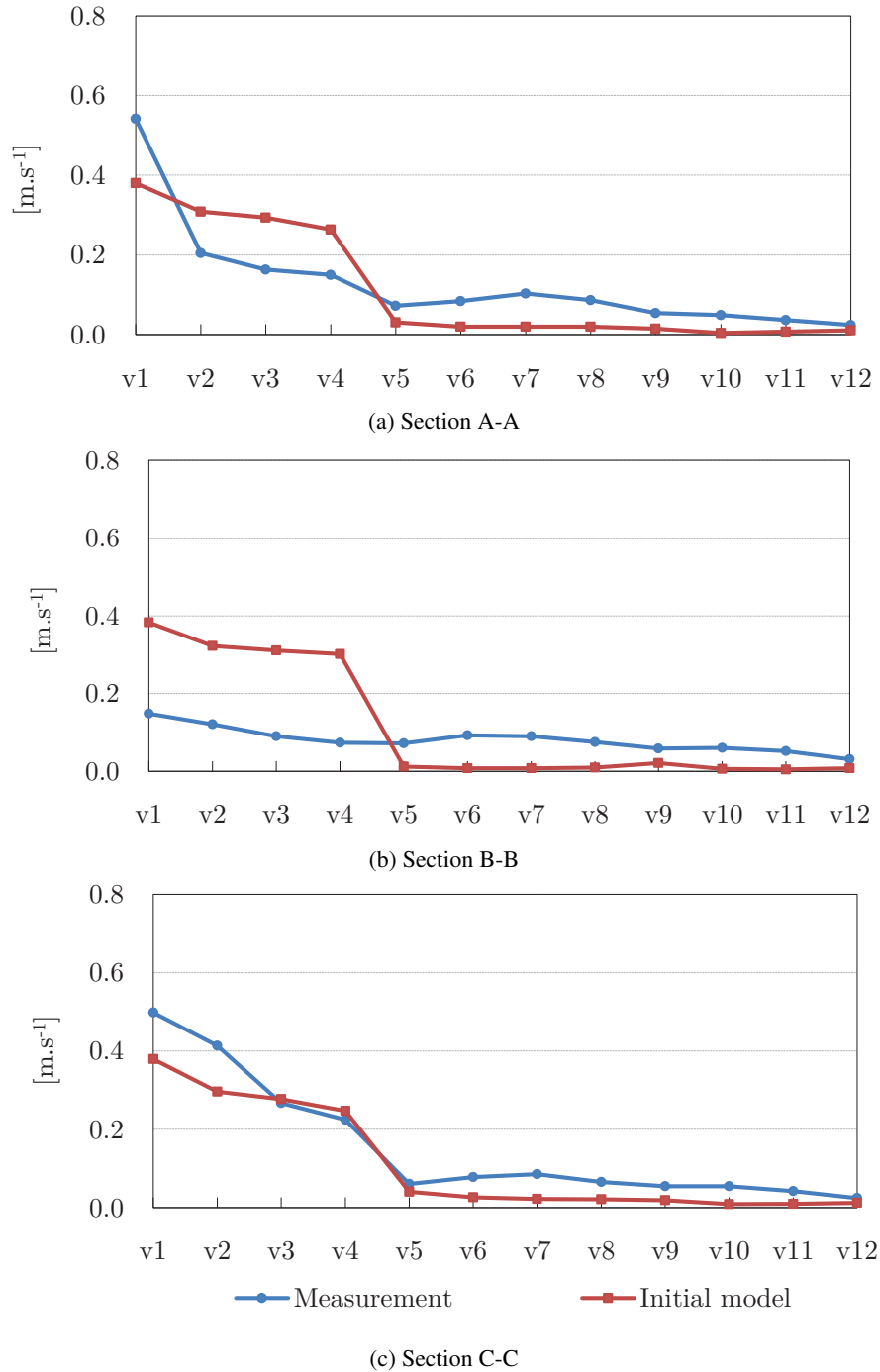
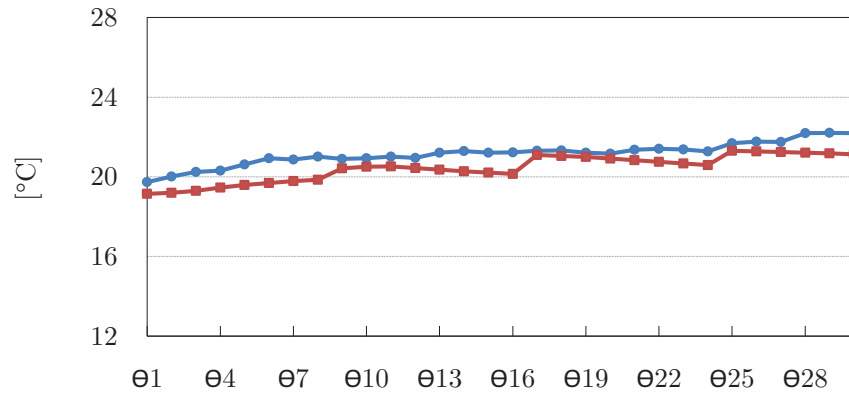
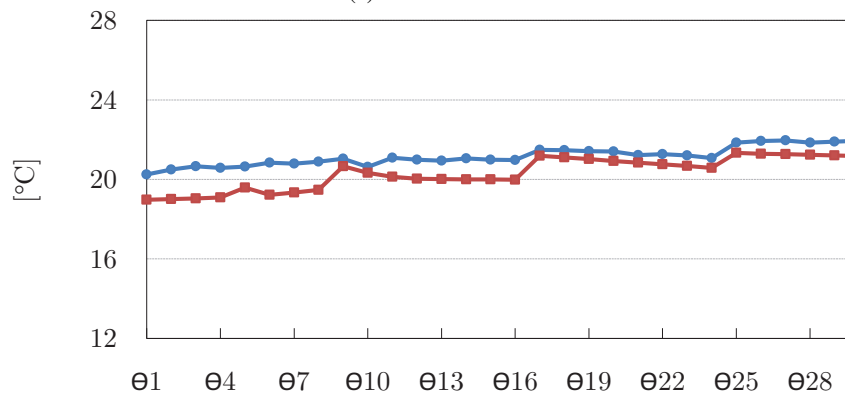


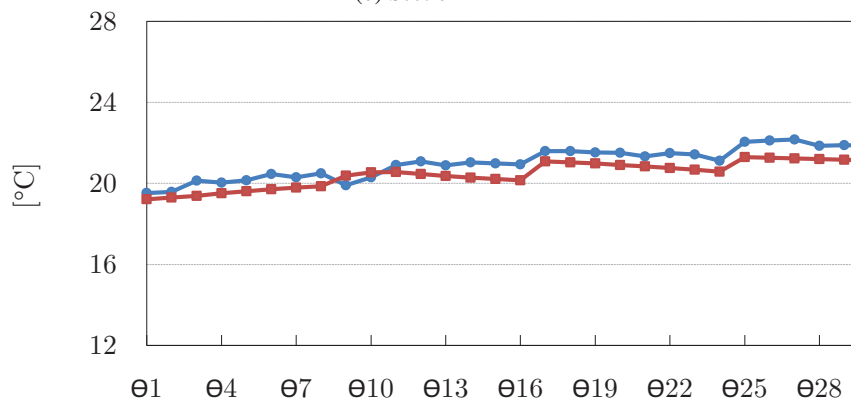
Figure 3.13: Measured and initially simulated velocity at positions v_1 to v_{12} in the laboratory test room (see Figure 3.6)



(a) Section A-A



(b) Section B-B



—●— Measurement —■— Initial model

(c) Section C-C

Figure 3.14: Measured and initially simulated temperature at positions θ_1 to θ_{30} in the laboratory test room (see Figure 3.7)

Table 3.9 summarizes the variables subjected to calibrations together with the initial and calibrated values at different calibration step.

Figure 3.15 and 3.16 compare the simulated airflow speed and temperature results of initial and calibrated models to measured values. Figure 3.15 reveals a considerable improvement in linear correlation between the calibrated and measured airflow speed values. The linear correlation between the calibrated and measured air temperature did not change significantly (Figure 3.16).

Table 3.9: Calibration variables in initial model and performed calibration steps

Model	Supply Diffuser	Flow rate [l.s ⁻¹]	X-discharge angle	X-discharge angle	Temperature [°C]	
Initial	SD	99	0	0	18.9	
Calibrated	Step 1	SD1	42	0	0	18.9
		SD2	12	0	0	18.9
		SD3	45	0	0	18.9
	Step 2	SD1	42	0	15	18.9
		SD2	12	-30	0	18.9
		SD3	45	-20	20	18.9
	Step 3	SD1	42	0	15	19.5
		SD2	12	-30	0	20.2
		SD3	45	-20	20	19.7

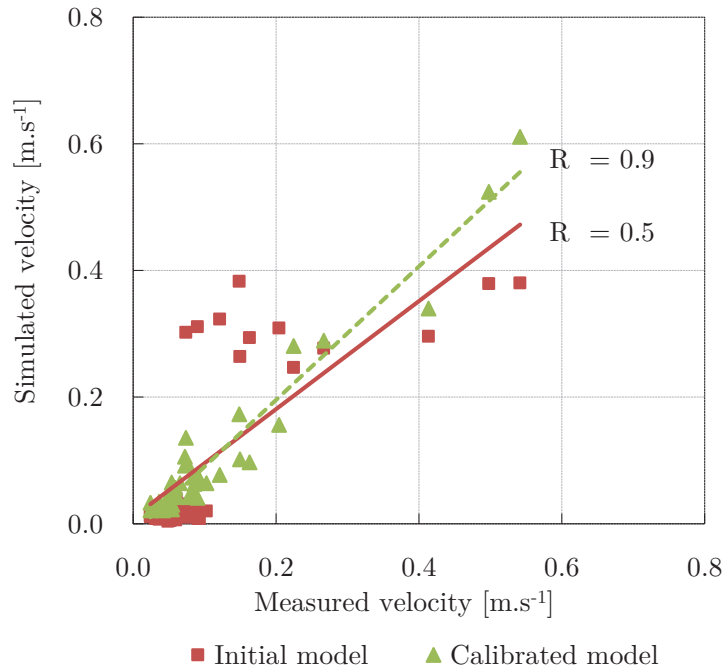


Figure 3.15: Measured versus simulated airflow speed in initial and calibrated model

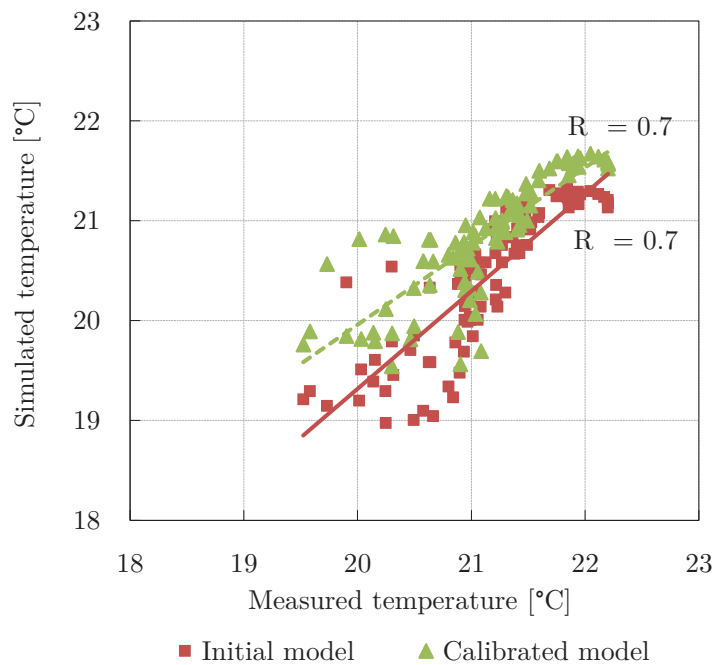


Figure 3.16: Measured versus simulated temperature in initial and calibrated model

Figure 3.17 illustrates the cumulative distribution of the velocity relative errors and Figure 3.18 shows the percentage of results within different bins of absolute error, for both the initial and the calibrated model. In case of the calibrated model, 85% of the calculated airflow speed rates display an absolute error less than $0.05 \text{ m}\cdot\text{s}^{-1}$. Such error magnitudes may be argued to be tolerable for many common applications of airflow field data in indoor environmental studies such as PMV calculations and human perception of the indoor climate (Loomans 1998).

Figure 3.19 shows the cumulative distribution of the temperature relative errors. In this case, 70% of the calculations display relative errors below 2%. This level of congruence would be acceptable for many application scenarios.

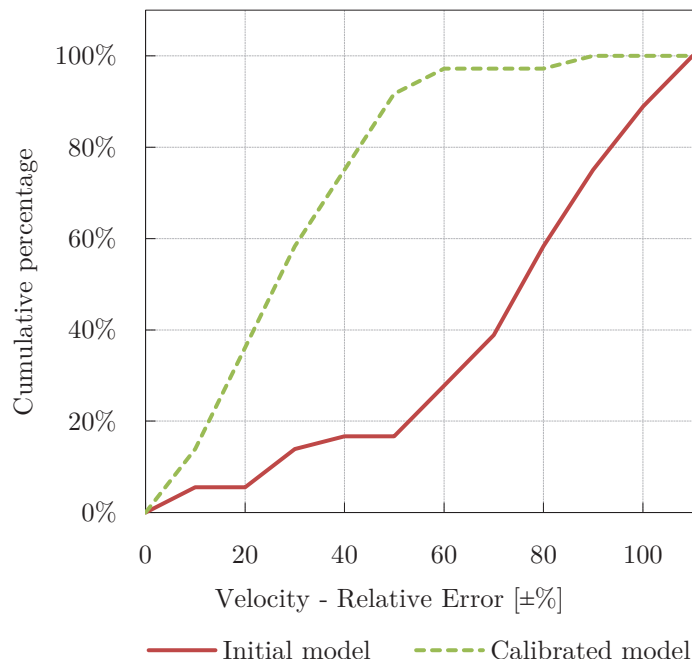


Figure 3.17: Cumulative distributions of velocity relative errors

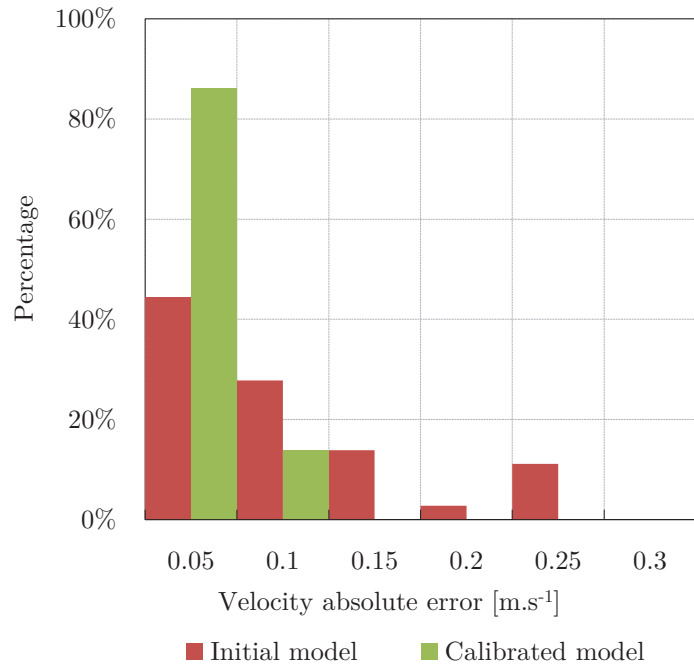


Figure 3.18: Absolute velocity error distributions

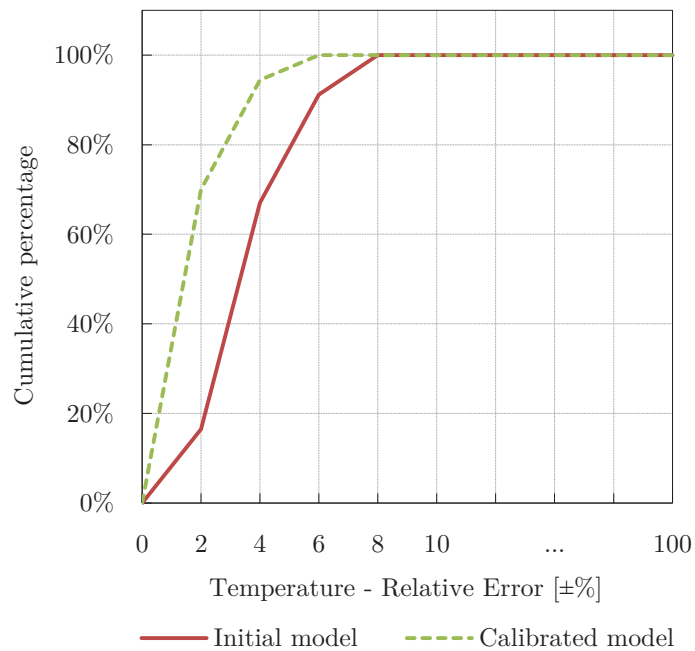


Figure 3.19: Cumulative distributions of temperature relative errors

3.3.2 Field office

Measurement results were used to set the airflow rate in and out as well as the supplied air temperature in CFD simulation model of the office space. Figure 3.20 and Table 3.10 present the detailed boundary conditions related to the flow rate in and out from the openings, supply diffusers and extract grilles in the office. Note that, in order to model the airflow in the space under the ventilation condition DV, the flow rate in and out of the other openings was set to zero. Moreover, an equal supply air temperature of 19.7 °C was assigned to the all seven supply diffusers. The surface temperature boundary conditions were also required for the simulation of the selected snap-shot in the time, i.e., January 12, 2013, 12:00 pm. Figure 3.21 demonstrates the related window in DesignBuilder CFD module to import the required temperature boundary conditions from the thermal simulation outcomes. Table 3.11 summarize the surface temperature boundary conditions for CFD simulations in this study.

Zone	Object	Boundary	Boundary Type	Flow In (l/s)	Flow Out (l/s)
Kriswang > Office	Wall	Window (External)	Window	0,000	0,000
Kriswang > Office	Partition	Hole (Internal)	Hole	0,000	0,000
Kriswang > Office	Partition	Hole (Internal)	Hole	0,000	0,000
Kriswang > Office	Partition	CFD Extract airflow boundary	Extract	0	19,730
Kriswang > Office	Partition	CFD Extract airflow boundary	Extract	0	19,730
Kriswang > Office	Wall	Window (External)	Window	0,000	0,000
Kriswang > Office	Wall	Window (External)	Window	0,000	0,000
Kriswang > Office	Wall	Window (External)	Window	0,000	0,000
Kriswang > Office	Wall	Window (External)	Window	0,000	0,000
Kriswang > Office	Wall	Window (External)	Window	0,000	0,000
Kriswang > Office	Wall	Window (External)	Window	0,000	0,000
Kriswang > Office	Wall	Window (External)	Window	0,000	0,000
Kriswang > Office	Wall	CFD Supply airflow boundary	Supply	13,160	0
Kriswang > Office	Wall	CFD Supply airflow boundary	Supply	10,670	0
Kriswang > Office	Wall	CFD Supply airflow boundary	Supply	13,160	0
Kriswang > Office	Wall	CFD Supply airflow boundary	Supply	11,510	0
Kriswang > Office	Wall	CFD Supply airflow boundary	Supply	14,800	0
Kriswang > Office	Wall	CFD Supply airflow boundary	Supply	13,160	0
Kriswang > Office	Wall	Window (External)	Window	0,000	0,000
Kriswang > Office	Wall	Window (External)	Window	0,000	0,000
Kriswang > Office	Wall	Window (External)	Window	0,000	0,000
Kriswang > Office	Wall	CFD Supply airflow boundary	Supply	5,760	0
Kriswang > Office	Wall	CFD Extract airflow boundary	Extract	0	11,520
Kriswang > Office	Wall	CFD Extract airflow boundary	Extract	0	10,690
Kriswang > Office	Wall	CFD Extract airflow boundary	Extract	0	9,040
Kriswang > Office	Partition	CFD Extract airflow boundary	Extract	0	11,510

Figure 3.20: Surface boundary conditions, flow balance specifications in DesignBuilder

Table 3.10: Boundary conditions pertain to supply diffusers (*SD1* to *SD7*) and extract grilles (*EG1* to *EG7*), defined based on measurements in the office space

Boundary type	ID	Flow rate [$\text{l}\cdot\text{s}^{-1}$]	Temperature [$^{\circ}\text{C}$]
Supply diffuser	SD1	13.16	19.70
	SD2	10.67	19.70
	SD3	13.16	19.70
	SD4	11.51	19.70
	SD5	14.80	19.70
	SD6	13.16	19.70
	SD7	5.76	19.70
Extract grille	EG1	19.73	-
	EG2	19.73	-
	EG3	11.51	-
	EG4	11.52	-
	EG5	10.69	-
	EG6	9.04	-

Table 3.11: Boundary conditions pertain to surface temperatures, imported from the thermal simulation outcomes

Boundary type	Temperature [$^{\circ}\text{C}$]
Floor	23.40
Ceiling	23.30
Walls	22.55/ 22.55/ 22.56
Partitions	22.58/ 23.62/ 18.74
Hole	26.25
Windows	23.58/ 22.51/ 22.50/ 22.50/ 22.50/ 22.50/ 22.50/ 22.53/ 26.90/ 26.89/ 26.89

3. Computational indoor climate assessment

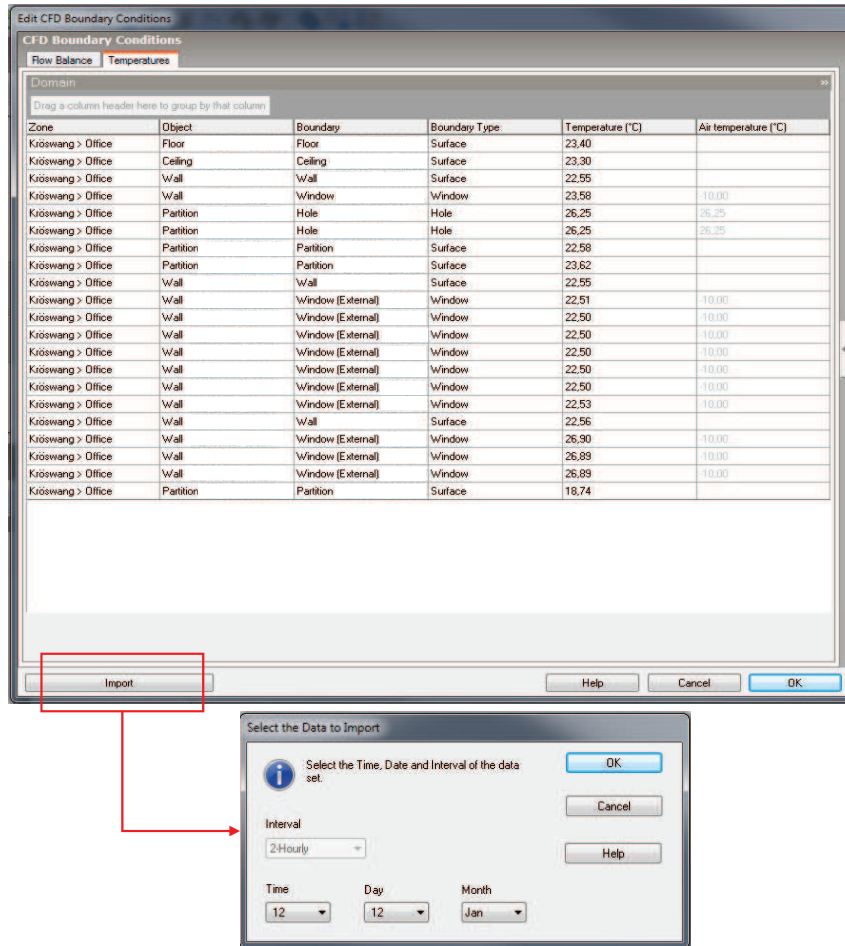


Figure 3.21: Importing surface boundary conditions from thermal simulation outcomes to the CFD simulation model in DesignBuilder

The initial CFD model was calibrated mainly by modifying the definition of the Y discharge angle of the air diffusers, which demonstrated a downward flow direction instead of the initial assumed horizontal flow. Figure 3.22 and 3.23 compare the initial and calibrated CFD model predictions of airflow speed and air temperature with measurements at multiple locations (see Figure 3.11 and 3.12). Note that, the results demonstrate higher differences between the measured and simulated airflow speed at locations v_1 , v_2 and v_3 . Given the downward discharge angle of the air diffusers, these locations may have been subjected to stronger turbulence. Figure 3.22 shows higher agreement between measurements and simulations at locations further away from the supply diffuser.

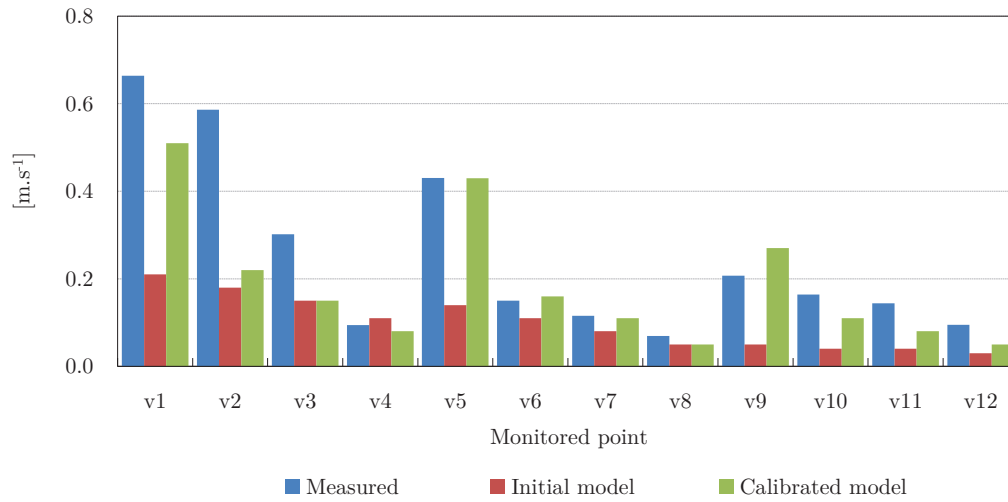


Figure 3.22: Measured values of airflow speed for specific positions in the office space (see Figure 3.11) together with corresponding CFD simulation results (both before and after calibration)

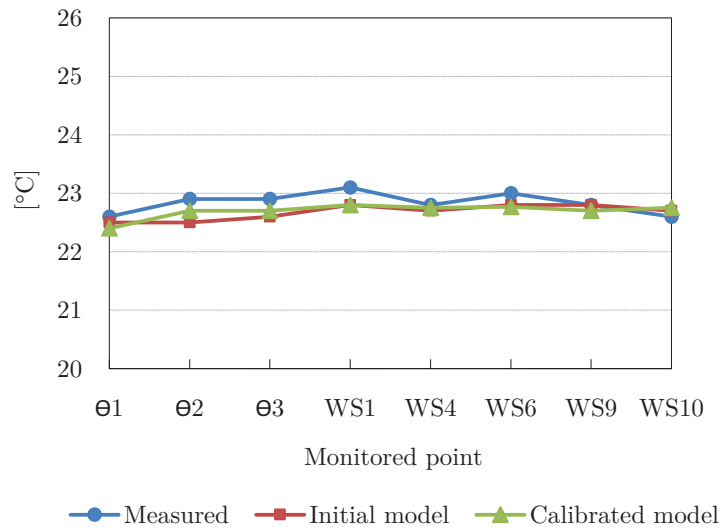
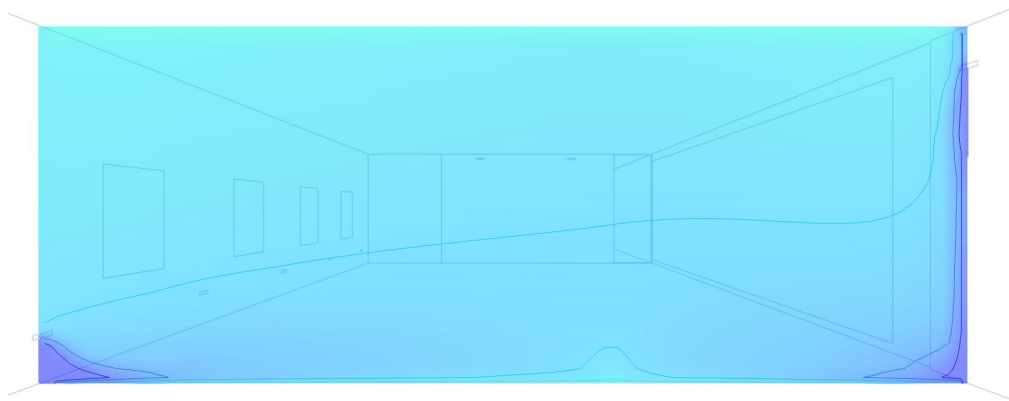


Figure 3.23: Measured values of air temperature for specific positions in the office space (see Figure 3.9 and Figure 3.12) together with corresponding CFD simulation results (both before and after calibration)

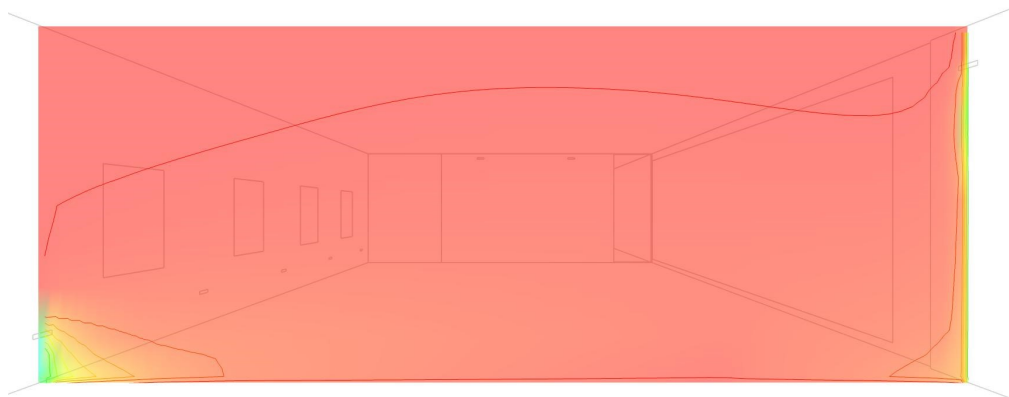
Following the CFD simulations, temperature and velocity were plotted in terms of planar slices through the space. The chromatic legends in the following figures illustrate the scale for temperature and velocity plots. According to the previous studies, the locations in the space with air velocity higher than $0.25 \text{ m}\cdot\text{s}^{-1}$ should not be occupied. Therefore, the maximum value for the velocity illustration has been set to 0.25.

Figures 3.24 and 3.25 illustrate the simulated air temperature and velocity distribution across a vertical plane perpendicular to a supply diffuser (section B-B, Figure 3.9), for winter and summer. According to Figures 3.24, the temperature stratification between the floor level and the occupants breathing zone is not considerable. In fact, the temperature difference is not enough to encourage the users to use the ductless PVs in order to transfer the cool and fresh air to their breathing zone (considering that the workstations are mostly equipped with ductless PVs). This result may explain the lower rate of ductless-PV usage by the occupants. The plots presenting the velocity distribution illustrate that the area close to the supply diffuser should not be occupied. This condition is already met in the actual office layout.

In this study, occupied locations with PMV ranging from -0.5 to +0.5 have been considered satisfactory. CFD-based PMV calculations suggest that the DV operation can provide a thermally comfortable environment (PMV around 0.14 in winter, and 0.23 in summer). The PMV results in summer present a slightly warmer indoor environment. The indoor temperature and PMV results may help explain the higher frequency of PV usage in the months of August and September (see Figure 2.21). The capacity of ducted PV stations to supply cooler and fresh air in warmer months would encourage higher usage rates.



(a) Winter condition



(b) Summer condition

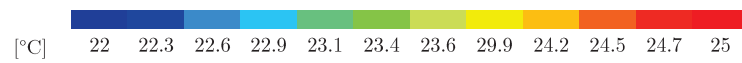


Figure 3.24: Air temperature in (a) winter and (b) summer conditions (section B-B, Figure 3.9)

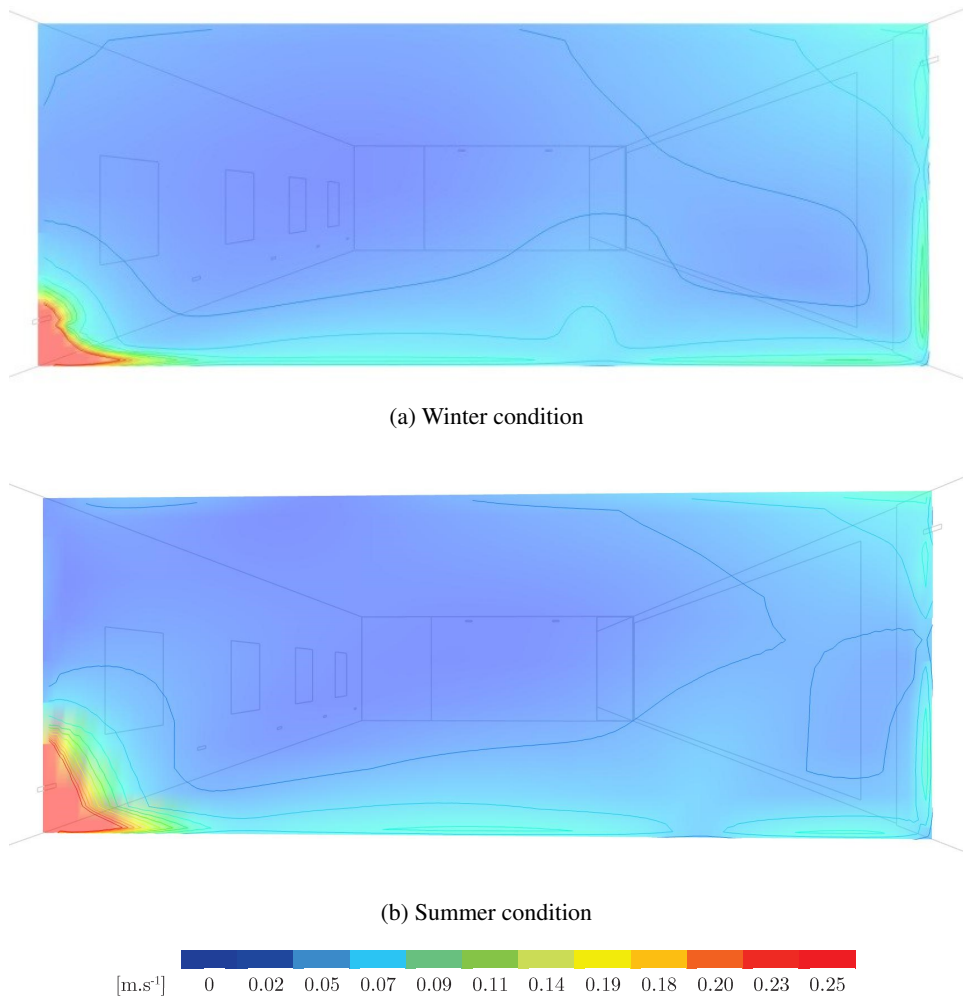


Figure 3.25: Velocity distribution in (a) winter and (b) summer conditions (section B-B, Figure 3.9)

3. Computational indoor climate assessment

Figure 3.26 presents the temperature and velocity distribution (summer conditions) across a vertical plane perpendicular to diffuser wall, but with a distance from the diffuser location (section C-C, Figure 3.9). This view displays slightly higher temperatures, insufficient vertical temperature stratification, and lower velocities.

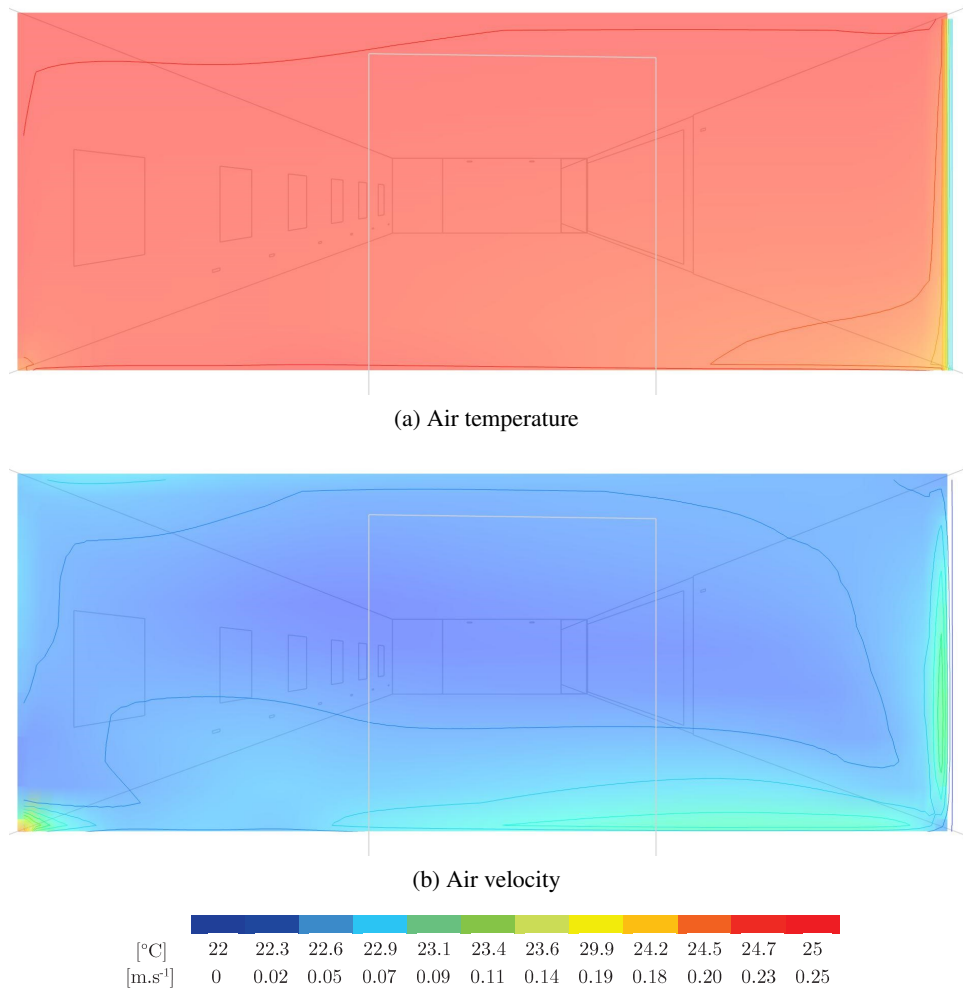


Figure 3.26: Air temperature and velocity distribution, summer conditions (section C-C, Figure 3.9)

The results provided here imply a couple of conclusions regarding the present ventilation system design in the office under study:

- The supply airflow rate and temperature cannot provide the temperature stratification level required for ductless PV application.
- The temperature distribution across the workstations (considering their distance and location relative to the supply diffusers) is rather non-uniform.

In the light of these observations, an alternative supply diffuser design was considered (Figure 3.27). The aim was to provide a more uniform temperature and velocity distribution across the workstations. Therefore, one linear supply diffuser along the western outside wall of the office at the height of 0.05 m from the floor level was modelled (width = 0.04 m). In the first set of simulations, the supply airflow rate and temperature are equal to the actual model in summer condition, i.e. 82.2 l.s^{-1} and $21\text{ }^{\circ}\text{C}$.

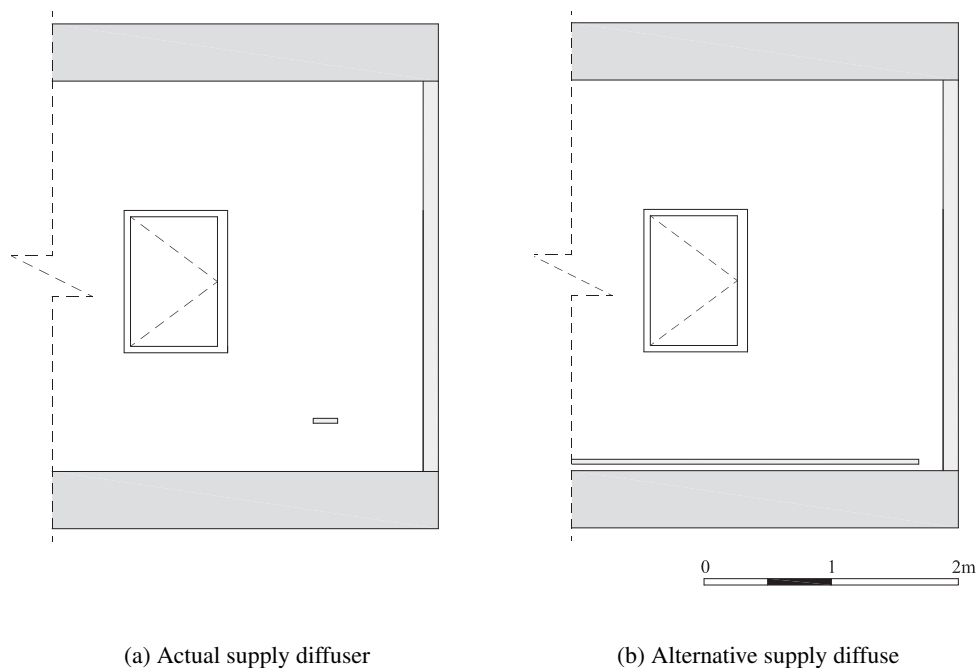


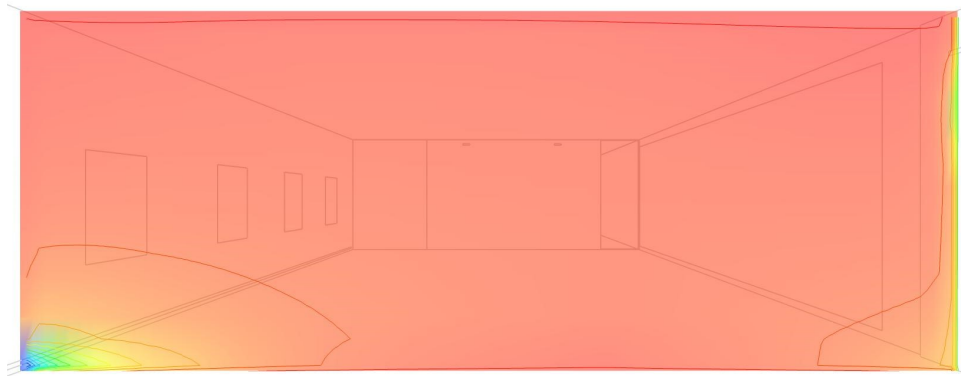
Figure 3.27: Illustration of the (a) actual and (b) alternative supply diffuser design (section D-D, Figure 3.9)

Figure 3.28 presents the air temperature and velocity results obtained from the CFD simulation (at section B-B, Figure 3.9). In this case too, the temperature stratification does not meet the PV application requirements. Hence, higher airflow rates and lower supply temperatures were considered. Assuming a ventilation rate equal to 4 air change per hour, the supply flow would be 480 l.s^{-1} . In addition, the supply air temperature was set to $18 \text{ }^\circ\text{C}$. The corresponding results are displayed in Figure 3.29, indicating a more uniform temperature and velocity distribution throughout the space. In addition, this most recent configuration yields a more pronounced vertical temperature distribution. Note that, in both cases the calculated PMV values in the occupied locations were in the defined acceptable range ($-0.5 < \text{PMV} < +0.5$).

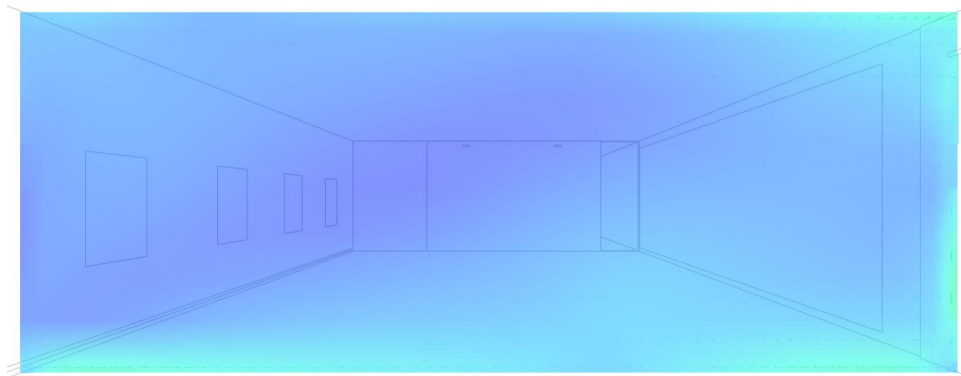
As past research has shown, achievable air quality improvement via PV systems depends on different parameters including the PV airflow rate and direction as well as the temperature difference between the PV air jet and the room air temperature. For instance, supply air temperature has been recommended to be 3 to 4 degrees cooler than the room air (Melikov 2004). This corresponds to conditions as in ducted PVs of our case, and is consistent with their more frequent operation by the occupants (as compared to the ductless PVs).

3.3.3 Concluding observations

This section presented CFD-based indoor airflow simulations assisted by monitored data to generate an accurate initial model as well as supporting simulation model calibration. The results presented here suggest that the predictive performance of CFD-simulations can be improved by systematic calibration procedures. Study of the temperature stratification in the field office model illustrated that the supply airflow rate and temperature cannot provide the temperature stratification level required for ductless PV application. Calibrated model assisted systematic investigation of different design alternatives and their implications for indoor environmental variables. Based on the observations an alternative supply diffuser configuration was explored. The CFD simulation outcomes suggest that higher difference between the room and supply air temperature as well as higher displacement supply airflow rate could provide the required temperature stratification for ductless PVs. In addition, the modified configuration resulted in a more uniform temperature and velocity distribution across the office space.



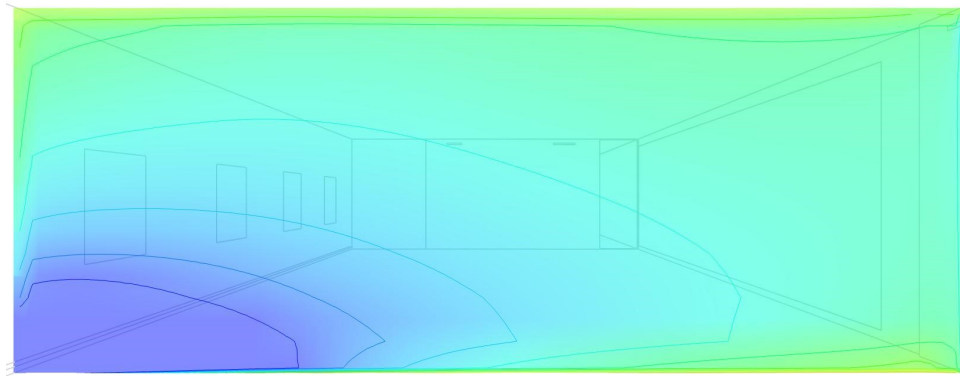
(a) Air temperature



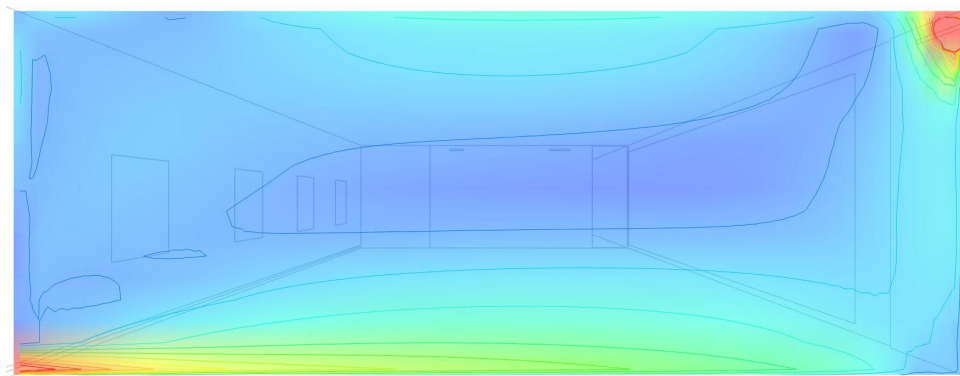
(b) Air velocity

[°C]	22	22.3	22.6	22.9	23.1	23.4	23.6	23.9	24.2	24.5	24.7	25
[m.s ⁻¹]	0	0.02	0.05	0.07	0.09	0.11	0.14	0.19	0.18	0.20	0.23	0.25

Figure 3.28: (a) Air temperature and (b) velocity in summer conditions (with original supply flow rate and temperature), (section B-B, Figure 3.9)



(a) Air temperature



(b) Air velocity

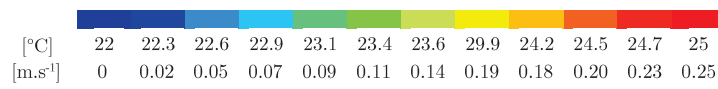


Figure 3.29: (a) Air temperature and (b) velocity in summer conditions (with modified supply flow rate and temperature), (section B-B, Figure 3.9)

Chapter 4

An Examination of the Reliability of Common Thermal Comfort Indicators

4.1 Background

Thermal comfort calculations that use environmental variables as input can facilitate indoor climate and thermal comfort evaluations (Bordass and Leaman 2009). The Predicted Mean Vote (PMV) model is a well-known thermal comfort model developed by Fanger 1970 on the basis of laboratory studies. In this model, thermally adapted occupant is assumed to be comfortable when the heat exchange between the human body and the thermal environment is in thermal balance. PMV is the most commonly used model to evaluate the human perception of thermal comfort (Fanger 1970). PMV index predicts the mean response of a large group of people on the ASHRAE thermal sensation scale based on the heat balance of the body (ASHRAE 2004). Human body's thermal balance happens when the heat loss to the environment is equal to the heat produced internally. The body automatically modifies the skin temperature to achieve the heat balance (EN ISO 7730 2005). Thereby, the heat generation is equal to the heat loss. The comfort equation or energy balance equation can be written as (Fanger 1970):

$$M - W = H - E_c + C_{res} + E_{res} \quad (4.1)$$

where:

$$H = 3.96 \times 10^{-8} f_{cl} [(t_{cl} + 273)^4 - (t_r + 273)^4] + f_{cl} h_c (t_{cl} - t_a), \quad (4.2)$$

$$E = 3.05 \times 10^{-3} [5733 - 6.99(M - W) - p_a] + 0.42(M - W - 58.15), \quad (4.3)$$

$$C_{res} = 0.0014M(34 - t_a), \quad (4.4)$$

$$E_{res} = 1.7 \times 10^{-5} M(34 - t_a). \quad (4.5)$$

In the above equations:

M denotes the metabolic rate [$W.m^{-2}$]¹,

W is the external work [$W.m^{-2}$],

H is the dry heat loss [$W.m^{-2}$],

E_c is the heat exchange by evaporation on the skin [$W.m^{-2}$],

C_{res} is the heat exchange by convection in breathing [$W.m^{-2}$],

E_{res} is the evaporative heat exchange in breathing [$W.m^{-2}$],

f_{cl} is the clothing surface area factor,

t_{cl} is the clothing surface temperature [$^{\circ}C$],

t_r is the mean radiant temperature [$^{\circ}C$],

h_c is the convective heat transfer coefficient [$W.m^{-2}.K^{-1}$],

t_a is the air temperature [$^{\circ}C$],

P_a is the water vapour partial pressure [Pa],

¹ 1 metabolic unit = 1 met = 58.2 ($W.m^{-2}$)

4. An examination of the reliability of common thermal comfort indicators

Calculation of PMV involves four environmental parameters, i.e., air temperature, mean radiant temperature, relative humidity, and air velocity, together with two personal factors, i.e., metabolic rate and clothing value. These factors are used in order to predict the average thermal sensation vote of a large number of subjects using the ASHRAE thermal sensation scale (ASHRAE 2004) (Figure 4.1). The seven point thermal sensation scale includes, hot (+3), warm (+2), slightly warm (+1), neutral (0), slightly cool (-1), cool (-2), and cold (-3) (see also Table 2.1). In a given space, PMV ranging from -0.5 to +0.5 can be considered satisfactory. PMV equal to zero means that combination of environmental parameters and the occupants' clothing and activity lead to a thermally neutral sensation (EN ISO 7730 2005). However, due to the differences between individuals and differences in perception of thermal comfort, there might be still some people dissatisfied with their environment.

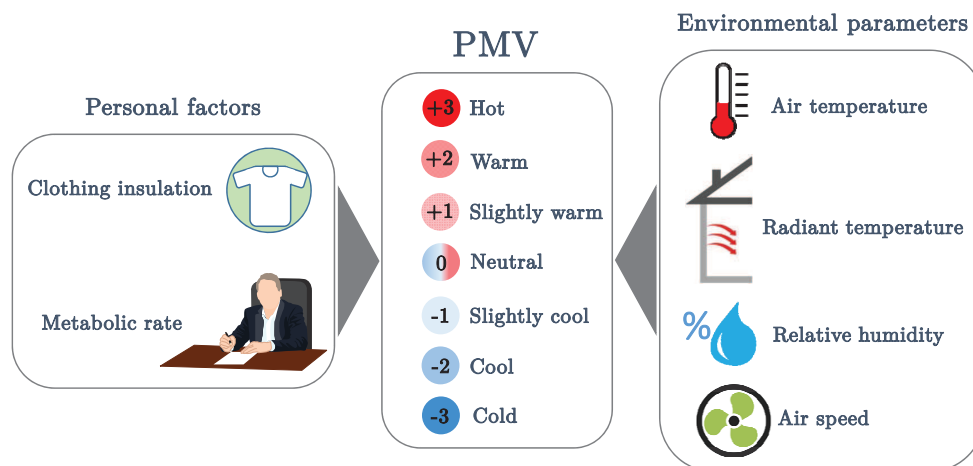


Figure 4.1: Six factors involved in PMV calculation

Fanger 1970 connected the PMV to the human body's thermal imbalance. Considering the imbalance between the required heat flow for thermal comfort and the heat flow from the human body, using personal and the environmental parameters, PMV equation is calculated as following (Fanger 1970):

$$PMV = (0.303 e^{-0.036M} + 0.028) [(M - W) - H - E_c - C_{res} - E_{res}] \quad (4.6)$$

Equations 4.2 to 4.5 together with Equation 4.6 result in Equation 4.7:

$$PMV = (0.303 e^{-0.036M} + 0.028) \{ (M - W) - 3.05 \times 10^{-3} \times [5733 - 6.99(M - V) - p_a] - 0.42 [(M - W) - 58.15] - 1.7 \times 10^{-5} M (5876 - p_a) + 0.0014 M (34 - t_a) - 3.96 \times 10^{-8} f_{cl} [(t_{cl} + 273)^4 - (\bar{t}_r + 273)^4] - f_{cl} h_c (t_{cl} - t_a) \} \quad (4.7)$$

where:

$$t_{cl} = 35.7 - 0.28(M - W) - l_{cl} \times \{ 3.96 \times 10^{-8} f_{cl} [(t_{cl} + 273)^4 - (t_r + 273)^4] + f_{cl} h_c (t_{cl} - t_a) \}, \quad (4.8)$$

$$h_c = \begin{cases} \text{if } 2.38 |t_{cl} - t_a|^{0.25} > 12.1 \sqrt{v_{ar}} \rightarrow & 2.38 |t_{cl} - t_a|^{0.25} \\ \text{if } 2.38 |t_{cl} - t_a|^{0.25} \leq 12.1 \sqrt{v_{ar}} \rightarrow & 12.1 \sqrt{v_{ar}}, \end{cases} \quad (4.9)$$

$$f_{cl} = \begin{cases} \text{if } l_{cl} \leq 0.078 (m^2.K.W^{-1}) \rightarrow & 1.00 + 1.29 l_{cl} \\ \text{if } l_{cl} > 0.078 (m^2.K.W^{-1}) \rightarrow & 1.05 + 0.645 l_{cl}, \end{cases} \quad (4.10)$$

$$v_{ar} = v_a + 0.005 \left(\frac{M}{A_{du}} - 58.15 \right), \quad (4.11)$$

l_{cl} is the clothing insulation [$m^2.K.W^{-1}$]¹, v_{ar} is the relative air velocity [$m.s^{-1}$], and A_{du} is the Dubois body surface area [m^2]. EN ISO 7730 2005 suggests to use the above mentioned PMV index for PMV ranging from -2 to +2 and when the main influencing parameters are within the ranges presented in Table 4.1.

¹ 1 clothing unit = 1 clo = 0.155 ($m^2.K.W^{-1}$)

Table 4.1: Main parameters for PMV calculations and their acceptable ranges

Parameter	Range	Unit
Metabolic rate [M]	0.8 to 4	met
Clothing insulation [I_{cl}]	0 to 2	clo
Air temperature [t_a]	10 to 30	°C
Mean radiant temperature [t_r]	10 to 40	°C
Air velocity [v_{ar}]	0 to 1	m.s ⁻¹
Water vapour partial pressure [P_a]	0 to 2700	Pa

4.2 Method

4.2.1 Overview

This section explores the utility of PMV for thermal comfort assessments in spaces equipped with DV and PV systems and tries to address the question, if PMV represents a viable indicator for the evaluations. The respective PMV values were calculated for two case studies of this research, i.e. laboratory and field office space, and were compared with the actual TSVs.

4.2.2 Laboratory experiment

Laboratory experiments involved two ventilation conditions PV and DPV. 26 students (13 male and 13 female, average age of 23 years old) participated in the experiment. Details of the experiment is fully discussed in Section 2.2.2.1. To obtain the environmental parameters required for PMV calculations, a precise thermal comfort sensor setup (Figure 2.6) was used to measure air temperature, mean radiant temperature, relative humidity, and air velocity near occupants. Moreover, the metabolic rate of occupants was assumed to be 1.2 Met (office work, seated) (ASHRAE 2005). Thermal resistance of the participants clothing was documented in the experiments (Figure 2.5).

4.2.3 Field experiment

To explore the utility of PMV the respective values were calculated for the aforementioned two full-day experiments in the office space, presented in Section 2.2.3.1. This includes the full-day experiments on two occasions 12.01.2013 and 10.08.2013, involving a small group of visiting individuals. As discussed before on each day, two distinct ventilation schemes were compared. One scheme involved DV alone, whereas the second scheme involved DV plus PV (DPV). For the purpose of PMV calculations, the metabolic rate of occupants was assumed to be 1.2 Met. Thermal resistance of the participants clothing was determined based on visual observation. For the period with combined operation of DV and PV, it was possible to use a precise thermal comfort sensor setup to measure humidity, air temperature, mean radiant temperature, and airflow velocity at the workstations. For the periods with only DV operating, the measured data provided the required temperature and humidity information (see Section 2.2.3.2), while the airflow velocity and mean radiant temperature had to be derived from the CFD simulation.

4.2.4 PMV versus TSV

The calculated PMV values were subsequently compared with the participants' expressed TSVs. Note that, the TSV's of each participant was compared with the PMV, calculated based on the environmental parameters, at the time when the survey was conducted (see also Sections 2.2.2.1 and 2.2.3.1).

4.3 Results and discussions

4.3.1 Laboratory experiment

Tables 4.2 and 4.3 demonstrate the values of required input data for the PMV calculations together with the respective calculated PMV values, from the experiments in laboratory test rooms with ducted and ductless PV, respectively.

Figure 4.2 shows a comparison between participants' expressed TSV and corresponding calculated PMV values for ducted and ductless workstations. As Figure 4.2 illustrates, calculated PMVs do not reflect the larger spread of the TSV results. Moreover, the room with the ducted PV is predicted to be warmer than it is perceived by participants (as reflected in their TSV results).

Table 4.2: Input data required for PMV calculations and respective calculated PMV values for the experiments in lab cell 1 with ducted PV

Experiment No.	θ [°C]	MRT	RH [%]	v [m.s ⁻¹]	Met	clo	PMV
1	26.4	26.8	38.9	0.03	1.2	1.6	1.4
2	27.4	27.6	37.3	0.03	1.2	0.4	0.7
3	28.3	28.5	33.4	0.03	1.2	0.5	1.1
4	27.2	27.5	31.4	0.03	1.2	1.0	1.2
5	27.7	28.1	32.1	0.03	1.2	0.6	0.9
6	28.3	28.6	30.1	0.02	1.2	1.0	1.4
7	26.2	26.3	38.1	0.04	1.2	1.0	1.0
8	26.0	26.2	33.8	0.03	1.2	0.8	0.7
9	27.2	27.5	32.1	0.04	1.2	0.6	0.8
10	26.4	26.5	31.9	0.04	1.2	0.4	0.3
11	27.0	27.3	31.2	0.02	1.2	0.8	1.0
12	27.6	27.9	28.7	0.03	1.2	0.4	0.6
13	27.1	27.3	328.8	0.02	1.2	0.5	0.7

Table 4.3: Input data required for PMV calculations and respective calculated PMV values for the experiments in lab cell 2 with ductless PV

Experiment No.	θ [°C]	MRT	RH [%]	v [m.s ⁻¹]	Met	clo	PMV
1	26.7	26.8	37.8	0.03	1.2	0.4	0.4
2	27.5	27.6	36.9	0.04	1.2	0.4	0.6
3	28.2	28.3	36.0	0.06	1.2	0.3	0.8
4	27.4	27.5	30.9	0.04	1.2	0.8	1.0
5	28.0	28.2	32.5	0.04	1.2	0.8	1.2
6	28.7	28.8	36.7	0.02	1.2	0.5	1.2
7	26.4	26.5	35.8	0.05	1.2	0.6	0.6
8	27.9	28.0	38.0	0.06	1.2	0.6	1.0
9	26.4	26.4	36.4	0.04	1.2	0.6	0.6
10	27.4	27.5	31.3	0.06	1.2	0.5	0.8
11	27.2	27.3	30.6	0.04	1.2	0.5	0.7
12	27.9	28.0	31.2	0.04	1.2	0.5	0.9
13	27.5	27.5	33.4	0.06	1.2	1.1	1.3

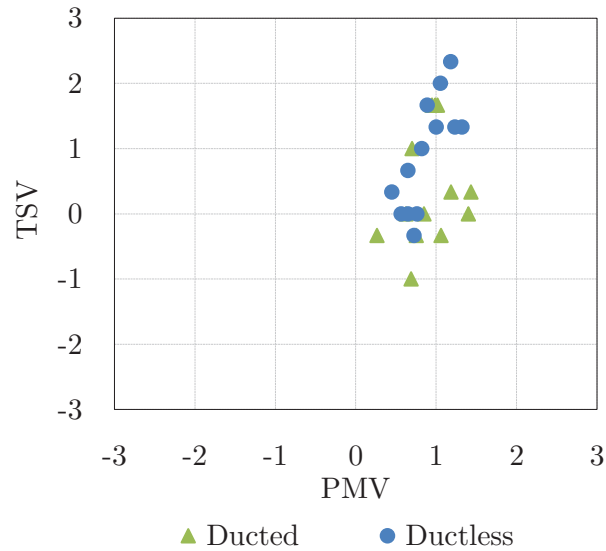


Figure 4.2: The calculated PMV and actual TSV of the participants of the laboratory experiment

4.3.2 Field experiment

Tables 4.4 and 4.5 present the required input data values for the PMV calculations together with the respective calculated PMV values, for the field experiments under the ventilation regime DV and DPV, respectively.

The result of subjective evaluations pertained to TSVs are compared to the calculated PMVs. Figures 4.3 and 4.4 show participants' expressed TSV and the corresponding calculated PMV. The actual TSVs are mostly lower than the calculated PMVs (especially in winter). PMV calculations involve some uncertainties, given the absence of precise information concerning the prevailing airflow velocities and the participants' clothing attributes. In our case (see description in Section 4.2.3 above), airflow speed input data for PMV calculations in case of ventilation conditions DV and DPV was derived using a calibrated CFD model and actual air velocity measurements, respectively.

4. An examination of the reliability of common thermal comfort indicators

Table 4.4: Input data required for PMV calculations together with respective calculated PMV values under the ventilation regime DV

Date	No.	θ [°C]	MRT	RH [%]	v [m.s ⁻¹]	Met	clo	PMV
12.01.2013	1	23.25	23.58	33.3	0.1	1.2	1.2	0.5
	2	23.25	23.58	33.3	0.1	1.2	0.8	0.04
	3	23.25	23.58	33.3	0.1	1.2	0.8	0.04
	4	23.2	23.59	32.9	0.02	1.2	0.8	0.09
	5	23.2	23.59	32.9	0.02	1.2	1.2	0.55
	6	23.2	23.59	32.9	0.02	1.2	0.8	0.09
10.08.2013	1	25.7	26.25	52.37	0.09	1.2	0.8	0.82
	2	25.7	26.25	52.37	0.09	1.2	0.8	0.82
	3	25.7	26.25	52.37	0.09	1.2	0.8	0.82
	4	26	26.29	51.9	0.07	1.2	0.5	0.51
	5	26	26.29	51.9	0.07	1.2	0.5	0.51
	6	26	26.29	51.9	0.07	1.2	0.5	0.51

Table 4.5: Input data required for PMV calculations together with respective calculated PMV values under the ventilation regime DPV

Date	No.	θ [°C]	MRT	RH [%]	v [m.s ⁻¹]	Met	clo	PMV
12.01.2013	1	22.86	23.47	31.2	0.15	1.2	1.2	0.36
	2	22.86	23.47	31.2	0.15	1.2	0.8	-0.15
	3	22.86	23.47	31.2	0.15	1.2	0.8	-0.15
	4	22.9	23.39	32.1	0.07	1.2	0.8	0.02
	5	22.9	23.39	32.1	0.07	1.2	1.2	0.49
	6	22.9	23.39	32.1	0.07	1.2	0.8	0.02
10.08.2013	1	25.4	26.31	46.6	0.16	1.2	0.8	0.61
	2	25.4	26.31	46.6	0.16	1.2	0.8	0.61
	3	25.4	26.31	46.6	0.16	1.2	0.8	0.61
	4	25.5	26.37	47.9	0.275	1.2	0.5	-0.04
	5	25.5	26.37	47.9	0.275	1.2	0.5	-0.04
	6	25.5	26.37	47.9	0.275	1.2	0.5	-0.04

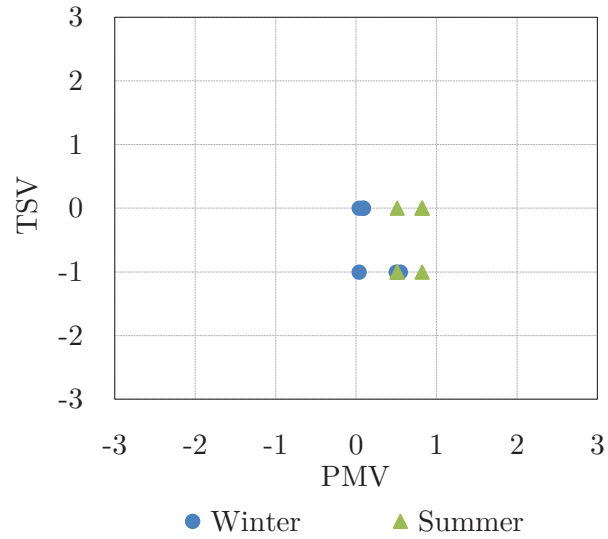


Figure 4.3: The calculated PMV and actual TSV of a small group of visiting participants under the ventilation regime DV

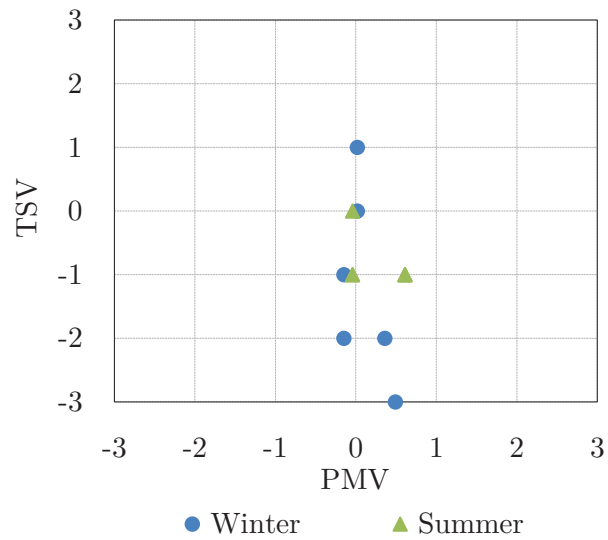


Figure 4.4: The calculated PMV and actual TSV of a small group of visiting participants under the ventilation regime DPV

4.3.3 Concluding observations

Comparison of the actual TSVs and calculated PMVs suggested that the application of PMV calculations for the conception and configuration of PV and DV systems may be problematic. According to the results provided here calculated PMVs, either with measured or simulated airflow velocity input, are usually higher than the actual TSVs. Moreover, based on the presented results calculated PMVs do not reflect the larger spread of the TSV results. As discussed before, in thermal comfort assessments by PMV calculations human factors such as physiological and psychological factors are not directly considered. Even though PMV is among the most recognized thermal comfort models, absence of these factors especially in rather more complex and non-uniform indoor environments can result to imperfect and misleading assumptions on thermal sensation.

Chapter 5

Parametric Assessment of Airflow Conditions Based on a Limited Set of CFD-based Simulation Runs

5.1 Background

Computational fluid dynamics (CFD) represents an effective method for indoor environmental studies. There have been many studies on the potential of CFD to assist building performance analysis and indoor air quality assessments (see, for instance, Chen and Zhai 2004, Meroney 2009, Wiercinski and Skotnicka-Siepsiak 2008, Taheri et al. 2016). CFD enables prediction of field properties such as air temperature and velocity in an architectural space by means of numerical methods (Chen and Srebric 2002). Instances of CFD application in building performance studies address heating, cooling, and ventilation systems designs, airflow pattern and velocity analysis, thermal comfort evaluations, and indoor air quality assessments. In fact, many cases of such studies would not be feasible without CFD (Wiercinski and Skotnicka-Siepsiak 2008). The application of CFD requires a fair amount of knowledge and experience. Specialized CFD packages (e.g., ANSYS Fluent, CLIMA 3D, PHOENICS, and STREAM) provide solutions for a wide range of fluid flow studies and advanced fluid mechanics problems (Chowdhury et al. 2010). One concern, when using the advanced-conventional CFD packages, is the extensive level of required expertise and effort. Proper use of CFD requires knowledgeable specialists (den Hartog et al. 2000). Consequently, easy-to-use CFD modelling packages have been developed (see, for example, DesignBuilder 2011*a*). Nonetheless, CFD simulations require large amount of time when conducting parametric

studies of alternative design and configuration options.

5.2 Method

5.2.1 Overview

This section investigates how a relatively comprehensive impact assessment of various design variables and input assumptions (e.g., number and location of diffusers and airflow rates in an architectural space) can be based on a detailed but small number of numerical simulations. In fact, the present section explores the following research question: Is it possible to obtain the basic airflow field information for a large variety of design configurations based on a small number of full-fledge CFD simulation runs? If possible, this approach would allow for an efficient deployment of advanced numerical simulation pertaining to the evaluation of airflow patterns in indoor environments. To explore the above mentioned research question, a number of variations of the design variables (i.e. airflow rates and diffuser configurations) of a basic room model were considered. Then, simple combinatorial manipulation options of a limited set of respective CFD simulation results were applied to estimate the airflow speed data for a larger set of design options.

5.2.2 CFD modelling scenarios

The study started with a shoebox model, i.e., a simple rectangular zone (width = 4 m, length = 4 m, height = 3.5 m, without openings). For the purpose of CFD simulations, the simulation program DesignBuilder was utilized (DesignBuilder 2011a). In this model multiple design variables pertaining to diffuser configurations and airflow rates were parametrically considered. Thereby, two scenarios were defined as follows.

5.2.2.1 First scenario

Let us assume CFD analysis is used to derive, from the knowledge of airflow rate into the space, the airflow speed at a certain location in the space. The question is if the respective result can be used - without additional CFD application - to predict the consequences of changes in airflow rates for airflow speed values. To address this question three shoebox models with different ceiling diffuser and extract configurations were modelled as illustrated in Figure 5.1. The CFD boundary conditions and simulation parameters including the zone mean temperature and surface temperatures as well as the supply air

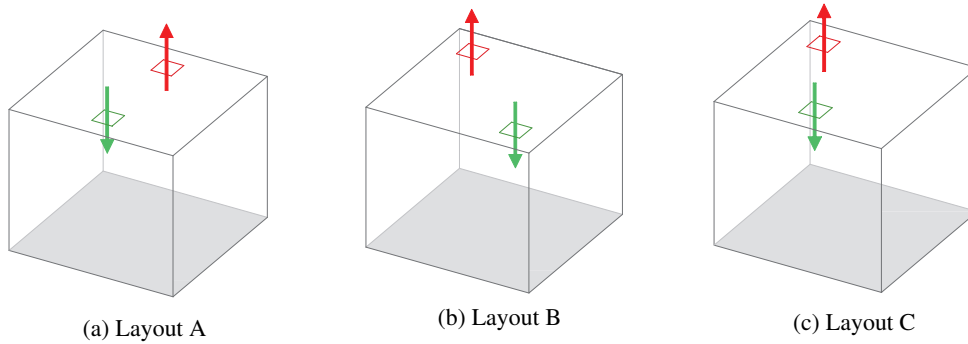


Figure 5.1: Illustration of the model geometry and location of the diffuser and extract grille in three layouts *A*, *B* and *C*, first scenario

Table 5.1: Simulation variants in the first scenario

Variant	Supply airflow rate [$l.s^{-1}$]	Supply air velocity [$m.s^{-1}$]
1	30	0.5
2	45	0.75
3	60	1.0
4	90	1.5
5	135	2.25

temperature were kept constant in the simulations. Table 5.1 presents five variations of airflow rates ($l.s^{-1}$) and supply air velocities ($m.s^{-1}$) modelled for each layout.

5.2.2.2 Second scenario

The second scenario assumes that, using CFD, the airflow field is separately simulated for two different supply air diffuser locations (see Figure 5.2, layouts *A* and *B*). The question is if the combined effect of the operation of both of these diffusers (see layout *C*, Figure 5.2) on the airflow field can be obtained without additional CFD analyses. Toward this end, three variations pertaining to the airflow rates ($l.s^{-1}$) and supply air velocities ($m.s^{-1}$) as per Table 5.2 were considered. Note that, the assumed airflow rate per diffuser is the same for all three layouts. This means that the total airflow rate in layout *C* is twice as high as those in layouts *A* and *B*.

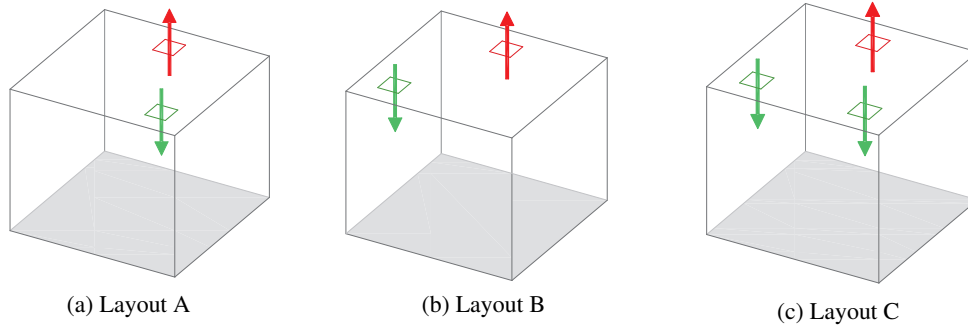


Figure 5.2: Illustration of the model geometry and location of the diffuser and extract grille in three layouts *A*, *B* and *C*, second scenario

Table 5.2: Simulation variants in the second scenario

Variant	Layout	Number of diffusers	Airflow rate of each diffuser [l.s^{-1}]	Total airflow rate [l.s^{-1}]	Supply air velocity [m.s^{-1}]
1	A and B	1	30	30	0.5
	C	2		60	
2	A and B	1	45	45	1.0
	C	2		90	
3	A and B	1	60	60	1.5
	C	2		120	

5.2.3 Investigation approach

CFD simulations were performed for all combinations of the layouts and variants corresponding to both scenarios, resulting in the air speed data for more than 350 grid nodes at the height of 1.1 m from the floor level. For the first scenario, the results corresponding to the paired sets of variants were compared to one another for all layouts (Table 5.1, Section 5.3.1). For the second scenario, the results of layout *A* and *B* were compared to Layout *C* for all variants (Table 5.2, Section 5.3.2). The results of the initial and altered models were analysed (primarily via curve-fitting techniques) to explore the potential for deriving simplified predictive relationships.

5.3 Results and discussion

In this section the results are presented in terms of a number of figures and tables together with discussions. Thereby the structure of the aforementioned methodology and research questions are followed.

5.3.1 First scenario

The consequence of changes in airflow rate alteration for the airflow speed was at the heart of this scenario. In Figure 5.3 and 5.4 the simulation result of variants 1 and 2 are compared to those with: *i*) doubled airflow rate, i.e. variant 3 and 4, and *ii*) tripled airflow rate, i.e. variant 4 and 5, respectively (see also Table 5.1). These figures reveal a strong linear relationship between the results (airflow speed rates) of the initial and altered scenarios.

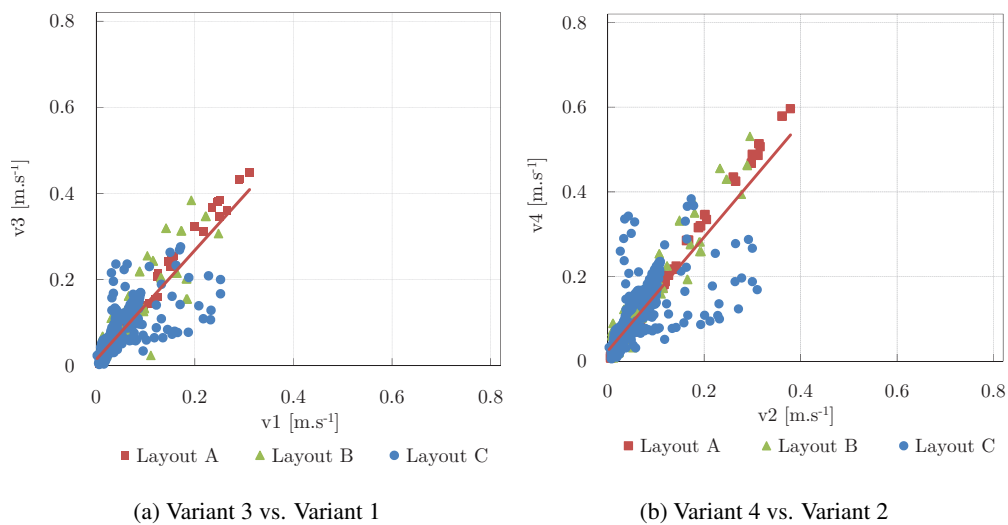


Figure 5.3: Airflow speed at grid nodes in variant 3 and 4 versus the corresponding nodes in variant 1 and 2, respectively

5. Parametric assessment of airflow conditions based on a limited set of CFD-based simulation runs

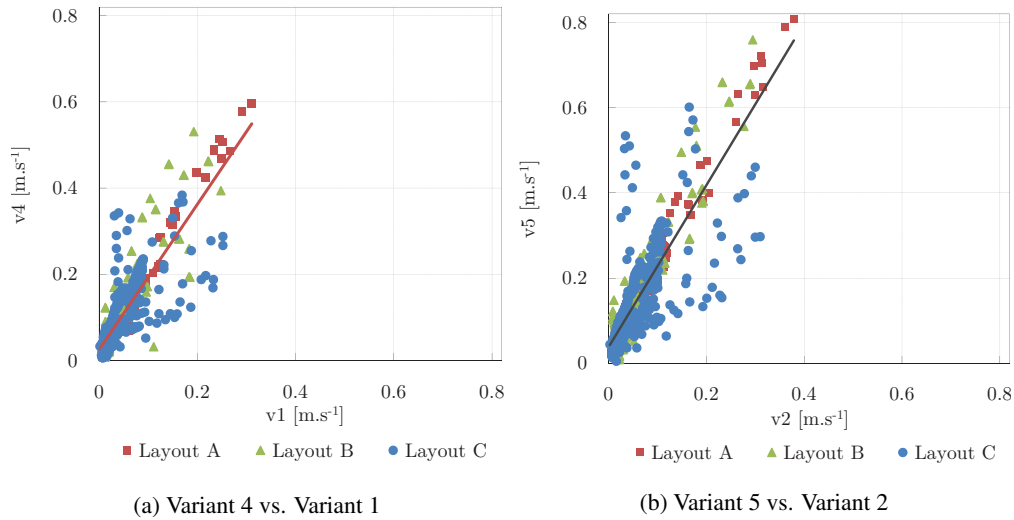


Figure 5.4: Airflow speed at grid nodes in variant 4 and 5 versus the corresponding nodes in variant 1 and 2, respectively

These results encourage the formulation and exploration of the validity of a relevant hypothesis. Let v_1 and v_2 be the simulated airflow speed for the initial and altered scenarios respectively. Let f_1 and f_2 be the corresponding assumed airflow rates. The hypothesis state that v_2 may be derived from v_1 using a linear equation as follows:

$$v_2 = \sqrt{\frac{f_2}{f_1}} \cdot v_1 \quad (5.1)$$

In order to evaluate the validity of Equation 5.1, four cases were defined based on the simulated variants (see Table 5.1). In each case the simulated airflow speed in the model with the flow rate f_2 was compared to its predicted value from Equation 5.1. Figure 5.5 illustrates cumulative distribution of the errors and Figure 5.6 shows the percentage of results within different bins of absolute error. These results may be interpreted to be encouraging, as even in the worst case (case 3), 95% of the calculated airflow speed rates display an absolute error of less than 0.1 m.s^{-1} . Such error magnitudes may be argued to be tolerable for many common applications of airflow field data in indoor environmental studies such as PMV calculations and human perception of the indoor climate (Loomans 1998). Table 5.3 presents the coefficient of correlations, R^2 , for different cases.

5. Parametric assessment of airflow conditions based on a limited set of CFD-based simulation runs

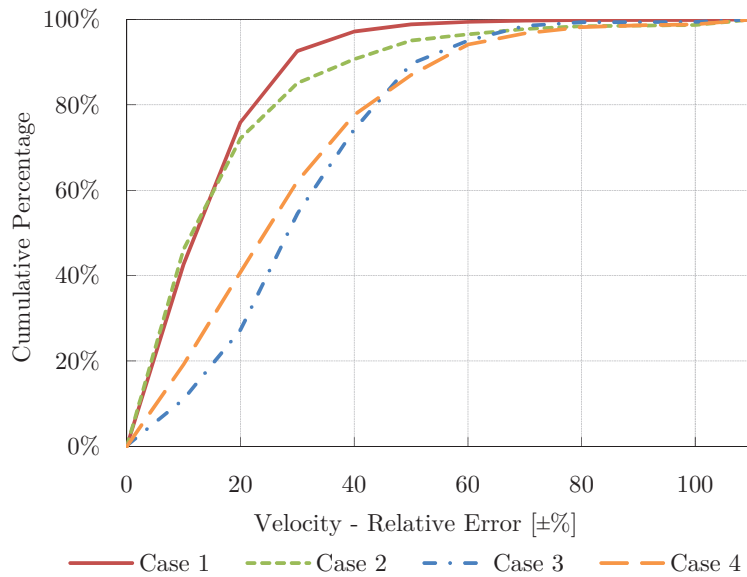


Figure 5.5: Cumulative distributions of relative errors of respective cases in the first scenario

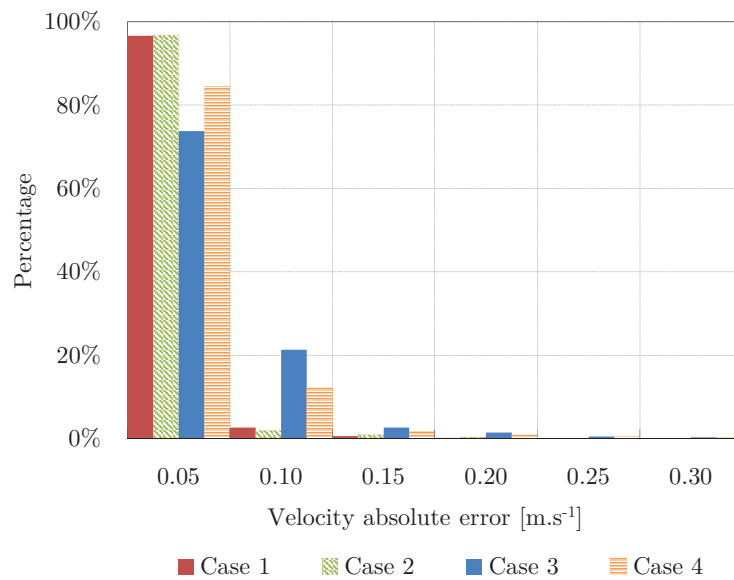


Figure 5.6: Percentage of result within various bins of absolute error (for respective cases in the first scenario)

Table 5.3: R^2 results for comparison of CFD-based and simplified calculations (Equation 5.1) of airflow speed for the four cases of the first scenario

Case	f_1	f_2	$\sqrt{f_1/f_2}$	R^2
1	30	45		1.0
	60	90	$\sqrt{1.5}$	1.0
	90	135		1.0
2	30	60	$\sqrt{2}$	0.8
	45	90		1.0
3	60	135	$\sqrt{2.25}$	0.9
4	30	90		0.8
	45	135	$\sqrt{3}$	0.9

5.3.2 Second scenario

Figure 5.7 illustrates airflow speed values for layouts *A*, *B*, and *C* for the respective variants in the second scenario. The comparison of results reinforces the idea that there is a potential to predict the airflow speed rates in layout *C* based on simulation results of layout *A* and *B*. This would require a mathematical superimposition of the results of *A* and *B*. Arguably, the simplest way to achieve this is averaging the values for each grid node of these two layouts. We implemented this option and compared the calculated results for layout *C* with the corresponding detailed simulation results. Figures 5.8 and 5.9 present the cumulative distributions of errors as well as the absolute errors. According to Figure 5.8, at least 80% of the calculations display relative errors below 20%. In the worst case (Variant 3), 65% have absolute errors less than $0.05 \text{ m}\cdot\text{s}^{-1}$ (87% in the best case). This level of congruence between detailed and simplified approaches would be acceptable for most application scenarios.

5.3.3 Concluding observations

This chapter presented the results of the effort to reliably evaluate basic design decisions pertaining to ventilation of architectural spaces based on a limited set of CFD simulation runs together with additional simple calculations. The results obtained from the implemented approach (airflow in a space with various diffuser configurations and/or flow rates) display an encouraging congruence with the corresponding results of a full CFD analysis.

5. Parametric assessment of airflow conditions based on a limited set of CFD-based simulation runs

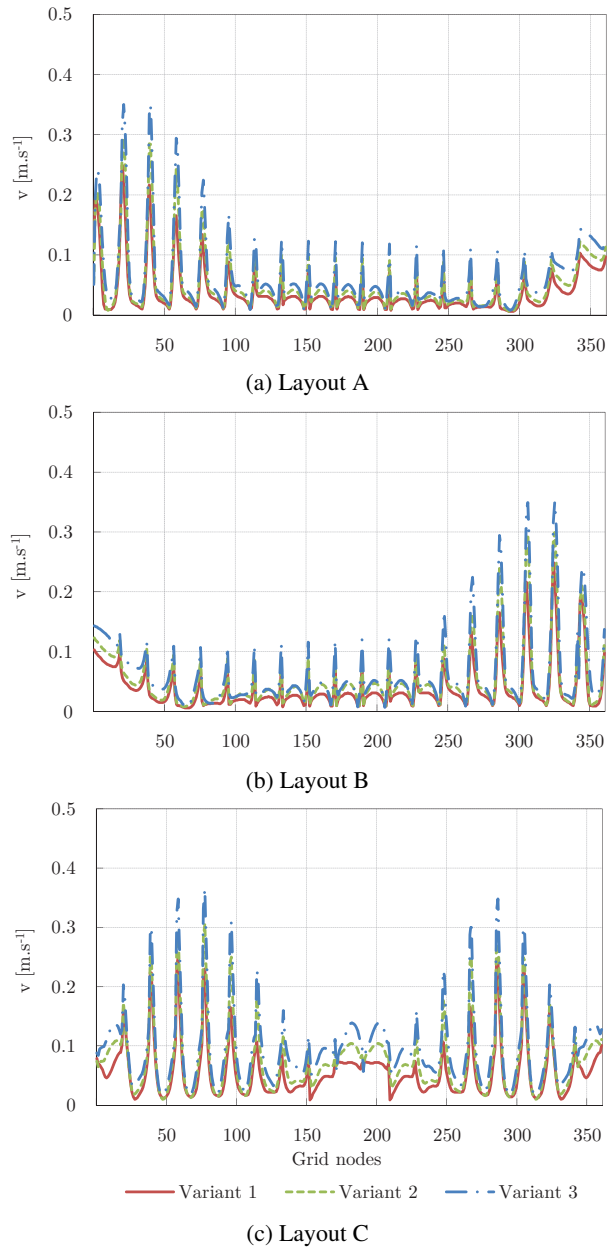


Figure 5.7: Airflow speed at grid nodes in layouts A, B, and C for respective variants of the second scenario

5. Parametric assessment of airflow conditions based on a limited set of CFD-based simulation runs

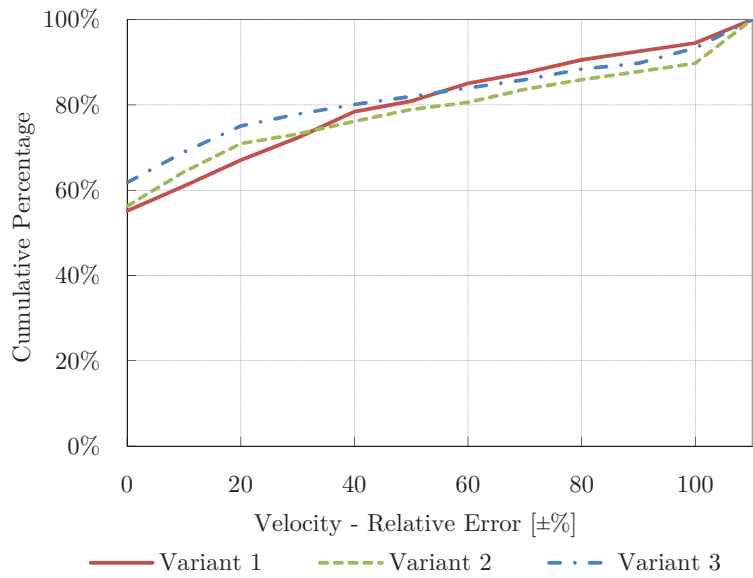


Figure 5.8: Cumulative distributions of relative errors for respective variants of the second scenario

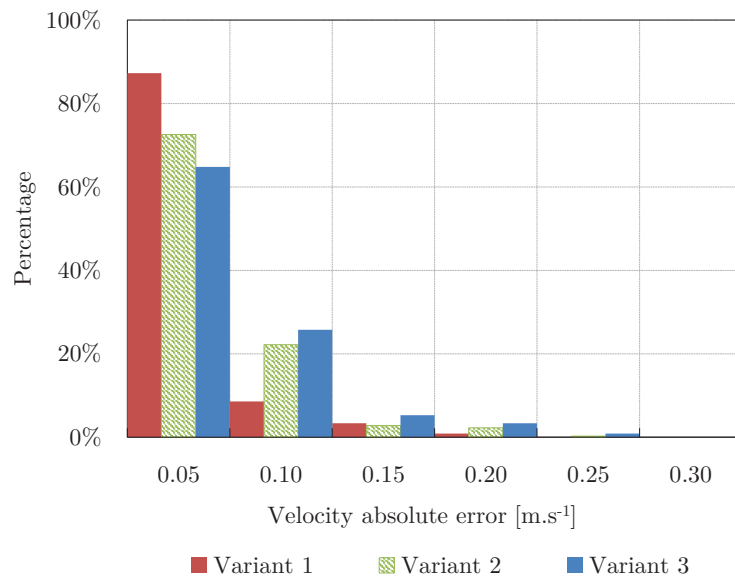


Figure 5.9: Absolute error distributions for respective variants in the second scenario

Chapter 6

Conclusions

6.1 Contribution

This dissertation presented the empirical and computational assessment of the functionality of ventilation systems and indoor environment condition in architectural spaces equipped with displacement ventilation, ducted and ductless personal ventilation. The functionality of the systems with respect to the indoor air quality and thermal comfort was evaluated based on the monitored data as well as user surveys. The results generally suggested acceptable indoor environmental conditions provided by the combined operation of the above mentioned ventilation systems. The combined operation of natural, displacement and personal ventilation systems was judged by the participants to result in a cooler indoor space, as compared to the solely natural ventilation option. In addition, the operation of displacement ventilation and personal ventilation together resulted in cooler thermal sensation votes as compared with displacement alone. The comparison between ducted and ductless personal ventilation represented that the ducted ones can provide a generally more desirable indoor environment. Regarding the air quality, ducted personal ventilation, and to a certain extent ductless one, improved the subjective impression of the freshness of the ambient air. The subjective evaluation of the systems suggested that the thermal perception of the office environment by those seated at workstations with operating personal ventilation is largely affected by the systems' supply air temperature. Therefore, careful control of the personal ventilation's supply air temperature highly affects the satisfaction of the occupants. Sufficiently lower supply temperatures required for ductless personal ventilation, however, may have repercussions for the energy demand.

This dissertation illustrated the utility of calibrated CFD models for better understanding

of the complex nature of the airflow and estimation of the airflow velocity and temperature field in the space. The main objective was to deploy monitored data to both populate the initial simulation model and to maintain its fidelity through a calibration process. In the course of multiple simulation and calibration steps, selected simulation input variables, including modeling of the diffuser, discharge angle of the air diffusers, and supply air temperature, were subjected to calibration. The calibration process aimed at minimizing the difference between monitored and simulated air speed and temperature. Through iterative calibration, the initial model was adjusted until a reasonable agreement between the measurements and CFD results was achieved. The study showed that CFD-based indoor airflow predictions can be noticeably improved, given monitored data to generate a more accurate initial model as well as supporting simulation model calibration. An instance of the use of calibrated CFD model was derivation of necessary input data for comfort calculations at different locations in the space. Furthermore, CFD model outcomes enabled the study of the temperature stratification in the space. The results illustrated that the supply airflow rate and temperature in the office space cannot provide the required temperature stratification level to encourage the users to use the ductless personal ventilation in order to transfer the cool and fresh air to their breathing zone. Calibrated model was then used to investigate design alternatives. A modified supply diffuser configuration with higher temperature difference between the room and supply air, and higher supply airflow rate provided a more acceptable temperature stratification for ductless personal ventilation, as well as a uniform temperature and velocity distribution in the space.

In this study, the comparison of actual thermal sensation votes and calculated predicted mean votes suggested that the application of PMV for evaluation of personal and displacement ventilation systems should be undertaken with great care. The experiences gained in this research point to the importance of continuous and comprehensive monitoring of indoor conditions, systems states, and occupants' feed-back toward systematic performance evaluation of indoor environmental control systems and methods.

This dissertation also presented the preliminary efforts in investigating how a relatively comprehensive impact assessment of various design variables and input assumptions regarding the ventilation systems in architectural spaces can be established based on a detailed but small number of numerical simulations. To explore this idea, a number of variations of the design variables of a basic shoe-box model was considered, which involved multiple airflow rates and diffuser configurations. Simple combinatorial manipulation options of a limited set of CFD based simulation results were applied to estimate airflow speeds for other design options. The results obtained from the implemented approach displayed an encouraging congruence with the corresponding results of a full CFD analysis. The proposed approach may thus entail the potential to reduce the extent of required computational resources for routine architectural ventilation tasks.

6.2 Future research

The introduced procedures and accordingly the results presented in this research appeared to be in compliance with the objectives of the research. This, therefore, implies the possibility to deploy this achievement for further studies. The author believes that the outcomes of this research is of indicative value and a pointer to issues that may be of interest to future research in this area. As suggestions, the author would like to address the followings:

- The observed possible deviation of the calculated thermal comfort indicators from the actual thermal sensation vote of the inhabitants underlines the necessity for clear understanding of the associated uncertainties with existing comfort models.
- The evaluation of the systems' energy use was not within the scope of the present study (the author agree of course that it would have provided additional insights but due to reasons pertaining to the ownership of the case study facility and related data issues, it could not be conducted, even if the author would have liked to include it). Therefore, study of the energy implications of the mentioned ventilation systems in details will be interesting.
- Future field studies shall increase the number of participants and additional operational schemes, which can provide further valuable insights.
- Future efforts are required to integrate the achievements of this study and similar studies in the standards addressing the ventilation requirements in spaces with personal ventilation systems.
- Additional efforts are needed to further evaluate the approach proposed in Chapter 5 involving a broader set of instances and options with regard to factors such as space geometry, diffuser configurations, and boundary conditions.

References

- Ahmed A. Saleem, Ali K. Abel-Rahman, Ahmed Hamza H. Ali and Shinichi Ookawara (2014), 'An analysis of thermal comfort and energy consumption within public primary schools in Egypt', *Sustainability, Energy & the Environment* **3**(1), 54–64.
- Arens, E. A., Zhang, H. and Huizenga, C. (2006), 'Center for the built environment sensation and comfort, part I: uniform environmental conditions', *Journal of Thermal Biology* **31**, 53–59.
- ASHRAE (2004), 'ANSI/ASHRAE Standard 55 - Thermal environmental conditions for human occupancy', *American Society of Heating, Refrigerating and Air-Conditioning Engineers, Inc., Atlanta, GA, United States*. .
- ASHRAE (2005), 'Handbook - Fundamentals', *American Society of Heating, Refrigerating and Air-Conditioning Engineers, Inc., Atlanta, GA, United States*. .
- ASHRAE (2007), 'ANSI/ASHRAE Standard 62.1 - Ventilation for acceptable indoor air quality', *American Society of Heating, Refrigerating and Air-Conditioning Engineers, Inc., Atlanta, GA, United States*. .
- Aswegan, J. and Pich, D. (2014), 'Designing for comfort & IAQ: Air distribution per ASHRAE 55 and 62.1'.
URL: <https://www.constructionspecifier.com/designing-for-comfort-iaq-air-distribution-per-ashrae-55-and-62-1/>
- Awbi, H. B. (2015), 'Ventilation and air distribution systems in buildings', *Frontiers in Mechanical Engineering* **1**(April), 1–4.
- B+B Thermo-Technik GmbH (2017), 'Präzisions-Temperatursensor TS-NTC-203'.
URL: <http://www.bb-sensors.com/en/products/temperature/>

- Bordass, B. and Leaman, A. (2009), 'An overview of post-occupancy evaluation'.
URL: <http://usablebuildings.co.uk/>
- Candido, C., de Dear, R., Lamberts, R. and Bittencourt, L. (2010), 'Air movement acceptability limits and thermal comfort in Brazil's hot humid climate zone', *Building and Environment* **45**(1), 222–229.
- Catalina, T., Virgone, J. and Kuznik, F. (2009), 'Evaluation of thermal comfort using combined CFD and experimentation study in a test room equipped with a cooling ceiling', *Building and Environment* **44**, 1740–1750.
- Cermak, R., Melikov, A. K., Forejt, L. and Kovar, O. (2006), 'Performance of personalized ventilation in conjunction with mixing and displacement ventilation', *HVAC&R Research* **12**(2), 295–311.
- Cetin, R. and Mahdavi, A. (2015), An empirically-based assessment of CFD utility in urban-level air flow studies, in 'BS2015, 14th Conference of International Building Performance Simulation Association, Hyderabad, India', pp. 796–803.
- Chakroun, W., Ghaddar, N. and Ghali, K. (2011), 'Chilled ceiling and displacement ventilation aided with personalized evaporative cooler', *Energy and Buildings* **43**(11), 3250–3257.
- Chanteloup, V. and Mirade, P.-S. (2009), 'Computational fluid dynamics (CFD) modelling of local mean age of air distribution in forced-ventilation food plants', *Journal of Food Engineering* **90**, 90–103.
- Chen, Q. and Srebric, J. (2002), 'A procedure for verification, validation, and reporting of indoor environment CFD analyses', *HVAC&R Research* **8**(2), 201–216.
- Chen, Q. and Zhai, Z. (2004), The use of CFD tools for indoor environmental design, in A. Malkawi and G. Augenbroe, eds, 'Advanced Building Simulation', Spon Press, New York, pp. 119–140.
- Chowdhury, A. A., Rasul, M. and Khan, M. M. K. (2010), Analysis of building systems performance through integrated computation fluid dynamics technique, in '13th Asian Congress of Fluid Mechanics, Dhaka, Bangladesh', pp. 625–628.
- Chung, L. P., Ahmad, M. H. B. H., Ossen, D. R. and Hamid, M. (2014), 'Application of CFD in prediction of indoor building thermal performance as an effective pre-design tool towards sustainability', *World Applied Sciences Journal* **30**, 269–279.
- Clarke, J. (2001), *Energy simulation in building design (Second edition)*, Adam Hilger Ltd, Techno House, Redcliffe Way, Bristol BS1 6NX, England.

References

- Conceição, E., Lúcio, M. M., Rosa, S., Custódio, A., Andrade, R. and Meira, M. (2010), 'Evaluation of comfort level in desks equipped with two personalized ventilation systems in slightly warm environments', *Building and Environment* **45**, 601–609.
- Dalewski, M., Melikov, A. K. and Vesely, M. (2014), 'Performance of ductless personalized ventilation in conjunction with displacement ventilation: Physical environment and human response', *Building & Environment* **81**, 354–364.
- Dalewski, M., Vesely, M. and Melikov, A. K. (2012), Ductless personalized ventilation with local air cleaning, in '10th International Conference on Healthy Buildings , Brisbane, Australia', pp. 1–6.
- den Hartog, J. P., Koutamanis, A. and Luscuere, P. G. (2000), Possibilities and limitations of CFD simulation for indoor climate analysis, in 'Fifth Design and Decision Support Systems in Architecture and Urban Planning - Part one: Architecture Proceedings, Nijkerk, the Netherlands', pp. 152–167.
- DesignBuilder (2011a), 'DesignBuilder CFD - Computational Fluid Dynamics'.
URL: <http://www.designbuilder.co.uk/content/view/152/226/>
- DesignBuilder (2011b), 'DesignBuilder simulation + CFD training guide'.
URL: <https://www.designbuilder.co.uk/training>
- Designbuilder (2011c), 'Technical CFD documentation'.
URL: <https://www.designbuilder.co.uk/downloadsv1/doc/CFDTechnical.pdf>
- EDR (2015), 'Design brief: Displacement ventilation 2.0'.
URL: <https://energydesignresources.com/resources/publications.aspx>
- Emmerich, S. J. and McDowell, T. (2005), Initial evaluation of displacement ventilation and dedicated outdoor air systems for U.S. commercial buildings, Technical report, U.S. Environmental Protection Agency Washington, DC, United States.
- EN ISO 7730 (2005), 'Ergonomics of the thermal environment - Analytical determination and interpretation of thermal comfort using calculation of the PMV and PPD indices and local thermal comfort criteria'.
- EnergyPlus (2011), 'EnergyPlus energy simulation software'.
URL: <http://apps1.eere.energy.gov/buildings/energyplus>
- EXHAUSTO (2016), 'Personalised ventilation - A healthy investment'.
URL: http://www.exhausto.com/ /media/Global/PDF/Products/broc_PV_GB.ashx
- Fanger, P. (1970), *Thermal comfort-analysis and applications in environmental engineering*, Copenhagen: Danish Technical Press.

- Faulkner, D., Fisk, W. J., Sullivan, D. P. and D. P. Wyon (1999), 'Ventilation efficiencies of task/ambient conditioning systems with desk-mounted air supplies'.
- Hagino, M. and Hara, J. (1992), Development of a method for predicting comfortable airflow in the passenger compartment, Technical report, SAE Technical Paper 922131.
- Halvonova, B. and Melikov, A. K. (2010a), 'Performance of ductless personalized ventilation in conjunction with displacement ventilation: impact of disturbances due to walking person(s)', *Building and Environment* **45**, 427–436.
- Halvonova, B. and Melikov, A. K. (2010b), 'Performance of ductless personalized ventilation in conjunction with displacement ventilation: Impact of intake height', *Building and Environment* **45**(4), 996–1005.
- Halvonova, B. and Melikov, A. K. (2010c), 'Performance of ductless personalized ventilation in conjunction with displacement ventilation: impact of workstations layout and partitions', *HVAC&R Research* **16**(1), 75–94.
- Hamilton, S. D., Roth, K. W. and Brodrick, J. (2004), 'Emerging technologies: displacement ventilation', *ASHRAE Journal, American Society of Heating, Refrigerating and AirConditioning Engineers*. **46**(9), 56–58.
- Hensen, J. (1990), 'Literature review on thermal comfort in transient conditions', *Building and Environment* **25**(4), 309–316.
- Hensen, J. L. M. and Hamelinck, M. J. H. (1995), 'Energy simulation of displacement ventilation in offices', *Building Services Engineering Research and Technology* **16**(2), 77–81.
- Hirsch, C. (2007), *Numerical computation of internal and external flows*, second edn, Elsevier.
- Iizuka, S., Sasaki, M., Yoon, G., Okumiya, M., Kondo, J. and Sakai, Y. (2011), Coupling strategy of HVAC system simulation and CFD part 2 : Study on mixing energy loss in an air-conditioned room, in 'Proceedings of Building Simulation 2011: 12th Conference of International Building Performance Simulation Association, Sydney, 14-16 November', pp. 2096–2101.
- Jackman, P. (1991), Displacement ventilation, in 'CIBSE National Conference', pp. 364–380.
- Junjing, Y., Sekhar, C., Cheong, D. and Raphael, B. (2014), 'Performance evaluation of an integrated personalized ventilation - personalized exhaust system in conjunction with two background ventilation systems', *Building and Environment* **78**, 103–110.

References

- Kaczmarczyk, J., Melikov, A. K. and Fanger, P. O. (2004), 'Human response to personalized ventilation and mixing ventilation', *Indoor Air* **14**, 17–29.
- Kaczmarczyk, J., Melikov, A. K. and Sliva, D. (2010), 'Effect of warm air supplied facially on occupants' comfort', *Building and Environment* **45**(4), 848–855.
- Kim, J., de Dear, R., Cândido, C., Zhang, H. and Arens, E. (2013), 'Gender differences in office occupant perception of indoor environmental quality (IEQ)', *Building and Environment* **70**, 245–256.
- Laborda, M. Á. C., Fernández-Agüera, J. and Domínguez-Amarillo, S. (2012), Development of a CFD simulation model to a classroom with radiant floor heating system case study in Mediterranean climate, in 'BuildSim-Nordic 2012, The Nordic regional affiliate of IBPSA-World, Oslo, Norway'.
- Lechner, N. (2001), *Heating, cooling, lighting : Design methods for architects*, 2nd edn, John Wiley & Sons.
- Lesbirel, M. (2012), 'LEED post-occupancy surveys: Designing a survey for maximum return'.
- Li, R., Sekhar, S. C. and Melikov, A. K. (2010), 'Thermal comfort and IAQ assessment of under-floor air distribution system integrated with personalized ventilation in hot and humid climate', *Building and Environment* **45**(9), 1906–1913.
- Lin, Y. and Lin, C. (2014), 'A study on flow stratification in a space using displacement ventilation', *International Journal of Heat and Mass Transfer* **73**, 67–75.
- Loomans, M. (1998), The measurement and simulation of indoor air flow, PhD thesis, Technische Universiteit Eindhoven, Eindhoven, the Netherlands.
- Loudermilk, K. J. (1999), 'Under-floor air distribution solutions for open office applications', *ASHRAE Journal, American Society of Heating, Refrigerating and AirConditioning Engineers* **105**, 605–613.
- Magnier, L., Zmeureanu, R. and Derome, D. (2012), 'Experimental assessment of the velocity and temperature distribution in an indoor displacement ventilation jet', *Building and Environment* **47**, 150–160.
- McDonough, J. M. (2003), 'Lectures in computational fluid dynamics of incompressible flow: Mathematics, algorithms and implementations'.
URL: <http://www.engr.uky.edu/acfd/me691-lctr-nts.pdf>
- Melikov, A. K. (2004), 'Personalized ventilation', *Indoor Air* **14**, 157–167.

- Melikov, A. K., Cermak, R. and Majer, M. (2002), 'Personalized ventilation: Evaluation of different air terminal devices', *Energy and Buildings* **34**, 829–836.
- Melikov, A. K., Grønbaek, H. and Nielsen, J. B. (2007), Personal ventilation: From Research to Practical Use, in 'Clima 2007 WellBeing Indoors, Helsinki.'
- Melikov, A. K. and Kaczmarczyk, J. (2012), 'Air movement and perceived air quality', *Building and Environment* **47**(1), 400–409.
- Meroney, R. N. (2009), CFD prediction of airflow in buildings for natural ventilation, in '11th Americas Conference on Wind Engineering Americas Conference on Wind Engineering', San Juan, Puerto Rico, pp. 1–11.
- Nielsen, P. V. (1998), 'The selection of turbulence models for prediction of room airflow', *ASHRAE Transactions* **104**, 1119–1129.
- Niu, J., Gao, N., Phoebe, M. and Huigang, Z. (2007), 'Experimental study on a chair-based personalized ventilation system', *Building and Environment* **42**, 913–925.
- Prajongsan, P. and Sharples, S. (2012), The Ventilation Shaft : An alternative passive cooling strategy for high-rise residential buildings in hot-humid climates, in 'PLEA2012 - 28th Conference, Opportunities, Limits & Needs Towards an environmentally responsible architecture Lima', p. 6.
- Rakesh, M., Janardhanan, S. and Vishnu, V. K. (2014), Subsonic flow analysis of a tailless aircraft by using CFD, Technical Report April, Dhanalakshmi Srinivasan Engineering College, India.
- Rees, S. J. and Haves, P. (2013), 'An experimental study of air flow and temperature distribution in a room with displacement ventilation and a chilled ceiling', *Building and Environment* **59**, 358–368.
- Ren, Z. (2002), Enhanced modelling of indoor air flows, temperatures, pollutant emission and dispersion by nesting sub-zones within a multizone model, PhD thesis, The Queen's University of Belfast, Northern Ireland.
- Rogers, G. (2015), 'ALMEMO system measuring instruments and data logging systems from IDS industry'.
URL: <http://inds.co.uk/almemo/index.htm>
- Russo, J. (2011), A detailed and systematic investigation of personal ventilation systems, Mechanical and aerospace engineering - dissertations, Syracuse University, New York, United States.
- Schiavon, S. and Melikov, A. K. (2009), 'Energy-saving strategies with personalized ventilation in cold climates', *Energy and Buildings* **41**, 543–550.

References

- Schiavon, S., Melikov, A. K. and Sekhar, C. (2010), 'Energy analysis of the personalized ventilation system in hot and humid climates', *Energy and Buildings* **42**, 699–707.
- Schiavon, S., Rim, D., Pasut, W. and Nazaroff, W. W. (2014), Sensation of draft at ankles for displacement ventilation and underfloor air distribution systems, in '13th International Conference on Indoor Air Quality and Climate, Indoor Air 2014, Hong Kong.', Center for the Built Environment UC Berkeley.
- Sekhar, S. C., Gong, N., Tham, K. W., Cheong, K. W., Melikov, A. K., Wyon, D. P. and Fanger, P. O. (2005), 'Findings of personalized ventilation studies in a hot and humid climate', *HVAC&R Research* **11**(4), 603–620.
- Shaharon, M. N. and Jalaludin, J. (2012), 'Thermal comfort assessment - A study toward workers' satisfaction in a low energy office building', *American Journal of Applied Sciences* **9**(7), 1037–1045.
- Sheta, W. and Sharples, S. (2010), A building simulation sustainability analysis to assess dwellings in a new cairo development, in 'SimBuild 2010, Fourth National Conference of IBPSA-USA, New York, USA', New York City, New York August 11 13, pp. 94–101.
- Taheri, M., Schuss, M., Fail, A. and Mahdavi, A. (2016), 'A performance assessment of an office space with displacement, personal, and natural ventilation systems', *Building Simulation* **9**(1), 89–100.
- Tawani, R. (2008), Discretization of convection-diffusion type equations by finite volume method, in '7th Indo German Winter Academy', Department of Chemical Engineering Indian Institute of Technology, Bombay.
- Testo (2015), 'We Measure It. testo'.
URL: <http://www.testo.com.cn/en/products/temperature/index.jsp>
- Thermokon (2015), 'Thermokon Sensortechnik GmbH'.
URL: <http://www.thermokon.de>
- Titus (2014), 'Displacement ventilation'.
URL: https://www.titus-hvac.com/docs/2014_catalog/displacement_2013.pdf
- Veselý, M. and Zeiler, W. (2014), 'Personalized conditioning and its impact on thermal comfort and energy performance A review', *Renewable and Sustainable Energy Reviews* **34**, 401–408.
- Webb, M. (2013), Building energy and CFD simulation to verify thermal comfort in under floor air distribution (UFAD) design, in 'BS2013: 13th Conference of International Building Performance Simulation Association, Chambéry, France, August 26-28', pp. 1886–1893.

References

- Wiercinski, Z. and Skotnicka-Siepsiak, A. (2008), 'Application of CFD for temperature and air velocity distribution calculation in a ventilated room', *Task Quarterly* **12**(3), 303–312.
- Wyon, D. and Sandberg, M. (1990), 'Thermal manikin prediction of discomfort due to displacement ventilation', *ASHRAE Journal, American Society of Heating, Refrigerating and AirConditioning Engineers* **96**(1), 67–75.
- Xu, Y. (2007), Modeling and evaluation of personal displacement ventilation system for improving indoor air quality, PhD thesis, University of Miami, US.
- Yang, B., Sekhar, S. C. and Melikov, A. K. (2010), 'Ceiling-mounted personalized ventilation system integrated with a secondary air distribution system - A human response study in hot and humid climate', *Indoor Air* **20**(4), 309–319.
- Zhai, Z., Chen, Q., Haves, P. and Klems, J. H. (2002), 'On approaches to couple energy simulation and computational fluid dynamics programs', *Building and Environment* **37**(8-9), 857–864.
- Zhai, Z., Chen, Q., JH, K. and P, H. (2001), Strategies for coupling energy simulation and computational fluid dynamics programs, in 'Building Simulation, Rio de Janeiro, Brazil', Vol. 01, pp. 59–66.
- Zhai, Z. J. and Chen, Q. Y. (2005), 'Performance of coupled building energy and CFD simulations', *Energy and Buildings* **37**(4), 333–344.
- Zhang, H. (2003), Human thermal sensation and comfort in transient and non-uniform thermal environments, PhD thesis, University of California, Berkeley, USA.

Curriculum vitae

Mahnameh Taheri

Department of Building Physics and Building Ecology
TU Wien, Karlsplatz 13 E2593, A-1040 Vienna, Austria

Educational background

- | | |
|-----------|--|
| 2013-2017 | PhD. , Engineering Sciences Architecture, Department of Building Physics and Building Ecology, TU Wien, Vienna, Austria |
| 2011-2013 | M.Sc. , Building Science and Technology, Department of Building Physics and Building Ecology, TU Wien, Vienna, Austria |
| 2003-2008 | B.Sc. , Civil Engineering, Technical Faculty, University of Mazandaran, Babol, Iran |
| 1999-2003 | High School Diploma , Mathematic-Physics, National Organization for Development of Exceptional Talents, Sari, Iran |

Research activities

- | | |
|--------------|---|
| | Department of Building Physics and Building Ecology, TU Wien, Vienna, Austria |
| 2016-Present | University assistant , Participating in research projects:
<i>Occupancy</i> : TU Wien Innovative Projects
<i>The Sun Houses of Konrad Frey</i> : Environmental Research and Solar Design Knowledge |

- 2012-2016 **Project assistant**, Participating in research projects:
- EDEN*: Entwicklung einer strukturierten und fehlerminimierten Datenaufbereitung und Dokumentation für Energieausweise
 - BAU WEB*: Ontologien für automatisierte Erschließung web-basierter Bauprodukt-daten für Industrie, Planer und Klienten
 - RESSEPE*: RETrofitting Solutions and Services for the enhancement of Energy Efficiency in Public Edification
 - FreshAir*: Nachhaltige Lüftungsstrategien für Bürogebäude: eine Untersuchung der Energieeffizienz, Innenklima und Nutzerkomfort
 - SEMERGY*: Semantic web-based tool for optimized energy-efficient building planning
 - Optimization-based calibration of building thermal performance simulation models

Publications

PhD project related publications

- Taheri, M., Schuss, M., Fail, A. and Mahdavi, A. (2016), 'A performance assessment of an office space with displacement, personal, and natural ventilation systems', *Building Simulation* **9**(1), 89–100.
- Taheri, M., Schuss, M., Lechleitner, J. and Mahdavi, A. (2016), Application of calibrated CFD models for the assessment of a displacement ventilation system, in 'CESBP Central European Symposium on Building Physics, and BauSIM 2016', Dresden, Germany, pp. 683–689.
- Taheri, M. and Mahdavi, A. (2016), An efficient approach to the parametric assessment of airflow conditions in architectural spaces based on a limited set of CFD-based simulation runs, in A. L. P. Hájek, J. Tywoniak, ed., 'CESB 2016: Central Europe towards sustainable building 2016 - innovations for sustainable future', Prague, Czech Republic, pp. 1497–1504.
- Schuss, M., Taheri, M., Pont, U. and Mahdavi, A. (2016), Performance evaluation of ducted and ductless personal ventilation systems, in J. Laverge, T. Salthammer and M. Stranger, eds, 'Indoor Air 2016, The 14TH International Conference of Indoor Air Quality and Climate', ISAIQ - International Society of Indoor Air Quality and Climate, Ghent, Belgium.
- Taheri, M., Schuss, M., Fail, A. and Mahdavi, A. (2014), Design analysis of an office ventilation system via calibrated CFD application, in 'BauSIM 2014, 5th German-

Austrian IBPSA Conference RWTH Aachen University', Aachen, Germany, pp. 53–59.

Taheri, M., Schuss, M., Fail, A. and Mahdavi, A. (2014), A comparative field study of space ventilation systems, *in* 'Indoor Air 2014, The 13th International Conference on Indoor Air Quality and Climate', ISAIQ - International Society of Indoor Air Quality and Climate, Hong Kong, China.

Other publications

Mahdavi, A., Taheri, M., Schuss, M., Tahmasebi, F. and Glawischnig, S. (2017), Structured building data management: Ontologies, queries, and platforms, *in* A. Wagner, W. O'Brien and B. Dong, eds, 'Exploring occupant behavior in buildings - Methods and challenges', Springer International Publishing.

Taheri, M., Tahmasebi, F. and Mahdavi, A. (2017), Consideration of inhabitants' diversity in building performance simulation: Does it matter?, *in* 'Building Simulation 2017, 15 IBPSA Conference, International Building Performance Simulation Association', San Francisco, United States.

Mahdavi, A., Ghiassi, N., Vuckovic, M., Taheri, M., Kiesel, K., Tahmasebi, F. and Glawischnig, S. (2017), High-resolution representations of internal and external boundary conditions in urban energy modelling, *in* 'Building Simulation 2017, 15 IBPSA Conference, International Building Performance Simulation Association', San Francisco, United States.

Covic, M., Pont, U., Ghiassi, N., Taheri, M., Bräuer, R. and Mahdavi, A. (2017), 'An inquiry into the current practice of building product data handling by different stakeholders in Austria', *Applied Mechanics and Materials* **861**, 547 – 555.

Vuckovic, M., Attila, S., Gomez, R. G., Hodzic, N., Lisyana, V., Risetto, P., Solman, M., Tezarek, T., Ghiassi, N., Taheri, M., Tahmasebi, F., Pont, U. and Mahdavi, A. (2017), The EMULATE Project course as an instance of Research-guided teaching, *in* 'Vienna Young Scientists Symposium', Vienna, Austria.

Schuss, M., Pont, U., Taheri, M., Lindner, C. and Mahdavi, A. (2017), Simulation-assisted monitoring-based performance evaluation of a historically relevant architectural design, *in* M. Baratieri, V. Corrado, A. Gasparella and F. Patuzzi, eds, 'Building Simulation Applications, 3rd IBPSA-Italy Conference', Bolzano, Italy.

Mahdavi, A. and Taheri, M. (2016), 'An ontology for building monitoring', *Journal of Building Performance Simulation* pp. 1–10.

URL: <http://dx.doi.org/19401493.2016.1243730>

Pont, U., Proskurnina, O., Taheri, M., Kropf, A., Sommer, B., Sommer-Nawara, M., Adam, G. and Mahdavi, A. (2016), Input data quality for building energy certification: Recent progress in the EDEN project, *in* 'Vienna Young Scientists Symposium', Vienna, Austria.

- Pont, U., Ghiassi, N., Taheri, M., Bräuer, R. and Mahdavi, A. (2016), The BAU WEB project: Exploring the potential of state of the art web technologies for building product data acquisition and management, *in* ‘Vienna Young Scientists Symposium’, Vienna, Austria.
- Pont, U., Proskurnina, O., Taheri, M., Mahdavi, A., Sommer, B., Sommer-Nawara, M. and Adam, G. (2016), Acquisition and processing of input data for building certification: An approach to increase the reproducibility of energy certificates, *in* S. Christodoulou and R. Scherer, eds, ‘ECPPM 2016, eWork and eBusiness in Architecture, Engineering and Construction’, Limassol, Cyprus, pp. 243–250.
- Ghiassi, N., Taheri, M., Pont, U. and Mahdavi, A. (2016), A semantic web approach to efficient building product data procurement, *in* S. Christodoulou and R. Scherer, eds, ‘ECPPM 2016, eWork and eBusiness in Architecture, Engineering and Construction’, Limassol, Cyprus, pp. 457–464.
- Ghiassi, N., Hammerberg, K., Taheri, M., Pont, U., Sunanta, O. and Mahdavi, A. (2015), An enhanced sampling-based approach to urban energy modelling, *in* ‘14 IBPSA Conference, International Building Performance Simulation Association’, Hyderabad, India.
- Taheri, M. and Mahdavi, A. (2014), ‘Optimization-based monitoring-supported calibration of a thermal performance simulation mode’, *International Journal of Optimization in Civil Engineering* **4**(2), 261–271.
- Tahmasebi, F., Taheri, M., Schuss, M. and Mahdavi, A. (2015), Improving energy efficiency through the optimization of buildings’ operational regime : simulation based case-studies, *in* ‘BSA 2015, 2nd IBPSA-Italy Conference’, Bolzano, Italy.
- Taheri, M., Tahmasebi, F. and Mahdavi, A. (2013), A case study of optimization-aided thermal building performance simulation calibration, *in* ‘Building Simulation 2013, 13 IBPSA Conference, International Building Performance Simulation Association’, Chambéry, France.
- Heurix, J., Fenz, S., Anjomshoaa, A., Neubauer, T., Tjoa, A. M., Taheri, M., Shayeganfar, F., Pont, U., Ghiassi, N., Sustr, C. and Mahdavi, A. (2013), Multi-objective optimization in the SEMERGY environment for sustainable building design and retrofit, *in* ‘CESBP, 2nd Central European Symposium on Building Physics’, Vienna, Austria, pp. 27–34.
- Pont, U., Shayeganfar, F., Ghiassi, N., Taheri, M., Sustr, C., Mahdavi, A., Fenz, S., Heurix, J., Anjomshoaa, A., Neubauer, T. and Tjoa, A. (2013), Recent advances in SEMERGY : A semantically enriched optimization environment for performance-guided building design and refurbishment, *in* ‘CESBP, 2nd Central European Symposium on Building Physics’, Vienna, Austria, pp. 19–26.

Taheri, M., Tahmasebi, F. and Mahdavi, A. (2013), Two case studies in optimization-based thermal building performance model calibration, *in* 'CESBP, 2nd Central European Symposium on Building Physics', Vienna, Austria, pp. 559–564.

Taheri, M. (2013), 'Optimization-based calibration of a building thermal performance simulation model', *Master Thesis, Department of Building Physics and Building Ecology, TU Wien, Vienna, Austria* .